

**ORGANIC SYNTHESSES: MODULAR DIVERGENT FORMATION  
OF ANTI-MALARIAL NATURAL PRODUCTS**

A Thesis  
Presented to  
The Academic Faculty

by

Kymerlee Alana Osborne-Benthaus

In Partial Fulfillment  
of the Requirements for the Degree  
Master of Science in the  
School of Chemistry and Biochemistry, Georgia Institute of Technology

Georgia Institute of Technology  
December 2017

**COPYRIGHT© 2017 BY KYMBERLEE OSBORNE-BENTHAUS**

**ORGANIC SYNTHESSES: MODULAR DIVERGENT FORMATION  
OF ANTI-MALARIAL NATURAL PRODUCTS**

Approved by:

Dr. Stefan France, Advisor  
School of Chemistry and Biochemistry  
*Georgia Institute of Technology*

Dr. David Collard  
School of Chemistry and Biochemistry  
*Georgia Institute of Technology*

Dr. Wendy Kelly  
School of Chemistry and Biochemistry  
*Georgia Institute of Technology*

Dr. Julia Kubanek  
School of Biology  
*Georgia Institute of Technology*

Date Approved: January 9, 2018

## **ACKNOWLEDGEMENTS**

I would like to thank my mother, father, husband and siblings for supporting me throughout my academic journey. Without their guidance and support, I would not be the woman that I am today.

## Table of Contents

|   |     |
|---|-----|
| ACKNOWLEDGEMENTS  | iii |
| LIST OF TABLES  | vi  |
| LIST OF FIGURES   | vii |
| LIST OF SYMBOLS AND ABBREVIATIONS                       | xii |
| SUMMARY   | xvi |
| CHAPTER 1   | 1   |
| 1.1 Introduction  | 1   |
| 1.2 Malaria   | 2   |
| 1.3 <i>Callophycus serratus</i> Terpenoids              | 6   |
| 1.4 Bromophycolide Biological Activity                  | 9   |
| 1.5 Thesis Overview                                     | 14  |
| CHAPTER 2   | 15  |
| 2.1 Bromophycolide Synthetic Strategy                   | 15  |
| 2.1.1 Bromonium Electrophilic $\pi$ -Cyclization        | 16  |
| 2.1.2 Objective   | 17  |
| 2.1.3 Significance- Modular Approach                    | 18  |
| 2.2 Results   | 21  |
| 2.2.1 Cyclohexyl Formation- Bromophycolides P, Q, and U | 22  |
| 2.2.2 Aryl-Allyl Cross-Coupling                         | 31  |
| 2.2.3 Linalool Fragment- Callophycolide A               | 40  |
| 2.2.4 Sulfone Stabilized Anionic Epoxide Ring Opening   | 41  |
| 2.2.5 Pyran Formation- Bromophycolide P, Q, and U       | 44  |
| 2.3 Outlook   | 46  |

|   |     |
|---|-----|
| 2.4 Conclusion                                      | 48  |
| CHAPTER 3- EXPERIMENTAL                             | 49  |
| 3.1 Cyclohexyl- Bromophycolides P, Q, and U         | 49  |
| 3.2 Aryl- Allyl Cross-Coupling                      | 56  |
| 3.3 Linalool Fragment- Callophycolide A             | 65  |
| 3.4 Sulfone Stabilized Anionic Epoxide Ring Opening | 67  |
| 3.5 Pyran Formation- Bromophycolides P, Q, and U    | 68  |
| APPENDIX A- NMR Data                                | 70  |
| REFERENCES  | 117 |

## LIST OF TABLES

|   |    |
|---|----|
| <b>Table 1</b> Bromophycolide family bio-activity profile featuring inhibitory concentration (IC <sub>50</sub> ) values for chloroquine resistant <i>P. falciparum</i> , methicillin-resistant <i>Staphylococcus aureus</i> (MRSA), and vancomycin-resistant <i>Enterococcus faecium</i> (VREF). <sup>10a, 13, 15</sup> .....         | 11 |
| <b>Table 2</b> Adapted from Snyder's BDSB study, table shows comparison of bromonium sources.....   | 16 |
| <b>Table 3</b> Adapted from Snyder's BDSB study, table shows concentration study for BDSB model system geranyl acetate. Image also provides description of diastereomeric products. <sup>1</sup> .....  | 17 |
| <b>Table 4</b> Bromonium $\pi$ -electrophilic cyclization using Snyder's reagent (BDSB, <b>40</b> ). Optimization table includes data for concentration dependence study in addition to results for the cyclization of substrates with variation at both terminal ends, "X" and "Y" position. <sup>1</sup> .....                      | 26 |
| <b>Table 5</b> Results from selective tertiary alcohol elimination study. <sup>24</sup> .....   | 29 |
| <b>Table 6</b> Optimization of the time needed for the generation of the aryl organometallic complex (Grignard/ <i>in situ</i> generated magnesate complex) and the actual coupling event with geranyl bromide. An overarching goal of this screen was to find conditions which reduced the formation of compound <b>71 (B)</b> ..... | 36 |
| <b>Table 7</b> Aryl-allyl coupling screen of various Grignard reagents.* .....  | 37 |
| <b>Table 8</b> Concentration study optimization table. ....   | 37 |
| <b>Table 9</b> Determined $\Delta\delta^{\text{SR}}$ and list data from most positive to most negative .....  | 45 |

## LIST OF FIGURES

|   |    |
|---|----|
| <b>Figure 1</b> Malaria life-cycle with temporal sequence. The <i>Plasmodium</i> parasite has three stages of development, a human liver stage, an erythrocytic stage (human blood cell) and an exogenous vector stage within <i>Anopheles</i> mosquitoes. <sup>5</sup>   | 2  |
| <b>Figure 2</b> Artemisinin ( <b>1A</b> ) and Chloroquine ( <b>1B</b> )   | 4  |
| <b>Figure 3</b> Macrolides belonging to bromophycolide family (A-I, S) extracted from Fijian red macro algae <i>C. serratus</i> . <sup>10a, 11, 13</sup>  | 6  |
| <b>Figure 4</b> <i>C. serratus</i> callophycoic acids and callophycols.   | 8  |
| <b>Figure 5</b> Diterpene benzoate lactone macrocyclic natural products associated with bromophycolide family extracted from Fijian red macro algae <i>C. serratus</i> . <sup>13, 15</sup>  | 10 |
| <b>Figure 6</b> Image features semi-synthetic derivatives from heme crystallization MOA study with chloroquine resistant <i>P. falciparum</i> inhibitory concentration values. Modifications from semi-synthesis are highlighted in red. FP = Fluorescent appendage. <sup>13,15</sup>   | 12 |
| <b>Figure 7</b> Bromophycolide D synthetic overview. <sup>20</sup>  | 15 |
| <b>Figure 8</b> Snyder's Reagent (BDSB) <sup>1</sup>  | 16 |
| <b>Figure 9</b> Mechanistic description for BDSB polyene electrophilic $\pi$ -cyclization   | 17 |
| <b>Figure 10</b> Modular approach to the synthesis of bromophycolides P, Q, and U. The macrolide is sectioned off into three pieces so conditions can be optimized individually. Upon completion, the segments will be joined. The cyclohexyl ring (A, red) is using a descriptor to symbolize that selective olefination can access the bromophycolides P, Q, and U. | 20 |
| <b>Figure 11</b> Modular approach used to access Callophycolide A, a <i>C. serratus</i> natural product. Methods utilized and optimized using this route are applicable to accessing other pertinent members of the bromophycolide family.  | 20 |
| <b>Figure 12</b> Retrosynthesis for the formation of the cyclohexyl unit of Bromophycolides P, Q, and U   | 22 |
| <b>Figure 13</b> Synthetic outline featuring substrates screened for formation of the cyclohexyl moiety (A, red). Blue and green are used to indicate attachment points to form macrolide ( <b>Figure 10</b> ).   | 23 |
| <b>Figure 14</b> Experimental data for the synthesis of cyclohexyl (A, red, <b>Figure 10</b> ) precursors. <sup>1, 22-23</sup>  | 24 |
| <b>Figure 15</b> Description of conditions used to functionalize the allylic "Y" position (green).  | 27 |

|  |    |
|--|----|
| <b>Figure 16</b> Most productive route to form cyclohexyl moiety for bromophycolide scaffold. <sup>1-2, 23</sup> .....   | 28 |
| <b>Figure 17</b> Mechanistic description of the product distribution for Swern elimination conditions listed in <b>Table 5</b> . .....   | 30 |
| <b>Figure 18</b> Retrosynthesis for the connection of aryl and terpene units.....  | 31 |
| <b>Figure 19</b> Scheme outlining initial attempts to access precursors for Stillie and Suzuki aryl-allyl cross coupling. <sup>29, 30</sup> .....  | 32 |
| <b>Figure 20</b> Model system for aryl-allyl cross-coupling via <i>in situ</i> generated magnesate complex. <sup>31, 32</sup> .....  | 32 |
| <b>Figure 21</b> Scheme outlining initial attempts towards accessing aryl-allyl cross coupled products for target bromophycolides and callophycolide A. ....   | 33 |
| <b>Figure 22</b> Scheme illustrates initial conditions for accessing the desired geranyl-aryl coupled product. Protection of the benzoate hydroxyl entailed the use of a methyl ether to prevent the protecting group from migration. ....   | 34 |
| <b>Figure 23</b> Scheme for allyl-aryl coupling with optimal conditions quenched with D <sub>2</sub> O to determine if the aryl organometallic complex was forming compound <b>71</b> upon deprotonation of an acidic proton within the desired product, <b>70</b> . No deuterium was observed to be incorporated into compound <b>70</b> . .... | 38 |
| <b>Figure 24</b> Sequence of steps leading to key intermediate ( <b>75</b> , point of divergence) for the synthesis of bromophycolide P, Q, U and callophycolide A. ....   | 38 |
| <b>Figure 25</b> Plan for modular divergent synthesis of bromophycolides P, Q, U, and callophycolide A. ....   | 39 |
| <b>Figure 26</b> Initial scheme for the formation of the linalool fragment, precursor for callophycolide A <sup>33</sup> . ....  | 40 |
| <b>Figure 27</b> Linalool epoxide protecting group screen precursors <sup>34, 35</sup> .....   | 40 |
| <b>Figure 28</b> Retrosynthesis for sulfone stabilized anionic ring opening .....  | 41 |
| <b>Figure 29</b> Model reaction and proof of concept for the sulfone stabilized anionic epoxide ring opening transformation <sup>36</sup> .....  | 42 |
| <b>Figure 30</b> Initial attempts to apply Trost's chemistry to <i>C. serratus</i> natural product point of divergence precursor, compound <b>75</b> .....   | 42 |
| <b>Figure 31</b> Linalool epoxide protecting group test reactions with model sulfone <b>87</b> .....   | 43 |
| <b>Figure 32</b> Attempt at forming callophycolide A precursor using sulfone, <b>75</b> , and benzyl protected linalool epoxide, <b>84</b> .....   | 43 |



|   |    |
|---|----|
| <b>Figure 33</b> Synthetic route to accessing the pyran module for bromophycolides P, Q, and U <sup>37, 39</sup> .....  | 44 |
| <b>Figure 34</b> Mosher ester formation for <sup>1</sup> H NMR analysis to confirm the correct stereochemistry of diol ( <b>102</b> ) formed via Sharpless asymmetric dihydroxylation <sup>38</sup> ..... | 44 |
| <b>Figure 35</b> Alternative route for accessing the pyran system for targets bromophycolide P, Q, and U. ....  | 46 |
| <b>Figure 36</b> Possible methods for desulfurization of callophycolide A precursor <sup>40, 41</sup> .....   | 47 |
| <b>Figure 37</b> Final steps towards the completion of the synthesis of callophycolide A. The methods applied to access this target should be transferrable to providing bromophycolides P, Q and U. .... | 47 |
| <b>Figure 38</b> HNMR of <b>38</b> .....  | 71 |
| <b>Figure 39</b> HNMR of <b>36</b> .....  | 72 |
| <b>Figure 40</b> HNMR of <b>43</b> .....  | 73 |
| <b>Figure 41</b> HNMR of <b>44</b> .....  | 74 |
| <b>Figure 42</b> HNMR of <b>47</b> .....  | 75 |
| <b>Figure 43</b> CNMR of <b>47</b> .....  | 76 |
| <b>Figure 44</b> HNMR of <b>46</b> .....  | 77 |
| <b>Figure 45</b> CNMR of <b>46</b> .....  | 78 |
| <b>Figure 46</b> HNMR of <b>55</b> .....  | 79 |
| <b>Figure 47</b> CNMR of <b>55</b> .....  | 80 |
| <b>Figure 48</b> HNMR of <b>54</b> .....  | 81 |
| <b>Figure 49</b> CNMR of <b>54</b> .....  | 82 |
| <b>Figure 50</b> HNMR of <b>56</b> .....  | 83 |
| <b>Figure 51</b> CNMR of <b>56</b> .....  | 84 |
| <b>Figure 52</b> HNMR of <b>60</b> .....  | 85 |
| <b>Figure 53</b> CNMR of <b>60</b> .....  | 86 |
| <b>Figure 54</b> HNMR of <b>62</b> .....  | 87 |

|                                   |     |
|-----------------------------------|-----|
| <b>Figure 55 CNMR of 62</b> ..... | 88  |
| <b>Figure 56 HNMR of 64</b> ..... | 89  |
| <b>Figure 57 CNMR of 64</b> ..... | 90  |
| <b>Figure 58 HNMR of 65</b> ..... | 91  |
| <b>Figure 59 CNMR of 65</b> ..... | 92  |
| <b>Figure 60 HNMR of 66</b> ..... | 93  |
| <b>Figure 61 CNMR of 66</b> ..... | 94  |
| <b>Figure 62 HNMR of 67</b> ..... | 95  |
| <b>Figure 63 CNMR of 67</b> ..... | 96  |
| <b>Figure 64 HNMR of 68</b> ..... | 97  |
| <b>Figure 65 HNMR of 69</b> ..... | 98  |
| <b>Figure 66 CNMR of 69</b> ..... | 99  |
| <b>Figure 67 HNMR of 70</b> ..... | 100 |
| <b>Figure 68 CNMR of 70</b> ..... | 101 |
| <b>Figure 69 HNMR of 73</b> ..... | 102 |
| <b>Figure 70 CNMR of 73</b> ..... | 103 |
| <b>Figure 71 HNMR of 75</b> ..... | 104 |
| <b>Figure 72 CNMR of 75</b> ..... | 105 |
| <b>Figure 73 HNMR of 83</b> ..... | 106 |
| <b>Figure 74 CNMR of 83</b> ..... | 107 |
| <b>Figure 75 HNMR of 84</b> ..... | 108 |
| <b>Figure 76 CNMR of 84</b> ..... | 109 |
| <b>Figure 77 HNMR of 85</b> ..... | 110 |
| <b>Figure 78 CNMR of 85</b> ..... | 111 |
| <b>Figure 79 HNMR of 92</b> ..... | 112 |

|   |     |
|---|-----|
| <b>Figure 80</b> HNMR of <b>101</b> ..... | 113 |
| <b>Figure 81</b> CNMR of <b>101</b> ..... | 114 |
| <b>Figure 82</b> HNMR of <b>103</b> ..... | 115 |
| <b>Figure 83</b> CNMR of <b>103</b> ..... | 116 |

## LIST OF SYMBOLS AND ABBREVIATIONS

|                      |   |
|----------------------|---|
| BDSB                 | bromodiethylsulfonium bromopentachloroantimonate(V) |
| MRSA                 | methicillin-resistant <i>Staphylococcus aureus</i>  |
| VREF                 | vancomycin-resistant <i>Enterococcus faecium</i>    |
| <i>P. falciparum</i> | <i>Plasmodium falciparum</i>                        |
| <i>P. vivax</i>      | <i>Plasmodium vivax</i>                             |
| ACTs                 | artemisinin combination treatments                  |
| CCTs                 | chloroquine combination treatments                  |
| <i>C. serratus</i>   | <i>Callophycus serratus</i>                         |
| DESI                 | desorption electrospray ionization                  |
| LC-MS                | liquid chromatography-mass spectrometry             |
| IC <sub>50</sub>     | half maximal inhibitory concentration               |
| μM                   | micromolar = 10 <sup>-6</sup> mole/liter            |
| MOA                  | mode of action                                      |
| FP                   | fluorescent appendage                               |
| SAR                  | structure activity relationship                     |
| π                    | pi  |
| TBCO                 | 2,4,4,6-tetrabromo-2,5-cyclohexadienone             |
| NBS                  | <i>N</i> -bromosuccinimide                          |
| DCM                  | dichloromethane                                     |
| mmol                 | millimole = 10 <sup>-3</sup> moles                  |
| M                    | mole/ liter   |
| S <sub>N</sub> 2     | bimolecular nucleophilic substitution               |
| THP                  | tetrahydropyran                                     |

|                     |   |
|---------------------|---|
| Ac                  | acetate   |
| Ts                  | tosylate  |
| TFAA                | trifluoroacetic anhydride                           |
| TEA                 | triethylamine                                       |
| DMAP                | 4-(dimethylamino)pyridine                           |
| TBHP                | <i>tert</i> -butyl hydroperoxide                    |
| <sup>1</sup> H-NMR  | proton nuclear magnetic resonance                   |
| <sup>13</sup> C-NMR | carbon nuclear magnetic resonance                   |
| TLC                 | thin-layer chromatography                           |
| TsCl                | tosyl chloride                                      |
| MsCl                | mesyl chloride                                      |
| DMSO                | dimethylsulfoxide                                   |
| THF                 | tetrahydrofuran                                     |
| DEPT                | distortionless enhancement by polarization transfer |
| COSY                | correlation spectroscopy                            |
| HSQC                | heteronuclear single quantum coherence              |
| R <sub>f</sub>      | retention factor                                    |
| EI                  | electron ionization                                 |
| m/z                 | mass-to-charge ratio                                |
| Å                   | angstrom  |
| TBTC                | tributyltin chloride                                |
| No rxn              | no reaction   |
| DMF                 | dimethylformamide                                   |
| CDI                 | 1,1'-carbonyldiimidazole                            |
| DBU                 | 1,8-diazabicyclo[5.4.0]undec-7-ene                  |

|         |                               |
|---------|-------------------------------|
| lit.    | literature                    |
| DCC     | N,N'-dicyclohexylcarbodiimide |
| TIPSCl  | triisopropylsilyl chloride    |
| TIPS    | triisopropylsilane            |
| t-Bu    | <i>tert</i> -butyl            |
| n-BuLi  | n-butyl lithium               |
| Hr      | hour                          |
| GBr     | geranyl bromide               |
| MgBr    | magnesium bromide             |
| w/o     | without                       |
| DIPT    | diisopropyl tartrate          |
| quant.  | quantitative                  |
| TsOH    | toluenesulfonic acid          |
| MeCN    | acetonitrile                  |
| DIPEA   | N,N-diisopropylethylamine     |
| MOMCl   | chloromethyl methyl ether     |
| MOM     | methoxymethyl acetal          |
| TBAI    | tetrabutylammonium iodide     |
| BnBr    | benzyl bromide                |
| Bn      | benzyl                        |
| DMPSCl  | dimethylphenylsilyl chloride  |
| DMPS    | dimethylphenylsilane          |
| eq      | equivalent                    |
| CSA     | camphorsulfonic acid          |
| MTPA-Cl | Mosher's acid chloride        |

|          |                               |
|----------|-------------------------------|
| ppm      | parts per million             |
| MHz      | mega hertz                    |
| $\Delta$ | difference; minus             |
| DMDO     | dimethyldioxirane             |
| boc      | <i>tert</i> -butoxy carbamate |
| g        | gram                          |

## SUMMARY

*Callophycus serratus*, a Fijian red macro alga, is the source of an interesting family of macrolides which have been elusive to the synthetic community. Sesquiterpene bromophycolides P, Q U, and related callophycolide A have highly conserved structural motifs which can be accessed through similar transformations therefore allowing for the application of a modular strategy. Formation of the modules features an expansion of electrophilic  $\pi$ -cyclizations with bromodiethylsulfonium bromopentachloroantimonate(V) (BDSB), and stereoselective Sharpless epoxidation and dihydroxylation conditions. Connection of the modules entail optimization of a magnesate assisted aryl-allyl coupling and a sulfone stabilized anion epoxide ring opening. The strategies explored can be applied to access a family of approximately 30 molecules. The development of a synthetic strategy is desirable due to notable anti-bacterial (MRSA and VREF), anti-malarial properties, and low natural abundance. Herein, I report results for the progress towards the total synthesis of bromophycolides P, Q, U, and callophycolide A utilizing a modular strategy.



# **CHAPTER 1**

## **1.1 Introduction**

Synthetic chemists make contributions in fields such as education, materials, and medicine by manipulating matter. We aim for controlled shuffling of electrons, enticing of charges, and exploitation of potentials to obtain coveted information or create useful substances. The power behind obtaining insight into the basis for chemical transformations propels the field forward, allowing for the development of novel reactions which produce compounds with a myriad of benefits. The work of synthetic chemists can lead to the mass production of beneficial therapeutic agents which have increased the life-span for humans by either being able to treat or eradicate potentially fatal ailments thereby increasing quality of life.

Many compounds that are pharmacologically relevant are born in nature and it is the task of the synthetic chemist to replicate what nature has evolved. There is a continual need for medicinal chemical innovation and the proof is in evolution. This can be described as a constant battle raging between humans and pathogens. Pathogens cause disease, people find a way to treat the disease, the pathogen evolves to evade treatment and the cycle continues. An example of an illness involved in the aforementioned battle which is currently plaguing tropical and sub-tropical regions is malaria. This thesis outlines synthetic strategies used to access natural products which contain anti-malarial and anti-bacterial properties against parasites and bacteria which have gained resistance to current medications.

## 1.2 Malaria

Malaria is a treatable and preventable illness that is transmitted by female *Anopheles* mosquitoes. The illness in humans is caused by four parasites, *Plasmodium falciparum*, *Plasmodium vivax*, *Plasmodium malariae*, and *Plasmodium ovale*. *P. falciparum* is the most lethal of the four and also one of the most common parasites, along with *P. vivax*.<sup>3</sup> Transmission is prevalent globally in tropical and sub-tropical regions posing a risk to over 3 billion people. In 2013, malaria was estimated to afflict over 2 million causing more than 600,000 fatalities.<sup>3d</sup> Africa is the most vulnerable region accounting for a mortality rate of 90%.<sup>3c, 3d</sup> African children below the age of 5 compose 78% of malaria deaths.<sup>3d</sup> Transmission to pregnant women is a major factor for maternal, perinatal, and neonatal mortalities in sub-Saharan Africa.<sup>4</sup>

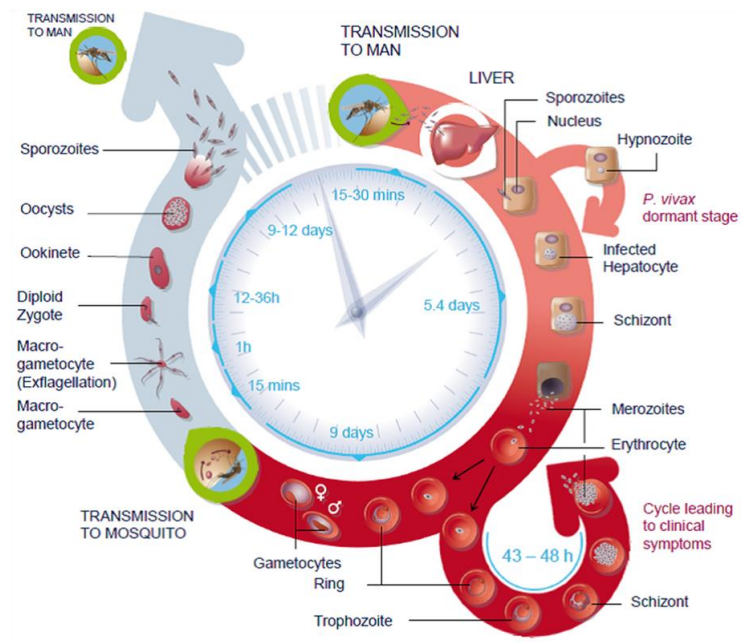


**Figure 1** Malaria life-cycle with temporal sequence. The *Plasmodium* parasite has three stages of development, a human liver stage, an erythrocytic stage (human blood cell) and an exogenous vector stage within *Anopheles* mosquitoes.<sup>5</sup>

Malaria has three distinct stages: a human liver stage, human blood stage, and an exogenous stage within the vector (mosquito) (Figure 1).<sup>3c, 5</sup> Infection begins as a consequence of being bitten by an *Anopheles* mosquito carrying *Plasmodium* parasites.<sup>3a, 3c, 3d, 5</sup> After the initial bite, the parasite undergoes an incubation period, within the human liver stage, which can last from 7-30 days.<sup>3b, 5-6</sup> If someone is administered anti-malarial prophylaxis, the incubation period can last for weeks or months.<sup>6</sup> The symptomatic stage of the illness occurs in the erythrocytic stage (human blood stage). Initial symptoms for uncomplicated malaria cases include: fever, chills, sweats, headache, body aches, nausea and vomiting.<sup>3b, 5-6</sup> If not treated within 24 hours of exhibiting these signs and symptoms, infections caused by *P. falciparum* can result in severe illness leading to death.<sup>3b</sup> Many aid groups are working towards the prevention of transmission of malaria. Awareness of vector breeding conditions and altering living spaces to avoid said conditions is one route. Organizations have also made insecticides and spatial repellants available, in addition to insecticide treated nets.<sup>3b, 3d, 7</sup> These methods are effective but not accessible to everyone in need. Other methods include intermittent and seasonal preventative treatments. In most cases, these preventative treatments consist of a full administration of anti-malarial medicines. These treatments are prioritized to high-risk groups of pregnant women and small children while seasonal treatments are administered during the rainy season. It also should be noted that as of July 2014, four vaccinations are in field clinical trials.<sup>3d</sup>

Despite preventative measures, transmission does still occur at staggering rates with tragic consequences. In many countries, the first line of defense upon parasitic invasion includes the use of artemisinin (**1A**) combination treatments (ACTs, Figure 2).

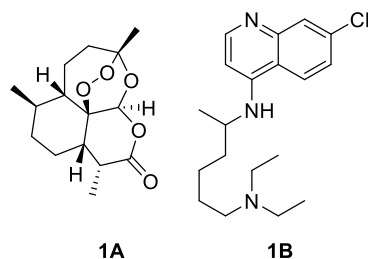


**Figure 2** Artemisinin (1A) and Chloroquine (1B)

ACTs are typically administered to children and can be distributed as pediatric doses. Chloroquine (**1B**) combination treatments (CCTs) are one of the preferred treatments for pregnant women (Figure 2).<sup>4</sup> It should be noted that these therapies are not limited to only being administered to the age groups mentioned. Combination treatments are used to avert the emergence or combat the presence of *Plasmodium* strains that are resistant to chemotherapy products.<sup>3d, 4</sup>

*Plasmodium* resistance to commonly used therapeutic agents was first observed in South-East Asia and now includes countries in Africa, South America and the West Indies.<sup>3d, 8</sup> Parasites are said to have gained resistance after diagnostic tools found evidence of *Plasmodium* after the third day of receiving treatment.<sup>3d</sup> *Plasmodium* resistance for both artemisinin and chloroquine have been shown to be linked to prescription practices, such as administration of monotherapies, subpar medication, and sub-therapeutic levels of combination treatments.<sup>3d, 8a, 8b</sup>

A retro-active case study of prescription practices in Nigeria illustrated that chloroquine resistance emerged as a result of private sector facilities not following World Health Organization dosage guidelines during a period of 1992-1997. CCTs were once the first line of defense in Nigeria. Now ACTs are prescribed for treatment since *P. falciparum*

clinical sensitivity decreased from 100% to 40%. Investigators from this study worry about the clinical shelf-life of ACTs if proper dosage guidelines are not followed.<sup>8b</sup>

Investigations into the efficacy of artemisinin in Guyana and Surinam highlighted the issue of counterfeit and poor quality medication, while also discussing the spreading of *Plasmodium* resistance via migrant workers.<sup>8a</sup> Spreading parasites that have built-up a resistance to some of the most potent drugs on the market is a real concern. A way of addressing single and multi-drug resistance is through the development of new treatments effective against *Plasmodium* insensitive to current clinical remedies. Many of the treatments currently utilized are derived from natural products.<sup>9</sup> Compounds derived from natural sources may hold the key for conquering *P. falciparum* that have adapted resistance to current treatments.

### 1.3 *Callophycus serratus* Terpenoids

In 2005, Kubanek and coworkers described the first known occurrence of brominated natural products consisting of a diterpene benzoate lactone (macrolide) scaffold. Bromophycolide A (**2**), bromophycolide B (**4**) and debromophycolide were initially isolated from Fijian red macro-alga, *Callophycus serratus* (Figure 3). Preliminary bio-activity analysis indicated that bromophycolides A and B exhibit moderate anti-bacterial activity and anti-fungal activity. Bromophycolide A is highlighted due to it being the most natural abundant (0.8% dry biomass) of the three terpenoids described from this initial investigation.<sup>10</sup> Further extractions of *C. serratus* the following year illuminated the presence of bromophycolides C-I (**3-8** and **10-11**) (Figure 3).<sup>11</sup>

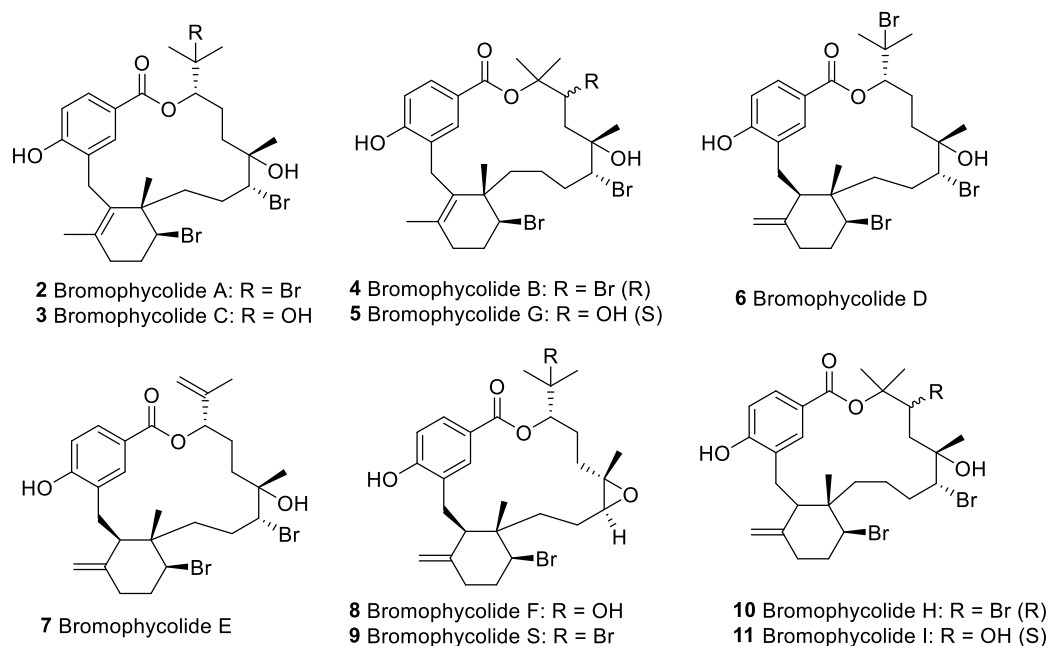


**Figure 3** Macrolides belonging to bromophycolide family (A-I, S) extracted from Fijian red macro algae *C. serratus*.<sup>10a, 11, 13</sup>

Delving deeper into determining the chemical constituents of *C. serratus*, investigators from the Kubanek lab isolated 10 more bio-active compounds termed callophycoic acids A-H (**12-19**) and callophycols A and B (**20** and **21**) (Figure 4). These compounds respectively contain diterpene-benzoic acid and diterpene-phenol scaffolds. These were the first examples of said scaffolds in macroalgae. These novel compounds also exhibited modest anti-malarial, anti-tumor, and anti-bacterial activity. The *C. serratus* samples used for the isolation and characterization of callophycoic acids and callophycols were collected at a different site in Fiji from *C. serratus* samples used for identification of bromophycolides. An interesting observation describes the lack of callophycoic acids and callophycols in samples containing bromophycolides, with the opposite observation also holding true. Therefore, where callophycoic acids and callophycols were present, bromophycolides were absent. This illustrates the possibility of having two chemotypes for *C. serratus*, or two cryptic species.<sup>12</sup>

Bio-assays were conducted to probe the biological roles of these secondary metabolites with the use of analytical mass-spectrometry. The bio-assays established that all of the bromophycolides known at this point (A-I, **2-11**, and debromophycolide A) and some callophycoic acids (C/**14**, G/**18** and H/**19**) inhibit the growth of pathogenic marine fungi *Lindra thalassiae*.<sup>12a</sup> Utilizing ambient ionization method, desorption electrospray ionization (DESI), researchers were able to map and quantify these secondary metabolites found on the surface of *C. serratus* with minimal or no sample preparation maintaining algal surface integrity during analysis.<sup>10b, 12a, 14</sup>

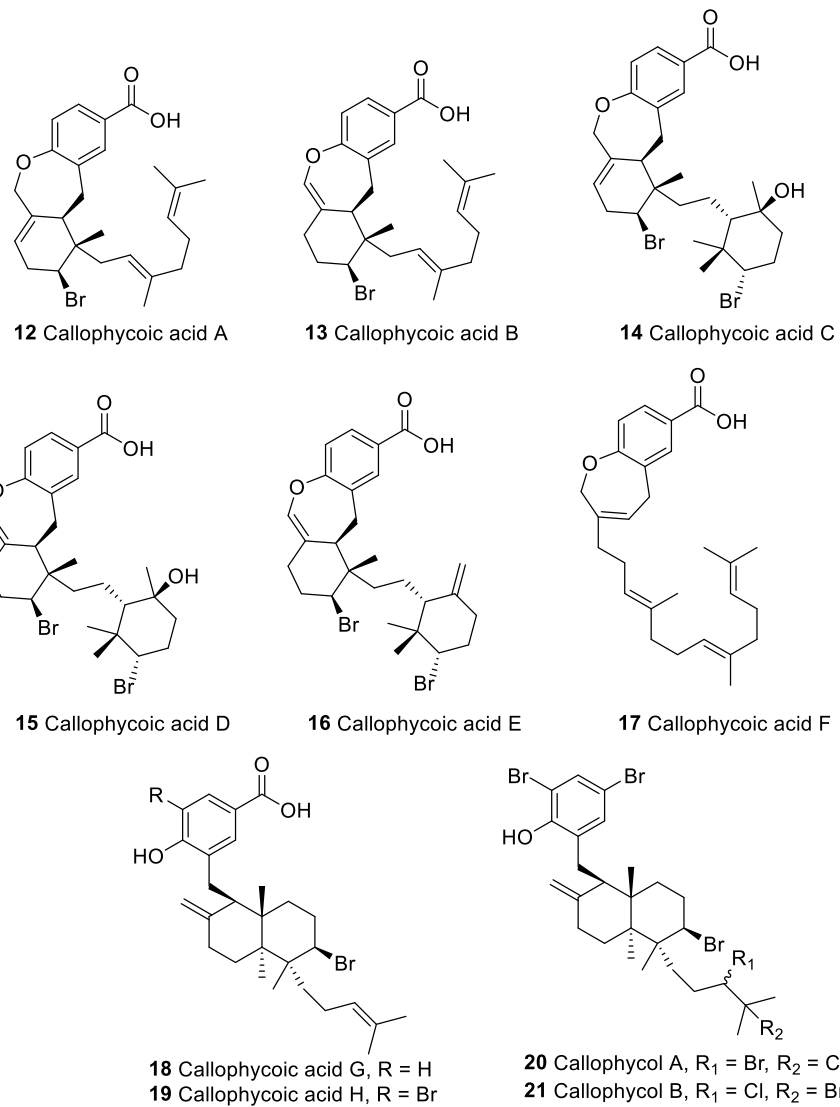


**Figure 4** *C. serratus* callophycoic acids and callophycols.



## 1.4 Bromophycolide Biological Activity

Continuing into the investigation for *C. serratus* secondary metabolites, members of the Kubanek lab isolated bromophycolides J-Q (**22-29**) (Figure 5). This additional study was prompted because LC-MS data from *C. serratus* extracts hinted that there might be more molecules not yet characterized. They speculated that these molecules contain a scaffold similar to the previously identified bromophycolides. Bromophycolides P and Q (**28** and **29**) illustrated a variant of the core structure consisting of a tetrahydropyran ring. They also exhibited potent anti-bacterial activity for methicillin-resistant *Staphylococcus aureus* (MRSA) and vancomycin-resistant *Enterococcus faecium* (VREF) bacteria, in addition to anti-malarial activity for chloroquine-resistant *Plasmodium falciparum* (Table 1).

Other members of the bromophycolide family which do not contain a rigid pyran unit have less anti-bacterial activity. Alluding to the possibility that the pyran unit is responsible for anti-bacterial potency. Results indicating potent anti-malarial activity, prompted the investigators to check *P. falciparum* inhibition for bromophycolides previously described.<sup>13a</sup> Comparison of inhibitory activity and the carbon frame showed that the macro-cycle is essential for anti-malarial activity. Bromophycolides are more potent than their analogs lacking a macro-cyclic scaffold, callophycols and callophycoic acids.<sup>12b</sup>

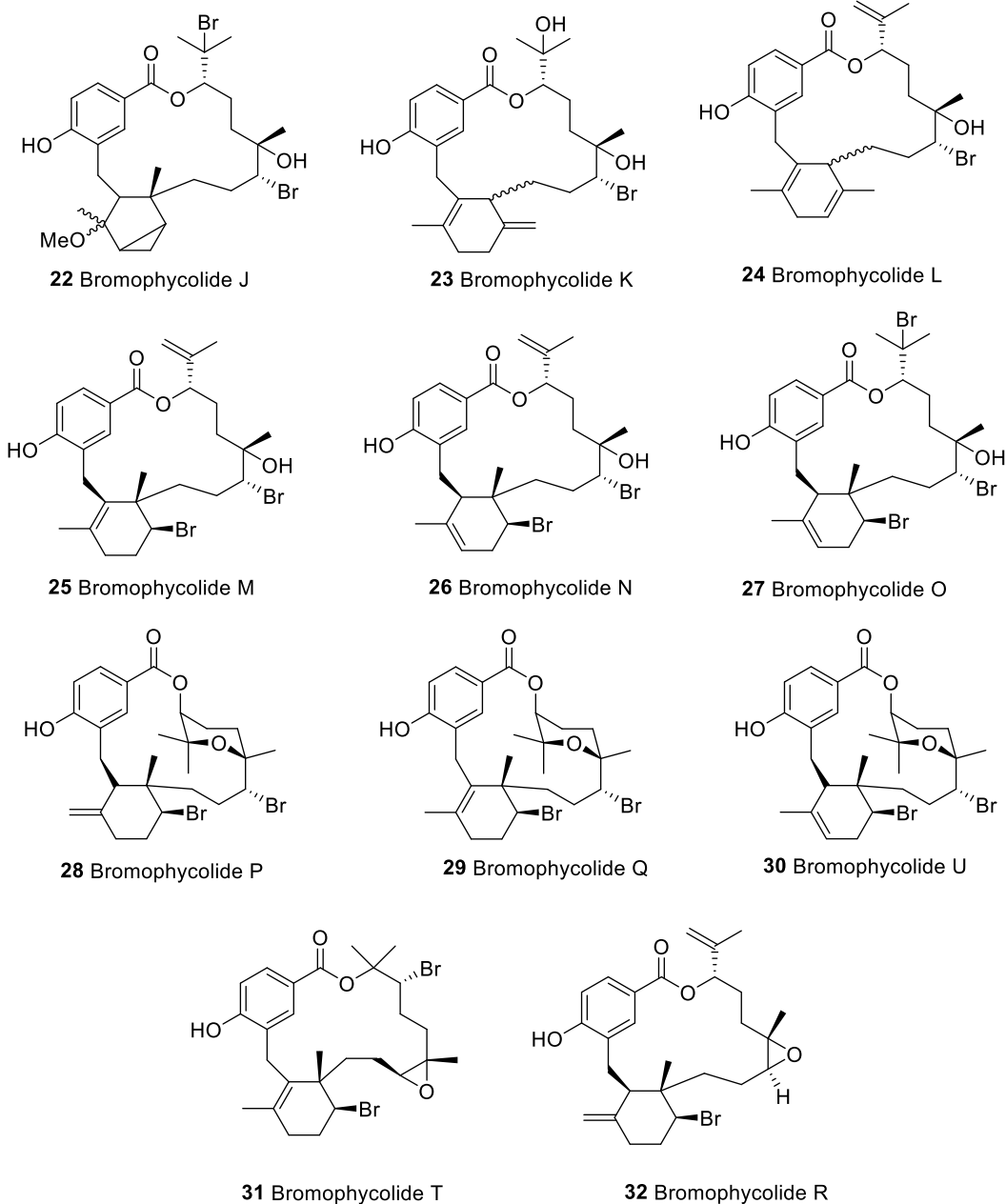


**Figure 5** Diterpene benzoate lactone macrocyclic natural products associated with bromophycolide family extracted from Fijian red macro algae *C. serratus*.<sup>13, 15</sup>

Four more bromophycolides (R/32, T/31, U/30) were reported in the subsequent year, expanding the array of bio-active molecules known for *C. serratus* (Figure 5). Notably, bromophycolide U, exhibited potent anti-malarial activity for chloroquine-

resistant *P. falciparum*. Sub-micromolar anti-bacterial activity for MRSA and VREF were also observed for bromophycolide U which also contains a pyran unit similar to previously identified bromophycolides P and Q that exhibited similar bio-activity.<sup>15a</sup> Of the bromophycolides identified, bromophycolides Q and U exhibit the widest range of pharmacological activity containing notable inhibitory potencies for chloroquine-resistant *P. falciparum* (anti-malarial), MRSA (anti-bacterial), and VREF (anti-bacterial). Bromophycolides P, Q, and U also exhibit a synthetically interesting scaffold of a di-terpene benzoate macrolide with a pyran moiety.<sup>13a, 15a</sup>

**Table 1** Bromophycolide family bio-activity profile featuring inhibitory concentration (IC<sub>50</sub>) values for chloroquine resistant *P. falciparum*, methicillin-resistant *Staphylococcus aureus* (MRSA), and vancomycin-resistant *Enterococcus faecium* (VREF).<sup>10a, 13, 15</sup>

| Bromophycolide | Anti-Malarial IC <sub>50</sub> (μM) | MRSA IC <sub>50</sub> (μM) | VREF IC <sub>50</sub> (μM) | Bromophycolide | Anti-Malarial IC <sub>50</sub> (μM) | MRSA IC <sub>50</sub> (μM) | VREF IC <sub>50</sub> (μM) |
|----------------|-------------------------------------|----------------------------|----------------------------|----------------|-------------------------------------|----------------------------|----------------------------|
| A              | 0.5                                 | 5.9                        | 5.9                        | L              | 9.8                                 | 8.2                        | 26                         |
| B              | 4.8                                 | 5.9                        | 3.0                        | M              | 0.5                                 | 6.7                        | 21                         |
| C              | 56                                  | -                          | -                          | N              | 1.4                                 | 7.2                        | 56                         |
| D              | 0.3                                 | -                          | -                          | O              | 1.4                                 | 8.9                        | 18                         |
| E              | 0.8                                 | -                          | -                          | P              | 2.9                                 | 1.4                        | 13                         |
| F              | 18                                  | -                          | -                          | Q              | 1.4                                 | 1.8                        | 5.8                        |
| G              | 14                                  | -                          | -                          | R              | 1.7                                 | >15                        | >15                        |
| H              | 0.9                                 | -                          | -                          | S              | 0.9                                 | >15                        | 3.8                        |
| I              | 2.5                                 | -                          | -                          | T              | 8.4                                 | >15                        | >15                        |
| J              | 2.7                                 | 80                         | 66                         | U              | 2.1                                 | 0.9                        | 0.9                        |
| K              | 44                                  | -                          | -                          |                |                                     |                            |                            |

Bromophycolide D is the most potent anti-malarial and bromophycolide A exhibits sub-micromolar activity along with being the most naturally abundant (Table 1).<sup>10a, 11, 13a</sup> Bromophycolide A is the most studied molecule in the family due to its relatively high natural abundance (0.8% dry bio-mass) and strong potency (IC<sub>50</sub> = 0.5 μM).<sup>10a, 13a, 15b, 16</sup> Studies were conducted on bromophycolide A and semi-synthetic derivatives to determine the mode of action (MOA) for anti-malarial activity (Figure 6). Co-localization studies

conducted with derivatives of bromophycolide A containing a fluorescent tag (**34** and **35**) illustrated that bromophycolide A disrupts heme crystallization while the parasite is in the erythrocytic stage (Figure 1).<sup>15b</sup> This is the same MOA for chloroquine based treatments.<sup>17</sup> Notably, some of the semi-synthetic derivatives also exhibit anti-malarial potency greater than bromophycolide D, the most potent in the family of compounds.<sup>15b</sup>

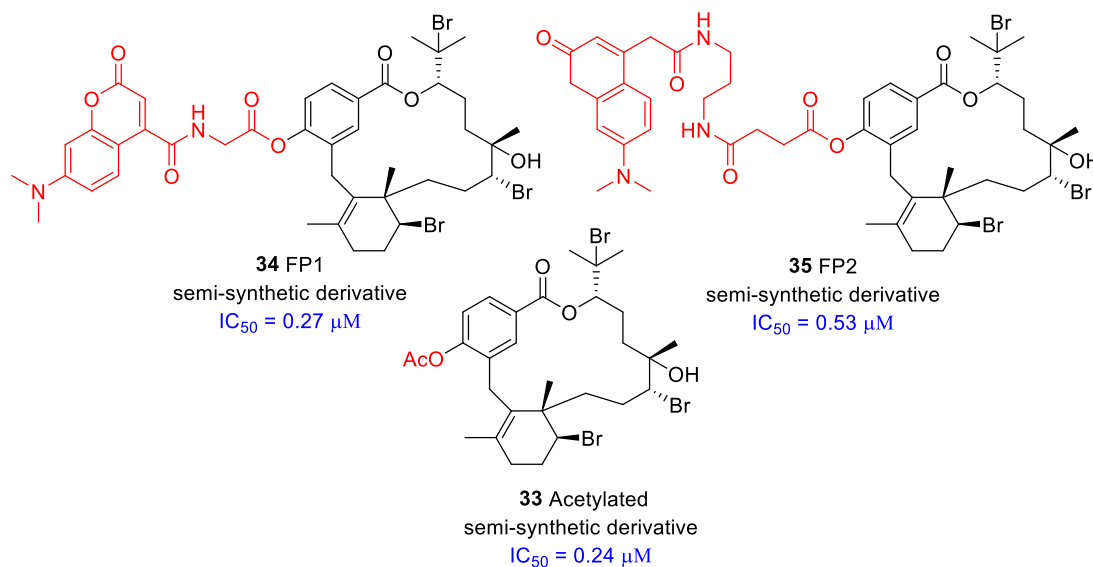


**Figure 6** Image features semi-synthetic derivatives from heme crystallization MOA study with chloroquine resistant *P. falciparum* inhibitory concentration values. Modifications from semi-synthesis are highlighted in red. FP = Fluorescent appendage.<sup>13,15</sup>

While in the erythrocytic stage (Figure 1), *P. falciparum* consumes heme in its food vacuole. The parasite forms crystalline heme (hemozoin) to circumvent toxicity of free heme.<sup>18</sup> Therefore, disruption of hemozoin formation has therapeutic benefits since it is detrimental to the life-cycle of the parasite. *P. falciparum* has developed a resistance to chloroquine based therapies by adapting integral membrane proteins that selectively lower the concentration of chloroquine in the parasites food vacuole where it is needed most.<sup>19</sup> Members of the bromophycolide family have demonstrated inhibition of *P. falciparum* that have evolved a resistance to chloroquine.<sup>13, 15</sup>

Pharmacokinetic profiles were established for bromophycolide A in pursuit of possible medicinal application. Murine studies showed that bromophycolide A is non-toxic and quickly eliminated from blood. Further tests established that bromophycolide A is metabolized by liver enzymes therefore limiting therapeutic bio-availability. Synthetic derivatives of bromophycolide A could address clearance issues pertaining to liver metabolism. Surprisingly, the lactone is not susceptible to degradation in the liver. Investigators suspect that hydroxylation within the liver, especially on the benzoate ring, contributes to degradation. Hence, they propose installation of electron withdrawing groups, such as halogens, to prevent said hydroxylations. Also, previous semi-synthetic SAR studies illustrated the importance of the phenolic group for anti-malarial activity. Researchers also proposed protection of the hydroxyl group so it is less susceptible to enzyme degradation in the liver.<sup>16</sup>

## 1.5 Thesis Overview

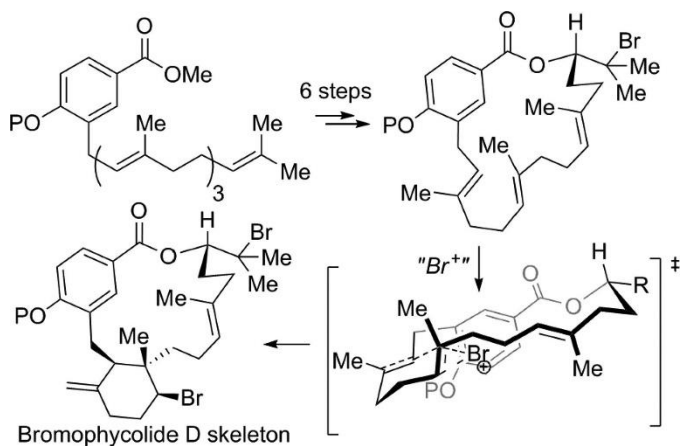
### Chapter 2

Previous attempts at the synthesis of the bromophycolide scaffold is presented in Chapter 2. A key transformation which allows for the construction of the cyclohexyl unit is a bromonium polyene electrophilic  $\pi$ -cyclization using Snyder's reagent, BDSB. Background information on the aforementioned transformation is presented. The synthetic strategy adopted for the synthesis of molecular targets bromophycolides P, Q, U and callophycolide A is also discussed. A modular strategy was adopted and a modular retrosynthetic plan is outlined for the reader. A significance of using a modular approach include facile formation of pharmacologically and synthetically interesting derivatives. Subsequent sections present results for module formation and methods explored for the joining of the modules to form the final completed structure.

## CHAPTER 2

### 2.1 Bromophycolide Synthetic Strategy

Structurally fascinating, the scaffold for the bromophycolide family has an almost intimidating allure for synthetic organic chemist. Consisting of multiple stereogenic centers (some of which are brominated), selective olefination, in some cases a pyran or epoxide moiety, and a highly conserved benzoate lactone system, this family is synthetically challenging to access with the efficiency nature has exhibited. Lin and coworkers (2011) have attempted to complete the synthesis of bromophycolides A and D (**2** and **6**) (Figure 7). They were able to access the carbon skeleton in six steps. However, completion was not attained due to difficulty in formation of the bromohydrin.<sup>20</sup>

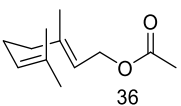
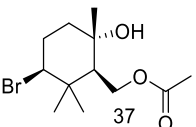
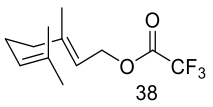
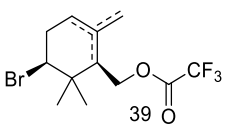


**Figure 7** Bromophycolide D synthetic overview.<sup>20</sup>

### 2.1.1 Bromonium Electrophilic $\pi$ -Cyclization

Additionally, for the first attempted synthesis of bromophycolide A yields were low for the bromonium electrophilic  $\pi$ -cyclization step using Snyder's reagent (bromodiethylsulfonium bromopentachloroantimonate, BDSB, **40**) (Figure 8).<sup>1, 20</sup> The transannular synthetic strategy adopted for the initial attempt was not modular and began with a benzoate geranylgeranyl system with subsequent formation of the macro-cycle before bromonium electrophilic  $\pi$ -cyclization.<sup>20</sup> Notably, yields for reactions of this class are inherently low with Snyder's bromonium source being the most efficient (Table 2 and Figure 8). BDSB is commercially available but can also be prepared rather easily.<sup>1</sup>

**Table 2** Adapted from Snyder's BDSB study, table shows comparison of bromonium sources for polyene electrophilic  $\pi$ -cyclizations.<sup>1</sup>

| Starting Material   | Product   | Yield [%] (Rxn Temp) (time)             |   |                             |                                |
|---|---|---|---|-----------------------------|--------------------------------|
|   |   | BDSB<br>CH <sub>3</sub> NO <sub>2</sub> | Br <sub>2</sub> /<br>AgBF <sub>4</sub> ,<br>CH <sub>3</sub> NO <sub>2</sub> | TBCO,<br>CH <sub>3</sub> CN | NBS/<br>PPh <sub>3</sub> , DCM |
|  |  | 80%<br>(0°C)<br>(5 min)                 | 22%<br>(0°C)<br>(5 min)   | <5%<br>(0°C)<br>(15 min)    | <5%<br>(-40°C)<br>(6 hrs)      |
|  |  | 56%<br>(25°C)<br>(5 min)                | <5%<br>(25°C)<br>(5 min)  | <5%<br>(25°C)<br>(15 min)   | <5%<br>(-40°C)<br>(6 hrs)      |

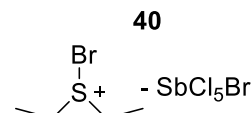


**Figure 8** Snyder's Reagent (BDSB)<sup>1</sup>

Despite the relative superior efficiency for BDSB as a bromonium source, the reaction for polyene systems does still have other limitations. The BDSB polyene electrophilic  $\pi$ -cyclization is dependent on concentration and requires dilute conditions (Table 3). Table 3 also illustrates how yields diminish when the reaction is scaled up, favoring formation of the major equatorial diastereomer. The scope presented in Snyder's



report is also limited. It lacks demonstration of incorporating functionality at the equatorial methyl group of the geminal system.<sup>1</sup> Addition of a functional group at this position could be useful for applications concerning the total synthesis of natural products.

**Table 3** Adapted from Snyder's BDSB study, table shows concentration study for BDSB model system geranyl acetate. Image also provides description of diastereomeric products.<sup>1</sup>

36  $\xrightarrow[0^\circ\text{C}, 5\text{ min}]{\text{BDSB, CH}_3\text{NO}_2}$  37 Major, OH equatorial      41 Minor, OH axial

| Entry | Scale [mmol] | Conc. [M] | BDSB equiv. | Yield [%] | d.r.  |
|-------|--------------|-----------|-------------|-----------|-------|
| 1     | 0.1          | 0.100     | 1.0         | 80        | 3.8:1 |
| 2     | 0.5          | 0.100     | 1.0         | 61        | 4.3:1 |
| 3     | 0.5          | 0.025     | 1.0         | 70        | 4.7:1 |
| 5     | 0.5          | 0.025     | 1.1         | 74        | 4.3:1 |
| 6     | 0.5          | 0.010     | 1.0         | 78        | 5.1:1 |
| 7     | 0.5          | 0.010     | 1.1         | 84        | 5.0:1 |
| 8     | 5.0          | 0.010     | 1.1         | 75        | 5.3:1 |

## 2.1.2 Objective

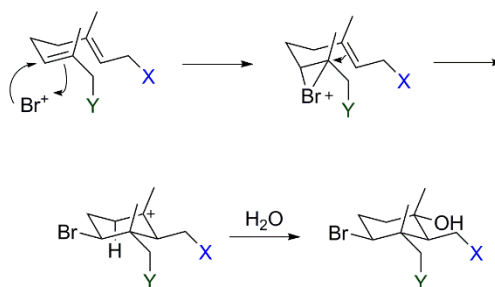


**Figure 9** Mechanistic description for BDSB polyene electrophilic  $\pi$ -cyclization

Despite the pitfalls concerning polyene electrophilic  $\pi$ -cyclizations, the transformation is synthetically useful. Figure 9 is an illustration of a general mechanism. Stereochemistry is established via adoption of a chair-like transition for bromonium

addition. Equatorial bromination and hydration occurs as a result of a syn-periplanar orbital alignment. Considering these limitations, the objective of this thesis is reporting progress on the total synthesis of bromophycolides P, Q, U, and derivatives incorporating a methodology development to increase the scope of substrates for BDSB polyene electrophilic  $\pi$ -cyclization.

Extracts of bromophycolides P, Q, and U (**28-30**) exhibit notable inhibition for chloroquine resistant *P. falciparum*. **29** and **30** also exhibit potent inhibition for MRSA, and VREF. Analysis of synthetic bromophycolides P, Q, and U should exhibit the same bio-activity as their naturally occurring counterparts. Synthetic derivatives of these natural products obtained via utilization of a modular approach will add to a bio-activity profile which currently is composed of information obtained from natural extracts and semi-synthetic derivatives. Additionally, structure activity relationship (SAR) studies will also be conducted on synthetic bromophycolides P, Q, U, and derivatives.

### 2.1.3 Significance- Modular Approach

The rise of pathogens which have evolved resistance to commonly used therapeutic agents is indicative of a need for the development of new compounds effective against pathogens insensitive to therapies on the market.<sup>3d, 4, 8-9, 13b, 21</sup> Bromophycolides with a pyran incorporated into their scaffold (especially bromophycolides Q and U) have exhibited notable inhibitory potency chloroquine resistant *P. falciparum*, MRSA and VREF. Natural abundance for these bio-active compounds are low: bromophycolide U (0.0049% of dry biomass), bromophycolide Q (0.023% of dry biomass), bromophycolide P (0.092% of dry biomass).<sup>13, 15a</sup> These bromophycolides have a broad pharmacological

profile, low natural abundance, and an intriguing molecular scaffold. Consideration of these factors exhibit the necessity for pursuing the completion of a synthetic route to efficiently access gram-scaled quantities of the listed bromophycolides.

A modular approach for the synthesis of bromophycolides P, Q, and U allows for formation of derivatives (Figure 10). A similar approach was utilized to access Callophycolide A, a *C. serratus* natural product which contains similar structural motifs as the target bromophycolides P, Q, and U (Figure 11). Callophycolide A does not contain the same bio-activity as bromophycolides P, Q, and U. However, methods used to access this less complex scaffold are applicable to the synthesis of desirable bromophycolides with useful bio-active properties. Derivatives can be screened for bio-activity and SAR studies conducted. The three bromophycolides (P, Q and U) which this study focuses on have scaffolds which are highly conserved. The only difference between the three structures is the location of the alkene associated with the cyclohexyl moiety. Selective olefination and formation of the cyclohexyl group allows access to other *C. serratus* terpenoids, therefore expanding the scope of this synthetic endeavor. Optimization of BDSB polyene electrophilic  $\pi$ -cyclization by introduction of functionality to expand the range for this useful transformation is also advantageous.

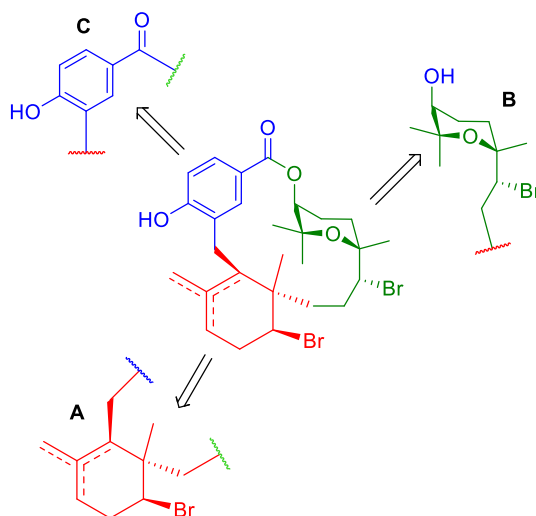


**Figure 10** Modular approach to the synthesis of bromophycolides P, Q, and U. The macrolide is sectioned off into three pieces so conditions can be optimized individually. Upon completion, the segments will be joined. The cyclohexyl ring (A, red) is using a descriptor to symbolize that selective olefination can access the bromophycolides P, Q, and U.

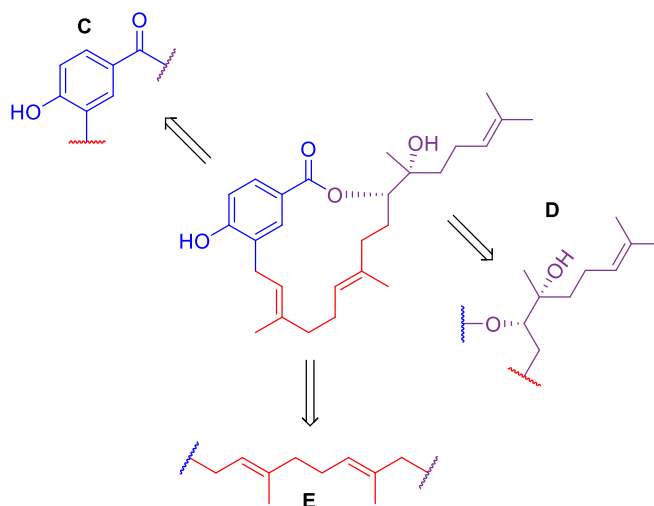


**Figure 11** Modular approach used to access Callophycolide A, a *C. serratus* natural product. Methods utilized and optimized using this route are applicable to accessing other pertinent members of the bromophycolide family.

## 2.2 Results

Recognizing the versatility of utilizing a modular approach, the scaffold for bromophycolides P (**28**), Q (**29**), U (**30**) was divided into three parts (Figure 10). The modules and attachments points for precursors are color coded in an attempt to clarify structural modifications and keep sight of the end-game objective. Upon consideration of possible disconnections to obtain viable precursors with compatible transformations, it becomes evident that the benzoate moiety (blue) can link to the cyclohexyl (**A**, red) via aryl-alkyl Suzuki coupling. The benzoate (**C**, blue) can also link to the pyran (**B**, green) via an esterification, possibly under Steglich conditions. While the cyclohexyl (red) and pyran (green) can either undergo alkyl-alkyl coupling (recently developed chemistry) or possibly an S<sub>N</sub>2 substitution.

### 2.2.1 Cyclohexyl Formation- Bromophycolides P, Q, and U

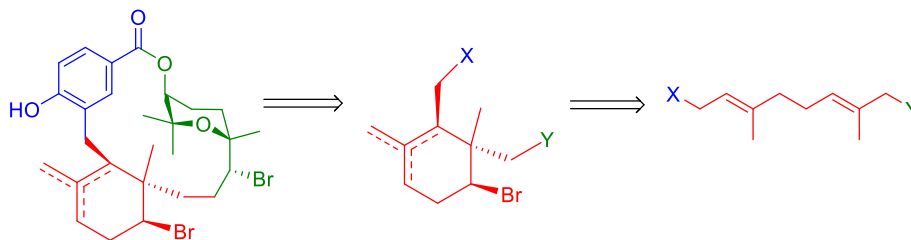


**Figure 12** Retrosynthesis for the formation of the cyclohexyl unit of Bromophycolides P, Q, and U

Strategies adopted and employed should be efficient, address asymmetric needs by induction of chirality, tolerant of functional groups (chemoselectivity), and regioselective when necessary. Figure 12 is an illustration of the retrosynthesis of the cyclohexyl module for target macrolides from terpene starting material. Figure 13 outlines the strategy used to access the cyclohexyl moiety (**A**, red). Beginning with commercially available geraniol (**42**), functionality will be introduced at position “X”. These groups (**43**, **36**, and **38**) are highlighted in blue to show connection to the benzoate unit (**C**).

Allylic oxidation of the model system, commercially available geranyl acetate (**36**), produces compound **44**. The geranyl acetate allylic alcohol is an ideal precursor for introduction of functionality at the “Y” position. Functional groups at the “Y” position are highlighted in green to indicate that it is the point of attachment to the pyran moiety (Figure 12, green). Compounds **45** – **49** in Figure 13 are the precursors for the bromonium electrophilic  $\pi$ -cyclization using Snyder’s reagent (**40**, Figure 8). Various functional groups were selected for both the “X” and “Y” position in order to investigate which system was most compatible with the strongly electrophilic bromonium source. Factors considered for compatibility would include tolerance to the transformation and increased yields. Compound **50** is an illustration of the general form for the cyclized product which will then

undergo selective elimination of the tertiary alcohol to form di- (**51**), tri- (**52**), or tetra-substituted (**53**) alkenes.

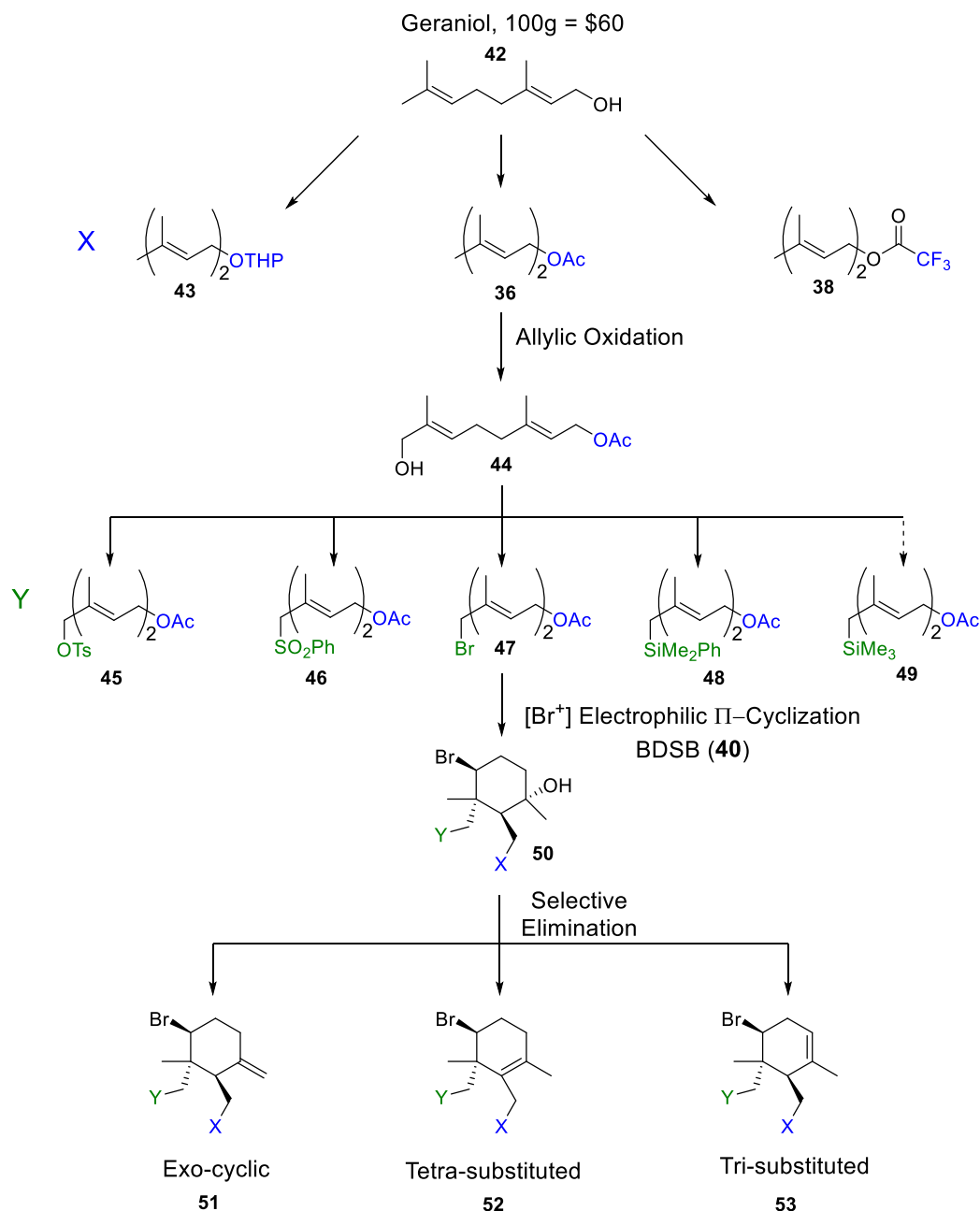


**Figure 13** Synthetic outline featuring substrates screened for formation of the cyclohexyl moiety (**A**, red). Blue and green are used to indicate attachment points to form macrolide (Figure 10).

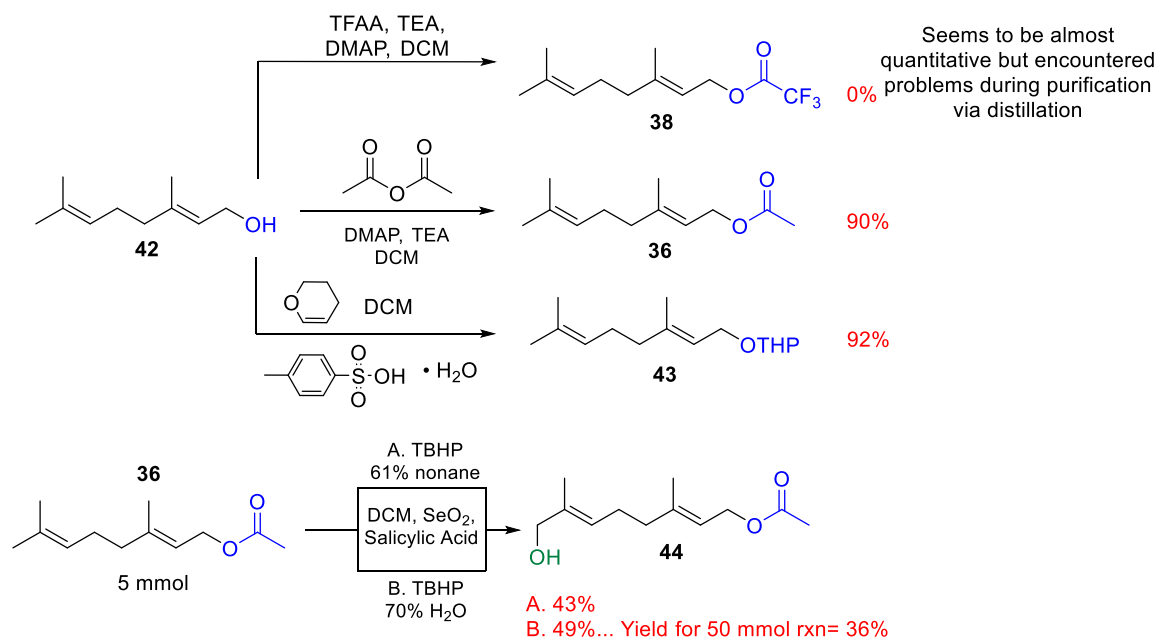


**Figure 14** Experimental data for the synthesis of cyclohexyl (A, red, Figure 10) precursors.<sup>1, 22-23</sup>

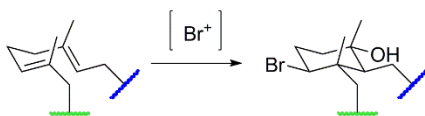
Conditions and yields for the introduction of various functional groups at the “X” position (blue) are provided in Figure 14. Deprotonation of **42** with triethylamine (TEA) and catalytic 4-(dimethylamino)pyridine (DMAP) in dichloromethane (DCM) then drop wise addition of trifluoroacetic anhydride (TFAA) produced compound **38**.<sup>1</sup> The product was bright pink (as described in literature), and <sup>1</sup>H-NMR of the crude showed almost full conversion to the desired product. However, efforts to purify the product via column chromatography (silica stationary phase) and vacuum distillation were unfruitful. Similar conditions were used for the synthesis of compound **36** (**42**, TEA, DMAP, and DCM). The acylating agent for this reaction was acetic anhydride.<sup>1</sup> Conversion to the product and isolation occurred smoothly with a 90% yield. 3,4-Dihydro-2H-pyran, *para*-toluenesulfonic acid monohydrate in DCM was combined with **42** to form *tetra*-hydropyran (THP) ether **43** in excellent yields (92%).<sup>22</sup>



Bromonium  $\pi$ -electrophilic cyclization was attempted with substrates **36** and **43**. Geranyl acetate (**36**) was selected as a model system since there is precedent for this transformation in the literature. Concentration studies were conducted to determine the optimal concentration to perform this reaction with the most amount of starting material (Table 4, entries 1-7). Electrophilic cyclization yields tend to diminish once the reaction is scaled up (Table 4, entry 8). To counter this limitation, the reaction must be extremely dilute. Table 4 entry 5 indicates the optimum concentration for scaling the reaction up without excessive yield decrease. Cyclization of **43**, resulted in degradation of the starting material (Table 4, entry 10). Specifically, the bromonium source was cleaving the THP ether and forming geraniol (**42**).

Due to tolerance for the BDSB cyclization, geranyl acetate (**36**), was selected for the continuation for the synthesis. The next step involved an allylic oxidation using selenium dioxide (SeO<sub>2</sub>), salicylic acid, DCM, and *t*-butyl hydrogen peroxide (TBHP) to form **44** (Figure 14).<sup>23</sup> The literature method was not clear as to what the TBHP was suspended in (nonane or water). Further investigation showed that better yields were slightly better accomplished using the water suspension (49% yield). Further investigation illustrated that yields diminish significantly to 36% when the reaction is conducted on a larger scale.

**Table 4** Bromonium  $\pi$ -electrophilic cyclization using Snyder's reagent (BDSB, **40**). Optimization table includes data for concentration dependence study in addition to results for the cyclization of substrates with variation at both terminal ends, "X" and "Y" position.<sup>1</sup>



| Entry     | Substrate              | Conc. [M] | Product       | Total Yield | Major                                       | Minor |
|-----------|------------------------|-----------|---------------|-------------|---|-------|
| <b>1</b>  | <br><b>36</b><br>1mmol | 0.02      | <br><b>37</b> | 69%         | 53%   | 16%   |
| <b>2</b>  | 1mmol                  | 0.03      | <b>37</b>     | 41%         | 41%   | 0%    |
| <b>3</b>  | 1mmol                  | 0.05      | <b>37</b>     | 54%         | 40%   | 14%   |
| <b>4*</b> | 1mmol                  | 0.05      | <b>37</b>     | 46%         | 46%   | 0%    |
| <b>5</b>  | 1mmol                  | 0.07      | <b>37</b>     | 58%         | 42%   | 16%   |
| <b>6*</b> | 1mmol                  | 0.07      | <b>37</b>     | 29%         | 29%   | 0%    |
| <b>7</b>  | 1mmol                  | 0.09      | <b>37</b>     | 38%         | 38%   | 0%    |
| <b>8</b>  | 129mmol                | 0.07      | <b>37</b>     | 35%         | 35%   | 0%    |
| <b>9</b>  | <br><b>47</b><br>1mmol | 0.01      | <br><b>54</b> | 35%         | Alcohol degrading to tri-substituted alkene |       |
| <b>10</b> | <br><b>43</b><br>1mmol | 0.01      | Degradation   | 0%          | 0%  | 0%    |
| <b>11</b> | <br><b>46</b><br>1mmol | 0.02      | <br><b>55</b> | 75%         | Alcohol degrading to tri-substituted alkene |       |

Conditions: BDSB (1.1 eq), Stirring for 5 minutes; \*Stirring for 10 minutes

Acquiring sufficient quantities of the allylic oxidation product of geranyl acetate (**44**) allowed for test reactions to be conducted to further modify said terminal position (Figure 15). Attempts to isolate **45** from **44** were unsuccessful after formation using TEA and *para*-toluenesulfonyl chloride (TsCl) in DCM. 2-D Thin-layer chromatography (TLC)

alludes to suspicion that the allylic tosylate is unstable on silica gel which resulted in degradation during column chromatography. Following a procedure from the literature, compound **47** was formed from **44** in excellent yields, 93%. This transformation involved generation of the mesylate *in situ* and subsequent S<sub>N</sub>2 displacement with lithium bromide.<sup>2</sup>

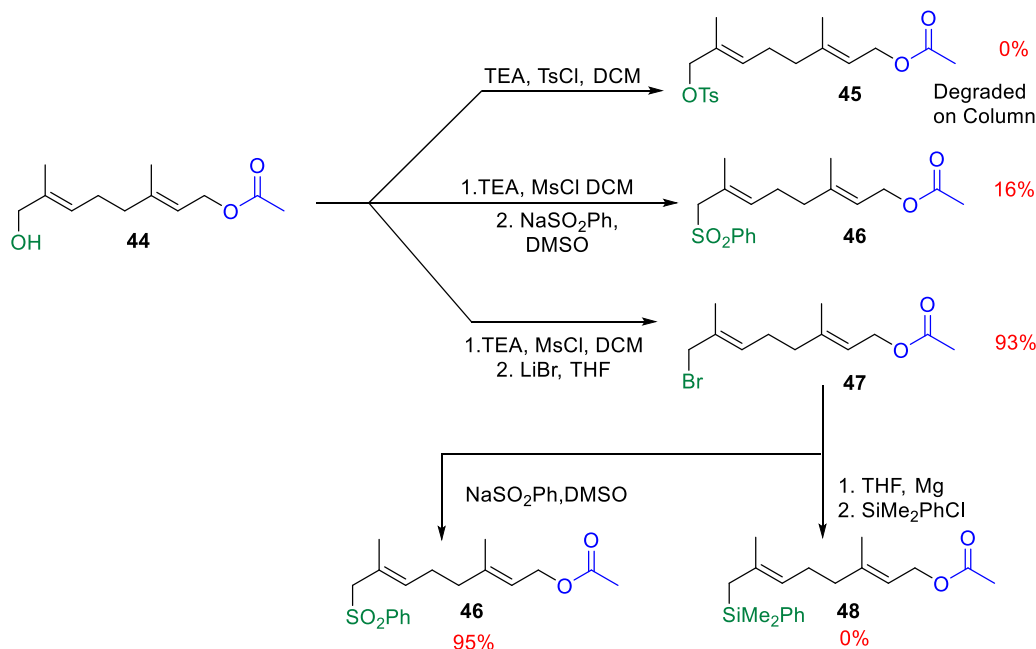


**Figure 15** Description of conditions used to functionalize the allylic “Y” position (green).<sup>2</sup>

Attempts to generate  $\pi$ -electrophilic cyclization substrate **46** using the same principles for acquiring substrate **47** resulted in low yields, 16% (Figure 15). Conversion to the allylic sulfone (**46**) was accomplished efficiently (95% yield) via a S<sub>N</sub>2 displacement of allylic bromine **47** with sodium sulfinate in dimethylsulfoxide. There is no known literature precedent for the formation of **46**. Accessing the allylic dimethylphenylsilane proved unsuccessful due to inability to form a Grignard from **47** (Figure 15). Various methods were tried to generate the Grignard including using different magnesium sources, treatment of the magnesium with 1 M HCl and ethanol, use of initiators such as crystalline

iodine, and consideration of weather conditions (preparation and reactions conducted on days with low humidity).

Successful acquisition of gram-scale quantities of substrates **47** and **46** allowed for test reactions to probe BDSB  $\pi$ -electrophilic cyclization reactivity. Subjecting allylic brominated substrate **47** to cyclization conditions resulted in formation of the alcohol which degrades to the tri-substituted alkene **54** with modest yields, 35% (Table 4, entry 9). Formation of cyclized sulfone **55** from substrate **46** was accomplished with relatively good yields, 75% (Table 4, entry 11). Similar to the allylic bromide system (**47**  $\rightarrow$  **54**), cyclization of the sulfone also produces the tri-substituted alkene. The tri-substituted alkene is found in target bromophycolide U. Considering the promising yields for formation of cyclized sulfone **55**, the synthetic strategy to access the bromophycolide cyclohexyl are outlined in Figure 16.

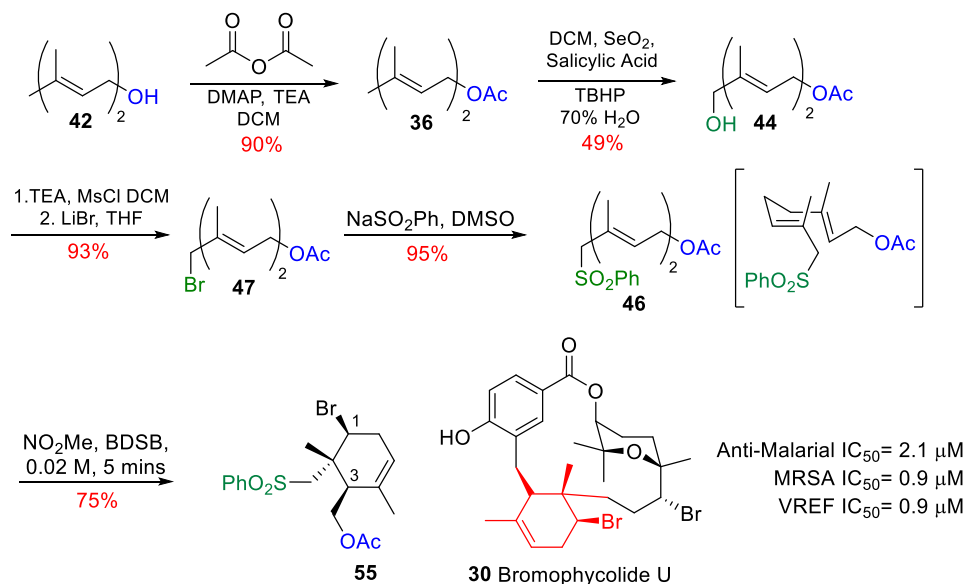
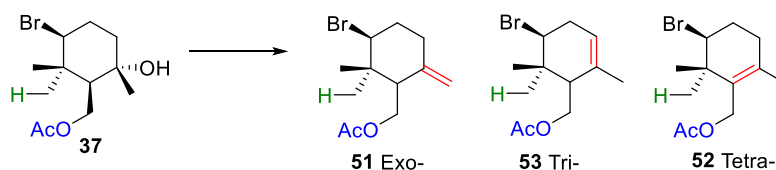


**Figure 16** Most productive route to form cyclohexyl moiety for bromophycolide scaffold.<sup>1-2, 23</sup>

As previously demonstrated in Table 4, geranyl acetate (**36**) is also used as a model system for probing selective tertiary alcohol elimination (Table 5). This elimination study was done in parallel with the determination of which terminal functional groups would be ideal for the bromonium  $\pi$ -cyclization. Initial attempts to use Swern oxidation conditions to facilitate the elimination resulted in diminished yields, 32%, and a less than ideal product distribution.<sup>24a</sup> Modifications to the conventional Swern oxidation to facilitate elimination includes significant increase of equivalence of oxalyl chloride ( $\text{COCl}_2$ ), DMSO and TEA.<sup>24b</sup> These modifications resulted in a significant increase in yield to 73% and a slight preference for the formation of the exo-cyclic alkene. When the alcohol is equatorial, the elimination favors formation of an exo-cyclic alkene (**51**). Figure 17 provides a mechanistic description for the product distribution noted in Table 5. When the alcohol is equatorial, the sulfur ylide is anti-periplanar to the geminal axial methyl. This desirable orbital overlap favors formation of the exo-cyclic alkene reflected in product distribution. **52** experiences allylic 1,2-strain ( $A^{1,2}$ ) and contains significant equatorial steric congestion which is reflected in the product distribution.

**Table 5** Results from selective tertiary alcohol elimination study.<sup>24</sup>



| Conditions   | Total Yield | Exo- | Tri- | Tetra- |
|--|-------------|------|------|--------|
| Swern Oxidation: 2.4eq ( $\text{COCl}_2$ ), 5eq TEA, 4.8eq DMSO    | 32%         | 1.4  | 1.6  | 1.0    |
| Swern Elimination: 5.3eq ( $\text{COCl}_2$ ), 24eq TEA, 9.5eq DMSO | 73%         | 3.2  | 1.1  | 1.0    |
| Amberlyst-15 dry, DCM (18 hrs)                                     | 24%         | 2.0  | 1.0  | 0.0    |
| Amberlyst-15 dry, 4Å DCM (18 hrs)                                  | 36%         | 4.5  | 8.0  | 1.0    |
| Amberlyst-15 dry, reflux, DCM (18 hrs)                             | 54%         | 1.0  | 3.0  | 0.0    |

Amberlyst-15 dry is a sulfonic acid based heterogeneous reusable catalyst which facilitates the dehydration of tertiary alcohols. This elimination has demonstrated selectivity for the tri-substituted olefin (**53**).<sup>24c</sup> Reactions seem to proceed to completion when analyzed via TLC (starting material seems to be fully consumed). However, yields are low (maximum yield: 54%) indicating that product is being lost along the way, probably during the work-up (Table 5). Some additional elimination methods include use of Burgess's reagent, mild Brønstead acids, Lewis Acids ( $\text{BF}_3 \cdot \text{Et}_2\text{O}$ ), and pyrolytic *syn*-elimination reactions (xanthate chemistry: Chugaev reaction).

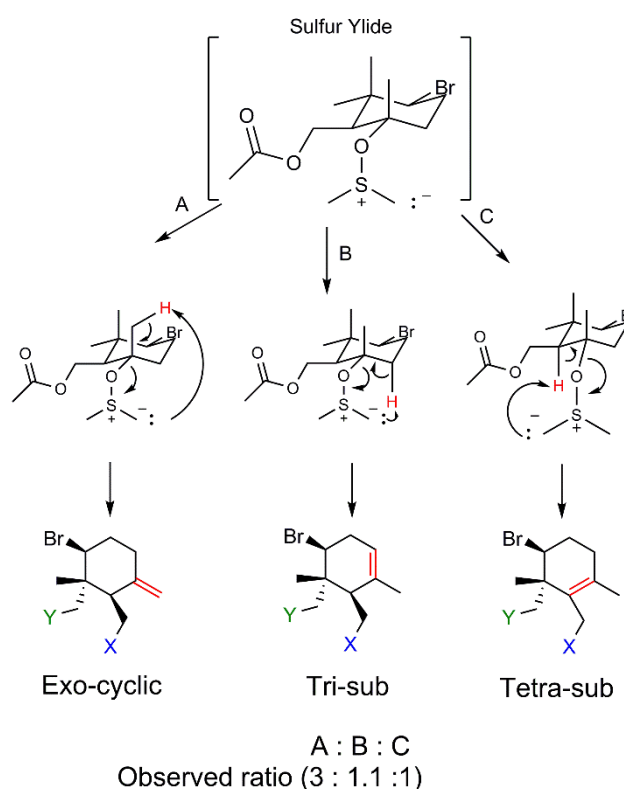


**Figure 17** Mechanistic description of the product distribution for Swern elimination conditions listed in Table 5.

### 2.2.2 Aryl-Allyl Cross-Coupling

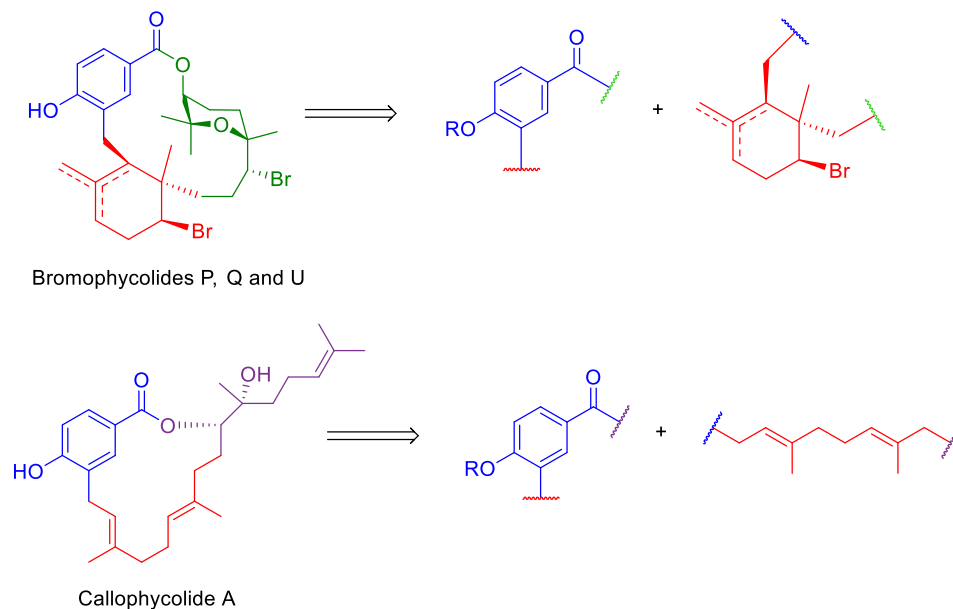


**Figure 18** Retrosynthesis for the connection of aryl and terpene units.

Continuing on the road towards accessing the scaffolds of bromophycolides P, Q, U and callophycolide A using the modular strategy outlined entailed determining a method for joining the benzoate and geranyl fragments (Figure 18). Three methods to perform the aforementioned aryl-allyl coupling were explored. Attempts to make geranyl substrates for Stille and Suzuki were explored but not fully developed either due to difficult preparation or avoidance of using highly toxic reagents which were difficult to purify.<sup>29, 30</sup> Figure 19 outlines initial attempts to produce geranyl stannane and geranyl pinacol boronate. Compound **57** was difficult to purify from residual tributyltin chloride (TBTC) and geranyl bromide via vacuum distillation after multiple attempts. Formation of **58** did not occur when subjected to reaction conditions and starting material was recovered.

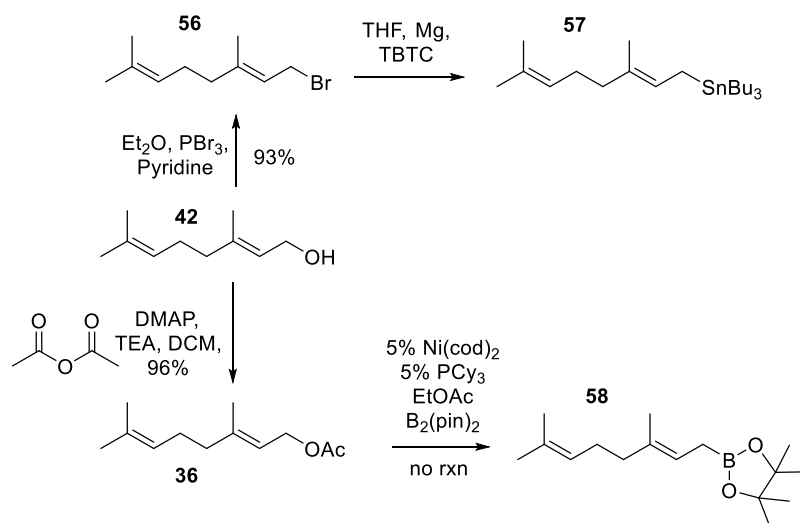


**Figure 19** Scheme outlining initial attempts to access precursors for Stillie and Suzuki aryl-allyl cross coupling.<sup>29, 30</sup>

Scouring the literature revealed a source for the desired aryl-allyl cross coupling using a magnesate complex generated from a Grignard and organolithiate. Pursuing this route was beneficial due to my ability to replicate the conditions outlined and my ability to optimize the transformation for systems pertinent to accessing *C. serratus* natural product scaffolds. The model system outlined in Figure 20 illustrates cross-coupling of *para*-bromo-*tert*-butyl benzoate (**60**) with allyl bromide (**61**) to provide compound **62** in decent yields, 51%. The magnesate complex allows for sufficient activation of the aryl bromide substrate and the presence of the *tert*-butyl group prevents nucleophilic addition to the ester.<sup>31, 32</sup>

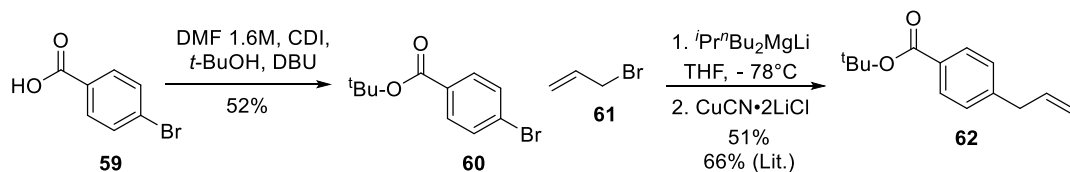


**Figure 20** Model system for aryl-allyl cross-coupling via *in situ* generated magnesate complex.<sup>31, 32</sup>



Successful acquisition of coupled product **62** in Figure 20 prompted the application of the transformation towards accessing coupled products which could be applied to the formation of natural product targets bromophycolides P, Q, U and callophycolide A. The two routes initially explored involved determination if the tert-butyl group was necessary for the prevention of nucleophilic addition to the ester. The sequence outlined in Figure 21 illustrates the formation of 4-hydroxymethylbromobenzoate **64**, 88% yield, and 4-hydroxy-tert-butylbromobenzoate **66**, 88% yield. Which were then protected with triisopropyl silane forming compounds **65** and **67** with quantitative recovery of the desired products. Conducting the aryl-allyl coupling with geranyl bromide and compound **65** resulted in an undecipherable mixture and not the desired product. Subjecting geranyl bromide and compound **67** resulted in migration of the triisopropyl silane protecting group, **68**, 89% yield. Considering the electronic implications of having a highly anionic charge adjacent to a silyl ether, it is not shocking that the migration occurred.

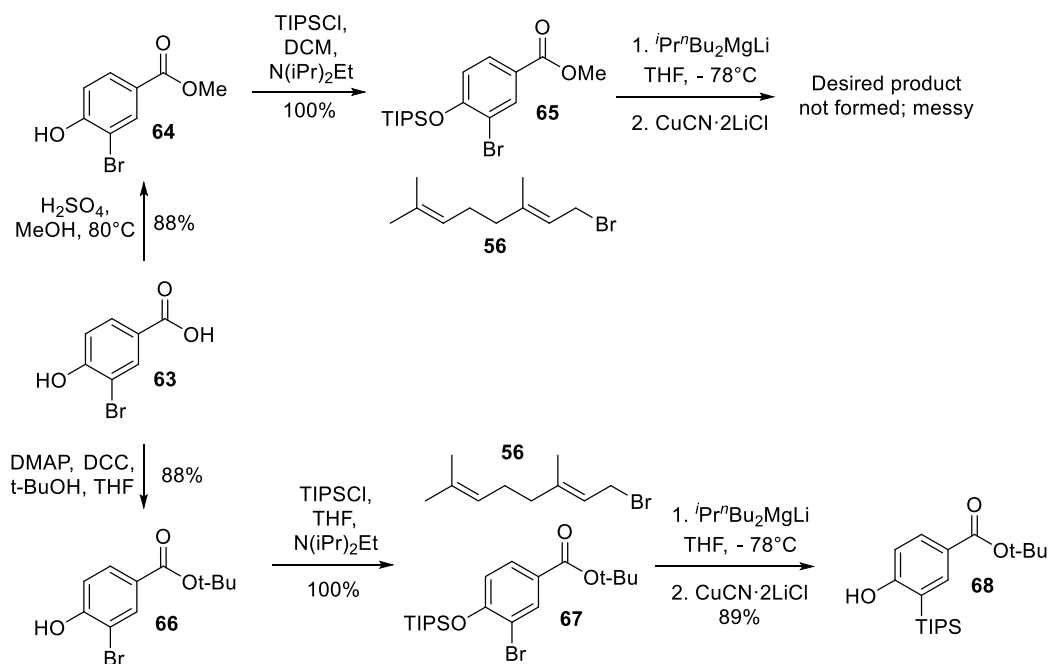


**Figure 21** Scheme outlining initial attempts towards accessing aryl-allyl cross coupled products for target bromophycolides and callophycolide A.

Migration of the TIPS protecting group (**68**, Figure 21) during the allyl-aryl coupling event was prevented with the use of a methyl ether protecting group in subsequent reactions. The methyl ether protecting group on the tert-butyl benzoate substrate (**69**, Figure 22) was obtained in excellent yield, 97%, after an evaluation of different conditions. Obtaining nearly quantitative yield for **69** required the use of a staggering 10 equivalence of methyl iodide with potassium carbonate in acetone. Subjecting **69** to the *in situ* generated magnesate complex in the presence of geranyl bromide (**56**) did finally provide the desired product which can be utilized to access natural product target bromophycolides P, Q, U and callophycolide A (Figure 22).

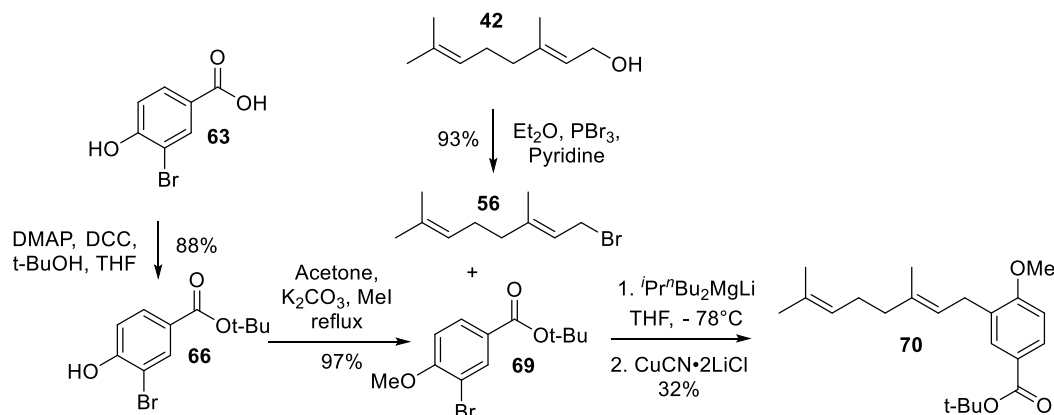


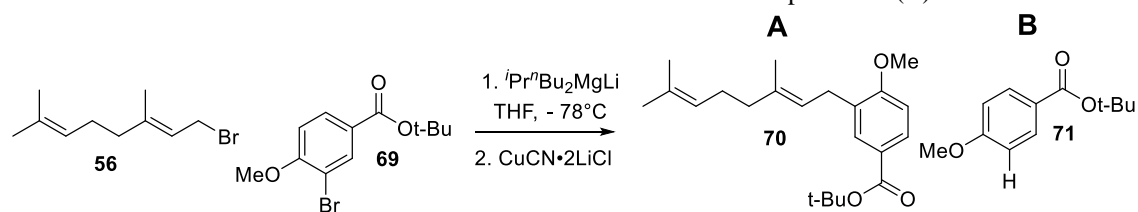
**Figure 22** Scheme illustrates initial conditions for accessing the desired geranyl-aryl coupled product. Protection of the benzoate hydroxyl entailed the use of a methyl ether to prevent the protecting group from migration.

These results were promising however further probing and optimization was necessary due to my observation of the formation of a deleterious side product (**71/B** Table 6) which makes purification of the desired product difficult due to similar retention factor values in various solvent systems. Compound **71** was verified by isolation using

preparative TLC. Table 6 (entry 4) shows that the best conditions which reduce the formation of undesirable compound **71** entail allowing the organometallic complex to form for 1 hour and the coupling event with geranyl bromide to stir for 0.5 hour and the use of  $\text{Li}_2\text{CuCl}_4$  as the copper source. Entries 1-3 from Table 6 demonstrated formation of the coupled product however, the presence of the quenched aryl substrate made these conditions less favorable. Although the aryl substrate, **69**, is formed in quantitative yield with a near pristine crude  $^1\text{H}$  NMR spectrum, without purification, the product distribution ratio shifts in favor of the formation of undesirable aryl species **71** (Table 6, entry 5).

A screen of Grignard reagents was also performed (Table 7). Results show that isopropenyl magnesium bromide is more efficient and provides a more clean reaction (Table 7, entry 2). Table 8, entry 6 shows that the optimal concentration to conduct the reaction on is 0.3 M of THF. Entries 10 and 11 are control reactions which confirm the need for the both the Grignard reagent and n-BuLi for the reaction to proceed. Attempts to increase the yield by allowing the reaction to gently warm to room temperature thereby driving the reaction to completion were also unsuccessful and resulted in diminished yields. Figure 23 shows an attempt to discern what was quenching the reactivity of the aryl halide to form **71**. This was accomplished by quenching the optimized aryl-allyl coupling conditions with deuterium oxide and observing where deuterium was incorporated. Results illustrated that deuterium was only incorporated into the aryl halide and not in the desired product. This quelled speculation that the active aryl magnesate complex was deprotonating the benzylic/allylic proton in **70** (Figure 23).

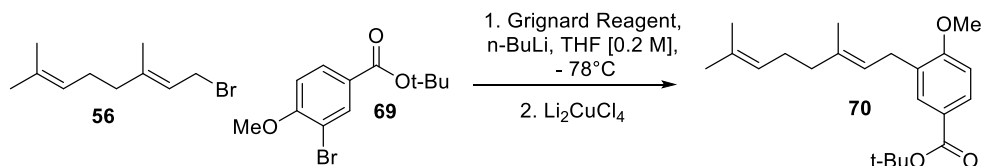
**Table 6** Optimization of the time needed for the generation of the aryl organometallic complex (Grignard/ *in situ* generated magnesate complex) and the actual coupling event with geranyl bromide. An overarching goal of this screen was to find conditions which reduced the formation of compound **71** (B).



| Time (Hr) |          |     |                 |      |      |
|-----------|----------|-----|-----------------|------|------|
| Entry     | Grignard | GBr | Yield, A+ B (%) | A    | B    |
| 1         | 0.5      | 0.5 | 64              | 1    | 0.28 |
| 2         | 1        | 1   | 59              | 1    | 0.25 |
| 3         | 0.5      | 1   | 38              | 1    | 0.33 |
| *4        | 1        | 0.5 | 59              | 1    | 0.11 |
| **5       | 1        | 0.5 | 52              | 0.56 | 1    |

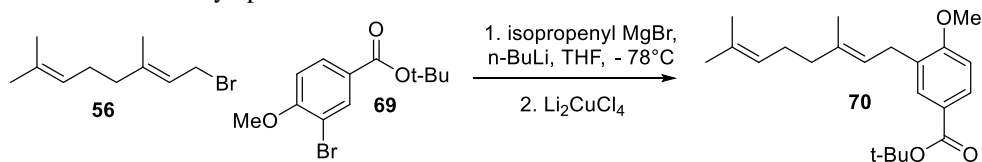
\* $\text{Li}_2\text{CuCl}_4$  used instead of  $\text{CuCN} \cdot 2\text{LiCl}$ ; \*\* Aryl halide not columned before use, and different set of NMR peaks used in ratio.

Attempts to increase the yield by allowing the reaction to gently warm to room temperature thereby driving the reaction to completion were also unsuccessful and resulted in diminished yields (Table 8, entries 12 and 13). Figure 23 shows an attempt to discern what was quenching the reactivity of the aryl halide to form **71**. This was accomplished by quenching the optimized aryl-allyl coupling conditions with deuterium oxide and observing where deuterium was incorporated. Results illustrated that deuterium was only incorporated into the aryl halide and not in the desired product. This quelled speculation that the active aryl magnesate complex was deprotonating the benzylic/allylic proton in **70** (Figure 23).

**Table 7** Aryl-allyl coupling screen of various Grignard reagents.\*

| Entry | Grignard Reagent                | Isolated Yield (%) |
|-------|---------------------------------|--------------------|
| 1     | isopropyl MgBr                  | 35                 |
| 2     | isopropenyl MgBr                | 45                 |
| 3     | Ethyl MgBr                      | 15                 |
| 4     | 1-Propenyl MgBr                 | 13                 |
| 5     | (1,3-dioxolan-2-yl methyl) MgBr | No desired product |

\*All reactions performed on a 1 mmol scale of aryl halide **69** with geranyl bromide (**56**, 4 eq), THF (0.2 M), n-BuLi (2.4 eq) and Li<sub>2</sub>CuCl<sub>4</sub>.

**Table 8** Concentration study optimization table.

| Entry | Scale (mmol)   | Conc. [M] | Yield (%) |
|-------|----------------|-----------|-----------|
| 1     | 6.5            | 0.2       | 55 (38)   |
| 2     | 3.5            | 0.2       | 20        |
| 3     | 1              | 0.15      | 14        |
| 4     | 1              | 0.2       | 19        |
| 5     | 1              | 0.25      | 33        |
| 6     | 1              | 0.3       | 58        |
| 7     | 7              | 0.3       | 38        |
| 8     | 1              | 1         | 20        |
| 9     | 1              | 2         | 47        |
| 10    | 0.5*           | 0.2       | N.R       |
| 11    | 0.5**          | 0.2       | messy     |
| 12    | 1 <sup>†</sup> | 0.3       | 22.5      |
| 13    | 1 <sup>‡</sup> | 0.3       | 10        |

Parenthesis= average yield; \* w/o n-BuLi; \*\* w/o isopropenyl MgBr; <sup>†</sup> Stirred for 1 hour at room temp; <sup>‡</sup> Stirred overnight at room temp.

Successful acquisition of the coupled geranyl aryl system (**70**) prompted the application of the strategies elucidated for the formation of the cyclohexyl unit allowing for functionalization at the terminal end of the geranyl-aryl system (Figure 24). The geranyl

sulfone (**75**) system is the point of divergence in the adopted modular strategy allowing for the formation of targets **28**, **29**, **30** and callophycolide A. It is also important to note that this strategy can be adopted to access *C. serratus* natural products.

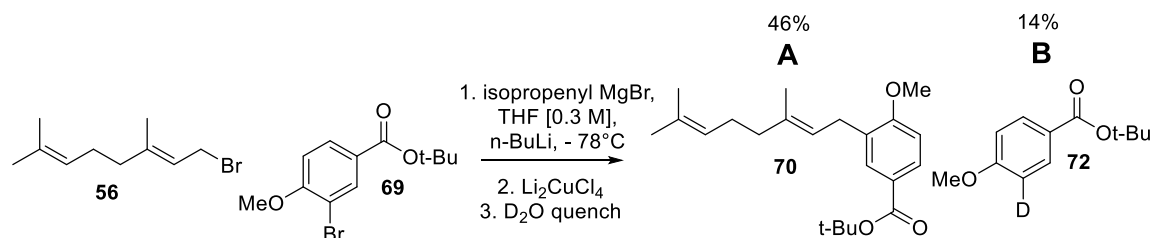


**Figure 23** Scheme for allyl-aryl coupling with optimal conditions quenched with D<sub>2</sub>O to determine if the aryl organometallic complex was forming compound **71** upon deprotonation of an acidic proton within the desired product, **70**. No deuterium was observed to be incorporated into compound **70**.

Allylic oxidation of **70** provided **73** in poor yields, 24%, despite efforts to increase the yield. These reactions are inherently low yielding and historically perform badly. However, starting material can be recovered and subjected to the oxidation conditions to help atom economy. All being said and done, enough material was generated to push forward allowing for the formation of allyl bromide **74** in excellent yields, 93%. Construction of aryl geranyl sulfone **75** occurred without any difficulty for the exception of the observation of the competing S<sub>N</sub>2' product which accounts for the slightly diminished yield of 87% (Figure 24).

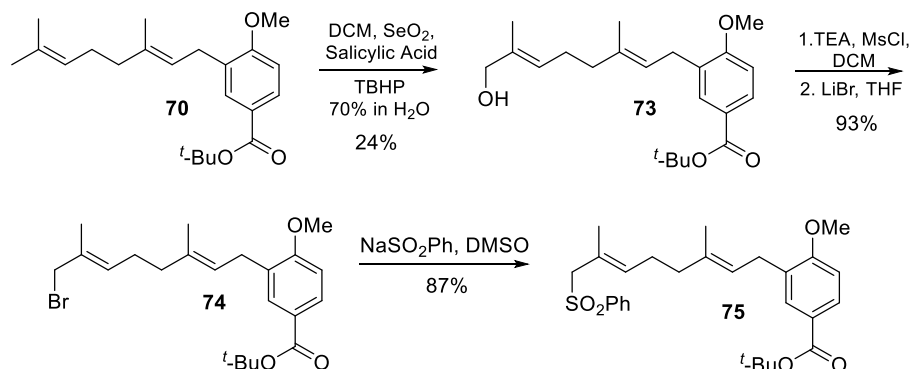


**Figure 24** Sequence of steps leading to key intermediate (**75**, point of divergence) for the synthesis of bromophycolide P, Q, U and callophycolide A.

As mentioned above, **75** is the point of divergence towards accessing bromophycolides P, Q, U and callophycolide A. The overarching strategy entails the use of **75** in a sulfone stabilized anionic epoxide ring opening event to join **75** to either the pyran (**B**, **78**) moiety or linalool (**D**, **76**) derivative featured in Figure 25. **77** is a precursor for callophycolide A and **79** a precursor for **28**, **29**, **30**.

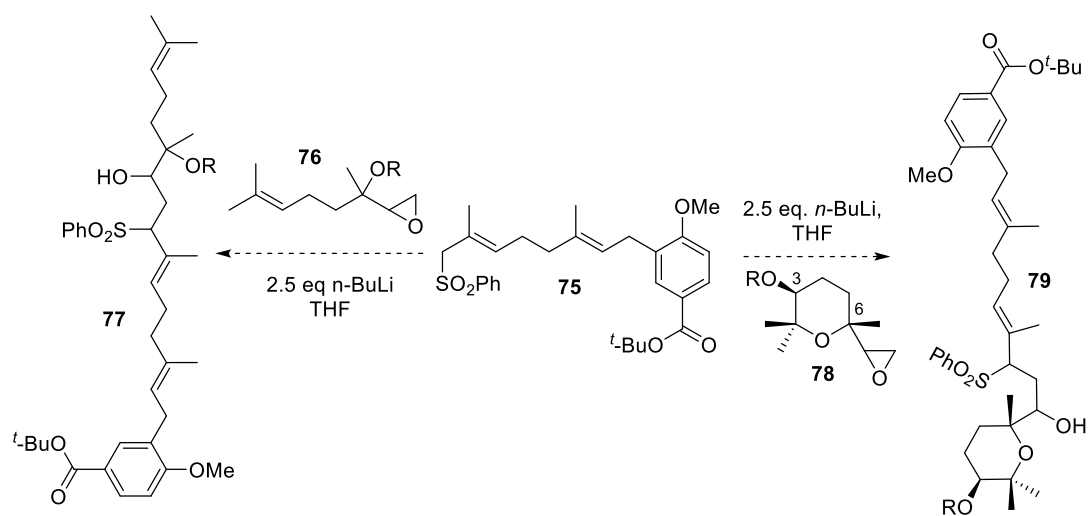


**Figure 25** Plan for modular divergent synthesis of bromophycolides P, Q, U, and callophycolide A.

### 2.2.3 Linalool Fragment- Callophycolide A

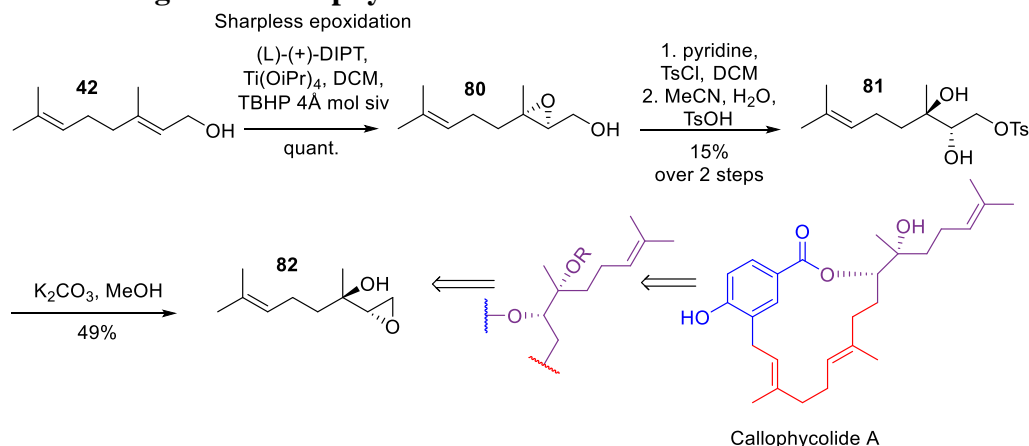


**Figure 26** Initial scheme for the formation of the linalool fragment, precursor for callophycolide A <sup>33</sup>.

Construction of the linalool fragment (**76**, Figure 25) to be joined with **75** began by performing an asymmetric Sharpless epoxidation on geraniol **42** (Figure 26). Epoxide formation (**80**) was followed by a primary hydroxyl tosylation and subsequent epoxide ring opening promoted with catalytic toluenesulfonic acid (**81**). Formation of terminal epoxide **82** occurred with an observation of isolable diastereomers (Figure 26) <sup>33</sup>. Successful acquisition of **82**, linalool epoxide, allowed for a protecting group screen to be performed to determine which protecting group can tolerate the sulfone stabilized anionic epoxide ring opening event proposed in Figure 25. Figure 27 presents the synthetic scheme for three protecting groups appended to the linalool epoxide system which were then subjected to the sulfone stabilized anionic epoxide ring opening conditions <sup>34, 35</sup>.

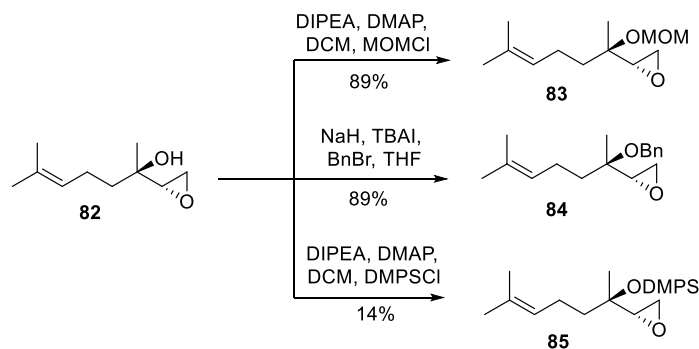


**Figure 27** Linalool epoxide protecting group screen precursors <sup>34, 35</sup>.



## 2.2.4 Sulfone Stabilized Anionic Epoxide Ring Opening

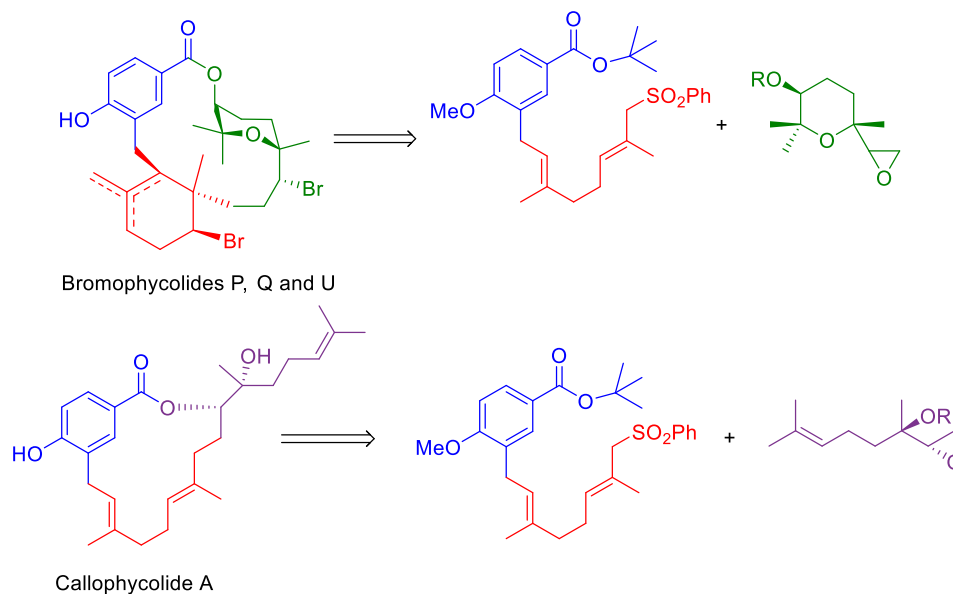


**Figure 28** Retrosynthesis for sulfone stabilized anionic ring opening

Inspiration for the connection of the pyran (**78**) and linalool (**76**) scaffold with **75** (point of divergence) arose from the work of B. Trost (1988) (Figure 28 and Figure 29). This entailed deprotonation of a proton alpha to the an isoprenyl/allylic sulfone and subsequent nucleophilic attack on a terminal epoxide inevitably joining two units. The sulfone forms a dianion when treated with at least 2 eq of n-BuLi which coordinates with the hydroxyl (formerly incorporated into the epoxide) providing the stereoselectivity desired for target bromophycolides and callophycolide A. Initial test reactions with model system **87** and styrene oxide, **88**, were promising and illustrated that the transformation can occur with simple systems (Figure 29) <sup>36</sup>.

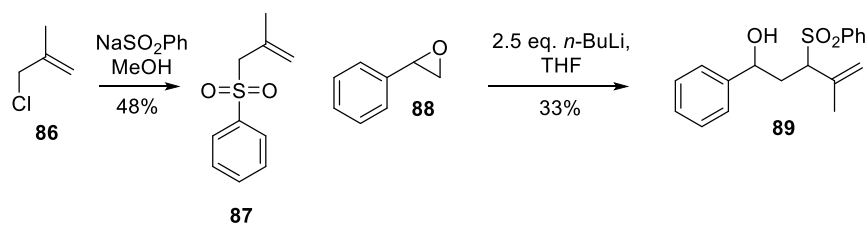


**Figure 29** Model reaction and proof of concept for the sulfone stabilized anionic epoxide ring opening transformation <sup>36</sup>.

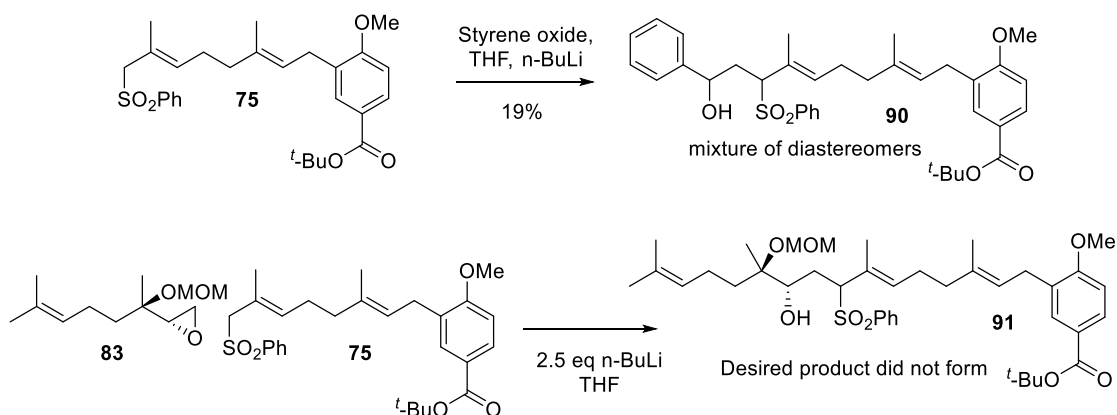


**Figure 30** Initial attempts to apply Trost's chemistry to *C. serratus* natural product point of divergence precursor, compound **75**.

Initial attempts to apply Trost's chemistry to *C. serratus* sulfone **75** by using commercially available styrene oxide showed modest yields. Although the transformation is not ideal, an unfruitful attempt was made to couple **75** with MOM protected linalool epoxide, **83** (Figure 30). It is speculated that the oxygen within the MOM protecting group disrupts the chelation necessary for the reaction to proceed down the desired pathway.

Considering the possibility of chelation disruption, benzyl (**84**) and dimethylphenyl silane (**85**, DMPS) protecting groups on linalool epoxide were screened using model sulfone **87**. Use of **87** provided modest results forming **92**. No reactivity was observed for the formation of **93** from **85** probably due to steric hindrance associated with the use of the bulky silane protecting group (Figure 31). Considering the possibility that the benzyl protecting group might be efficient for the transformation led to attempting the coupling of **84** with **75** (Figure 32). There was no evidence of product formation.

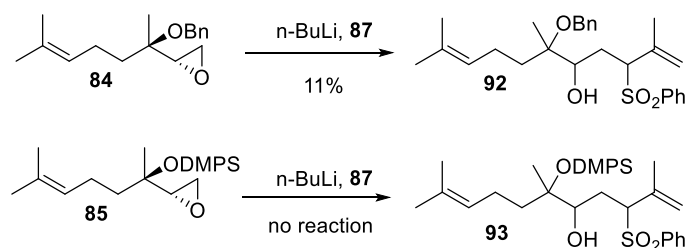


**Figure 31** Linalool epoxide protecting group test reactions with model sulfone **87**.

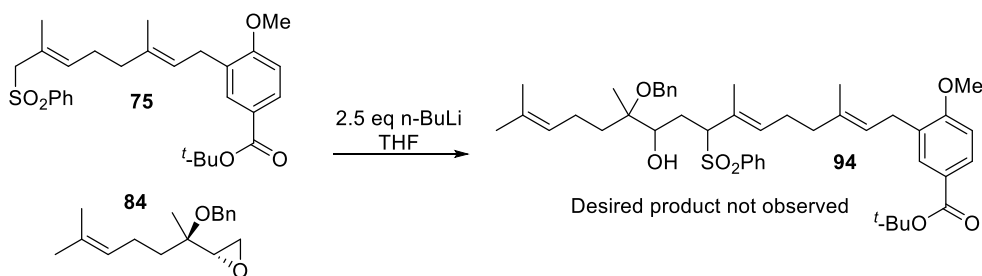


**Figure 32** Attempt at forming callophycolide A precursor using sulfone, **75**, and benzyl protected linalool epoxide, **84**.

## 2.2.5 Pyran Formation- Bromophycolide P, Q, and U

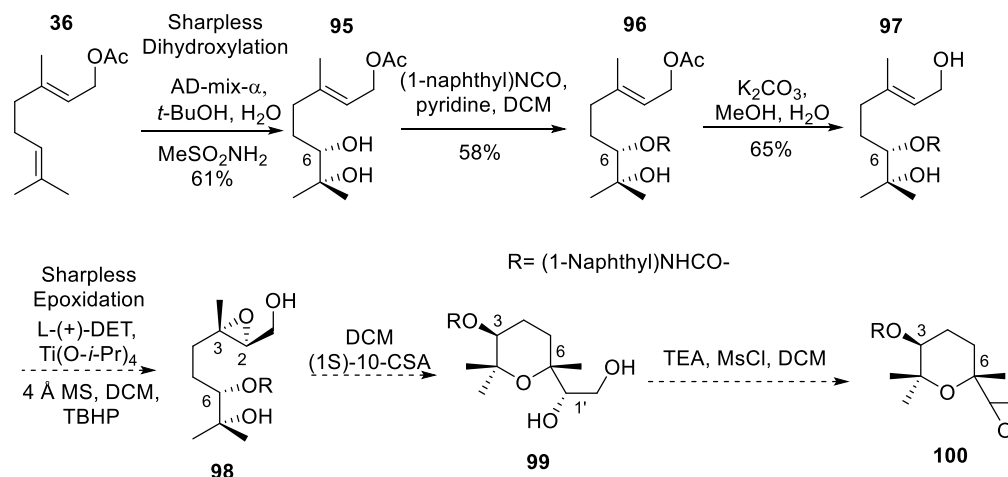


**Figure 33** Synthetic route to accessing the pyran module for bromophycolides P, Q, and U <sup>37, 39</sup>.

Formation of the pyran module has been worked out by Vidari and co-workers (2000) <sup>37</sup>. The multi-step synthesis began with a Sharpless dihydroxylation of geranyl acetate, **36**, forming diol **95** <sup>39</sup>. The less sterically hindered alcohol was selectively protected using 1-naphthyl isocyanate providing compound **96**. Saponification of the acetate yielded the primary alcohol handle essential for the subsequent Sharpless epoxidation **98** (Figure 33) <sup>37</sup>. The remainder of the synthesis was placed on hold while the stereochemistry for the dihydroxylation was confirmed via use of Mosher ester analysis.

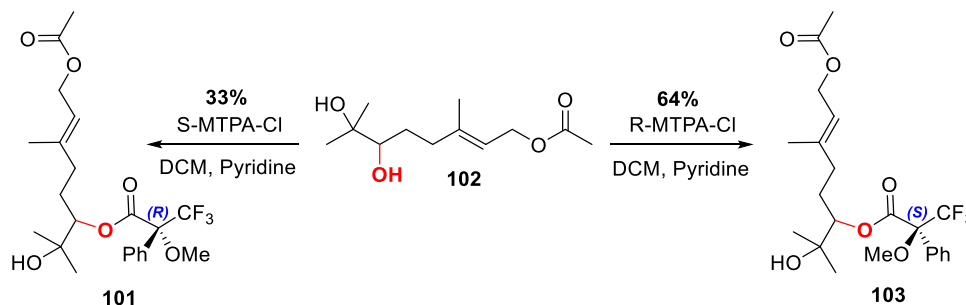
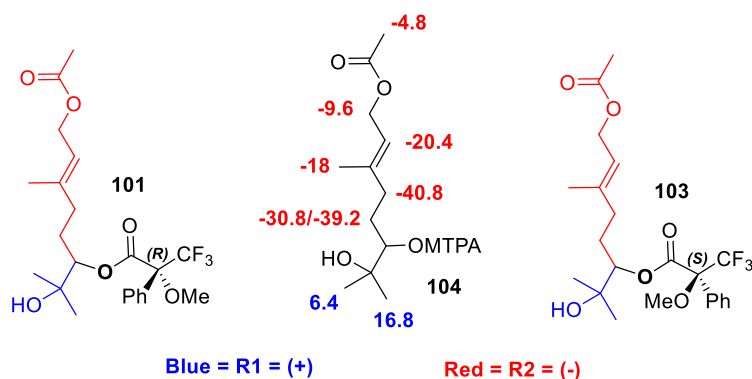


**Figure 34** Mosher ester formation for <sup>1</sup>H NMR analysis to confirm the correct stereochemistry of diol (**102**) formed via Sharpless asymmetric dihydroxylation <sup>38</sup>.

Mosher ester analysis began with the synthesis of the esters from diol, **102**, and acyl chlorides R-MTPA-Cl and S-MTPA-Cl forming esters **103** and **101** respectively (Figure 34) <sup>38</sup>. It is important to note that the S-acyl chloride forms the R-ester and the R-acyl chloride forms the S-ester. Unambiguous assignment for each peak of each diastereomeric ester in the <sup>1</sup>H NMR was essential for subsequent calculations which use the effects of differences in anisotropy and shielding of the Mosher ester appendages on the diol substrate to determine the absolute stereochemistry of the substrate in question, **102**. The use of Chan-Ingold Prelog convention to assign the absolute configuration confirmed formation of the S-diol (**95**, Figure 33) (Table 9).

**Table 9** Determined  $\Delta\delta^{SR}$  and list data from most positive to most negative



| Proton | R-ester (ppm) | S-ester (ppm) | (S - R) |              |
|--------|---------------|---------------|---------|--------------|
|        |               |               | ppm     | Hz (400 MHz) |
| i      | 1.172         | 1.214         | 0.042   | 16.8         |
| i'     | 1.138         | 1.154         | 0.016   | 6.4          |
| e      | 4.994         | 4.986         | -0.008  | -3.2         |
| g      | 2.058         | 2.046         | -0.012  | -4.8         |
| d      | 4.579         | 4.555         | -0.024  | -9.6         |
| h      | 1.655         | 1.61          | -0.045  | -18          |
| c      | 5.31          | 5.259         | -0.051  | -20.4        |
| k'     | 1.74          | 1.663         | -0.077  | -30.8        |
| k      | 1.882         | 1.784         | -0.098  | -39.2        |
| j      | 2.038         | 1.936         | -0.102  | -40.8        |

## 2.3 Outlook

Carrying forward with this project entails the continuing construction of the pyran moiety outlined in Figure 33. An alternative route which could access the pyran more readily involves chiral resolution of commercially available **105** and subsequent epoxide formation using either Shi conditions or DMDO as a reagent (Figure 35). Chiral resolution is envisioned to occur by forming a boc-protected phenyl alanine in hope that the diastereomers can be isolated.

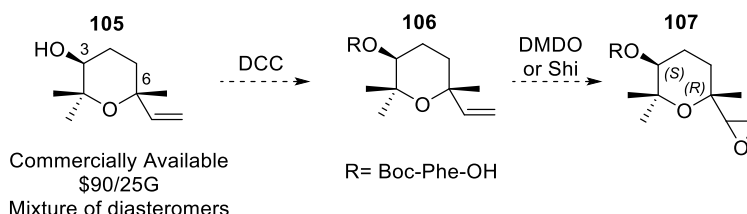


**Figure 35** Alternative route for accessing the pyran system for targets bromophycolide P, Q, and U.

Additionally, optimization for the sulfone stabilized anionic epoxide ring opening transformation featured in Figure 25 is required for a successful synthesis. Optimization of this step will allow for the synthesis of targets bromophycolides P, Q, U and callophycolide A in 3-4 steps. Desulfurization of the product resulting from the anionic ring opening event can occur with either sodium amalgam or superhydride (Figure 36). Figure 32 describes the final steps needed to complete the scaffold for callophycolide A. It is important to note that these transformations can also be applied to completing bromophycolides P, Q, and U. Formation of the macrolactone can occur by use of Corey-Nicolaou (via double activation of the ester) or Yamaguchi (via formation of a mixed anhydride) macrolactonization conditions (Figure 37). Both condition call for extremely dilute conditions (0.001- 0.002 M). Deprotection of the final precursor should provide *C. serratus* natural products callophycolide A and bromophycolide P, Q, and U.

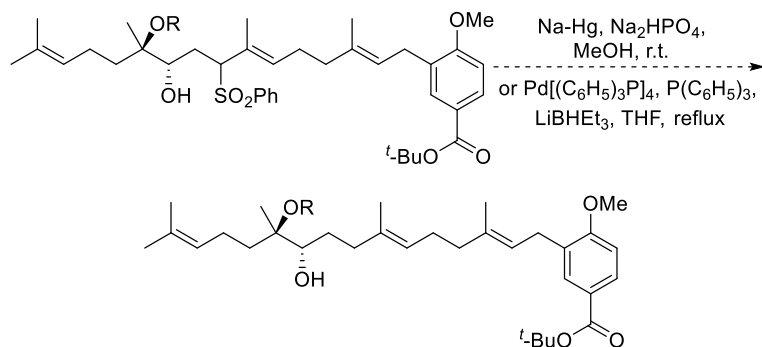


**Figure 36** Possible methods for desulfurization of callophycolide A precursor <sup>40, 41</sup>.

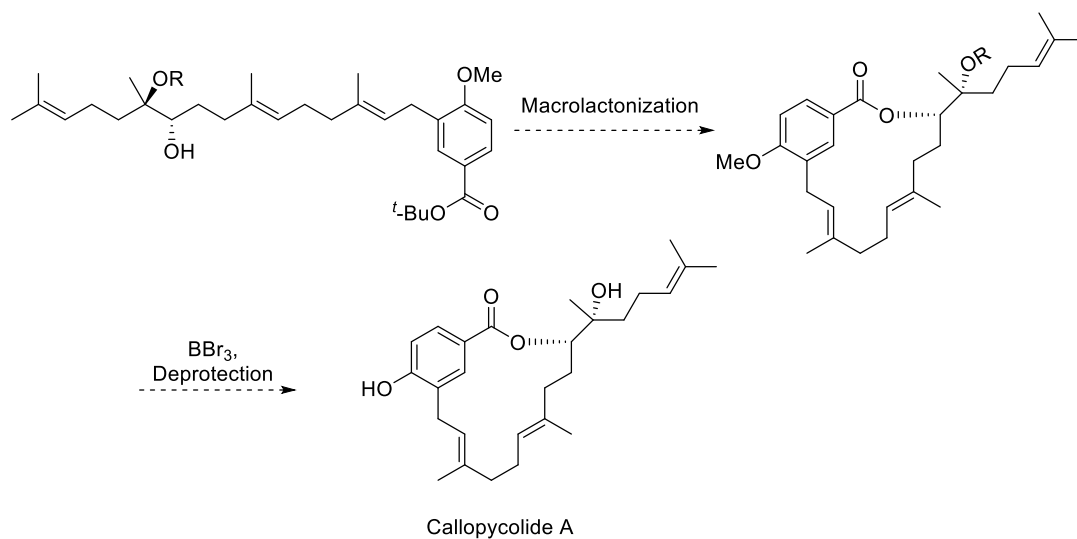


**Figure 37** Final steps towards the completion of the synthesis of callophycolide A. The methods applied to access this target should be transferrable to providing bromophycolides P, Q and U.

## 2.4 Conclusion

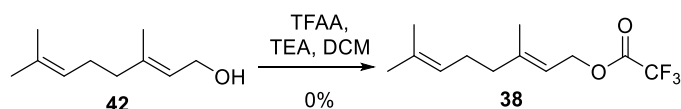
I was successful in obtaining the cyclohexyl module in 5 steps with an overall yield of 29%. Methods have been explored for the selective alkene formation of the cyclohexyl unit. With Swern elimination conditions selectively forming the exo-cyclic alkene. Use of heterogenous Amberlyst-15 dry resin allows for the selective generation of the tri-substituted alkene. Although these findings are useful, BDSB cyclization of sulfone **46** forms the tri-substituted alkene. Formation of the tri-substituted alkene is more desirable over the exo-cyclic and tetra-substituted alkene due to its increased bio-activity. Joining of the aryl and geranyl system using an *in situ* generate magnesate complex was optimized. This entailed finding a method which allowed for the facile generation of the geranyl coupling substrate, a phenolic protecting group that would withstand magnesate conditions, and concentrations for optimal product recovery.

Despite my efforts, I was unable to complete the synthesis of targeted bromophycolides P, Q, U and callophycolide A. This was due to difficulty encountered when attempting to join key units which would allow for the conjoining of the three modules that compose the scaffold of the targets. Steps to efficiently perform the sulfone stabilized anionic epoxide ring opening event need to be elucidated. Once the three modules are joined, macrolactonization would close the system bringing the project to its finishing leg.

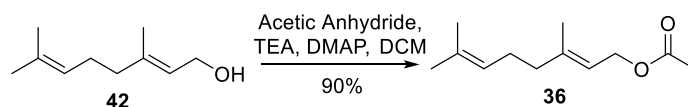


## CHAPTER 3- EXPERIMENTAL

### 3.1 Cyclohexyl- Bromophycolides P, Q, and U

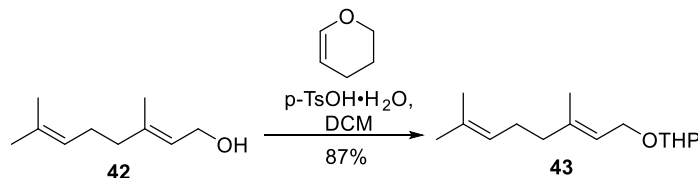


Under an inert atmosphere, a solution of TEA (3.62 mL, 26 mmol, 2 eq) in DCM (25 mL, 0.52 M) was prepared followed by the addition of **42** (2.00 g, 13 mmol, 1 eq). The resulting solution was stirred at 0° C and TFAA (2.35 mL, 16.9 mmol, 1.3 eq) was added dropwise and then stirred for 30 minutes. Upon reaction completion, the mixture was quenched with cold water and extracted with DCM. Combined organic layers were then treated with brine, dried over magnesium sulfate, filtered and concentrated. Purification was attempted with vacuum distillation but was unsuccessful (b.p.= 72° C, 2 mm Hg). Crude <sup>1</sup>H-NMR (400 MHz, CDCl<sub>3</sub>) δ 5.40 (dt, J = 1.2 Hz, 7.4 Hz, 1H), 5.07 (t, J = 2.7 Hz, 1H), 4.85 (d, J = 7.4 Hz, 2H), 2.12 (m, 5H), 1.74 (s, 3H), 1.67 (s, 5H), 1.59 (s, 4H)

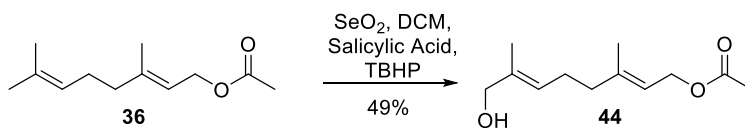


Under an inert atmosphere a solution of DMAP (139 mg, 1.14 mmol, 0.02 eq) and TEA (11.5 mL, 114 mmol, 1.5 eq) in DCM (120 mL, 0.47 M) was prepared followed by the addition of **42** (8.79 g, 57 mmol, 1 eq). The resulting solution was stirred at 0°C and acetic anhydride (6.46 mL, 68.4 mmol, 1.2 eq) was added and then stirred for 20 minutes. Upon reaction completion, the mixture was quenched with water and extracted with DCM. Combined organic layers were then treated with 1M HCl, saturated NaHCO<sub>3</sub> (aq), brine, dried over magnesium sulfate, filtered and concentrated. Purification using flash column chromatography provided **36** in 90% yield: R<sub>f</sub> = 0.63 (15% EtOAc/Hexane, resolved with vanillin stain) <sup>1</sup>H-NMR (400 MHz, CDCl<sub>3</sub>) δ 5.32 (t, J = 7.10 Hz, 1H), 5.07 (t, J = 5.38 Hz,

1H), 4.57 (d,  $J = 7.12$  Hz, 2H), 2.09 (m, 2H), 2.04 (s, 5H), 1.69 (s, 3H), 1.67 (s, 3H), 1.59 (s, 3H)

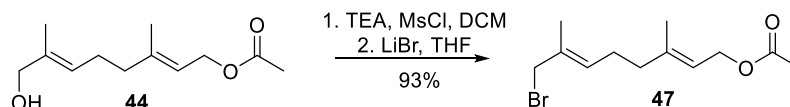


Under an inert atmosphere. A solution of **42** (20.0 g, 130 mmol, 1 eq), p-TsOH·H<sub>2</sub>O (0.24 g, 1.3 mmol, 0.01 eq) and 3,4-dihydropyran (16.4 g, 195 mmol, 1.5 eq) in DCM (130 mL, 1 M) was prepared and stirred at room temperature for 3 hours. Upon reaction completion, the mixture was quenched with water and extracted with diethyl ether. Combined organic layers were then washed with water (3x), brine, and dried over sodium sulfate, filtered and concentrated. Purification using flash column chromatography provided **43** in 92% yield:  $R_f = 0.73$  (20% EtOAc/Hexane, resolved with vanillin stain) <sup>1</sup>H-NMR (400 MHz, CDCl<sub>3</sub>)  $\delta$  5.35 (t,  $J = 6.74$  Hz, 1H), 5.09 (t,  $J = 6.38$  Hz, 1H), 4.62 (s, broad, 1H), 4.24 (dd,  $J = 6.4$  Hz, 11.84 Hz, 1H), 4.03 (dd,  $J = 7.5$  Hz, 11.8 Hz, 1H), 3.89 (t,  $J = 8.2$  Hz, 1H), 3.51 (m, 1H), 2.09 (m, 2H), 2.05 (m, 2H), 1.83 (m, 1H), 1.74 (m, 1H), 1.67 (s, 6H), 1.59 (s, 4H), 1.56 (m, 3H)

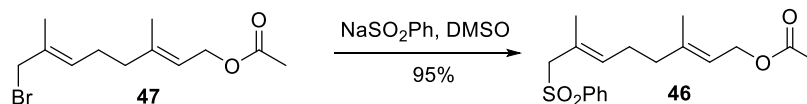


Salicylic acid (0.49 g, 3.6 mmol, 0.1 eq), SeO<sub>2</sub> (118.7 mg, 1.08 mmol, 0.03 eq) then DCM (53.4 mL, 0.62 M) was added to a flask at room temperature. TBHP (14.18 mL, 90 mmol, 2.5 eq, 70% in H<sub>2</sub>O) was added to the resulting solution and stirred for 15 minutes. The substrate, **36** (7.0 g, 36 mmol, 1 eq), was then added and the mixture was stirred for 20 hours. Flask contents was then concentrated under reduced pressure below 30° C. The residue was then diluted in Et<sub>2</sub>O and the organic layer was then washed with 10% KOH

(3x), H<sub>2</sub>O (3x), and brine (1x). The ether layer was then dried over magnesium sulfate, filtered and concentrated. Purification using chromatography provided **44** in 49% yield: R<sub>f</sub> = 0.16 (15% EtOAc/Hexane, resolved with vanillin stain) <sup>1</sup>H-NMR (400 MHz, CDCl<sub>3</sub>) δ 5.34 (m, 2H), 4.59 (d, J = 7.04 Hz, 2H), 3.99 (s, 2H), 2.16 (m, 2H), 2.10 (m, 2H), 2.05 (s, 3H), 1.70 (s, 3H), 1.66 (s, 1H)

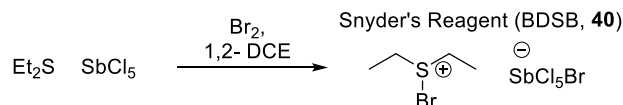


Under an inert atmosphere, make a solution of the alcohol substrate **44** (5.09 g, 24 mmoles, 1 eq) in DCM (99 mL, 0.24 M). The resulting solution was then cooled to -40° C then TEA (6.69 mL, 48 mmoles, 2 eq) was added to the vessel. MsCl (3.72 mL, 48 mmoles, 2 eq) was then added to the flask dropwise then stirred for 90 minutes. Get the flask to -15 °C then add a solution of LiBr (5.21 g, 60 mmoles, 2.5 eq) in THF (60 mL, 1 M) and stir the resulting solution overnight. Quench with saturated NH<sub>4</sub>Cl (aq), extract with DCM, dry over sodium sulfate, filter, and concentrate. **47** was provided in 93% yield. R<sub>f</sub> = 0.73 (15% EtOAc/Hexane, resolved with UV and vanillin stain) <sup>1</sup>H-NMR (400 MHz, CDCl<sub>3</sub>) δ 5.51 (dt, J = 6.66 Hz, 33.84 Hz, 1H), 5.34 (t, J = 7.09 Hz, 1H), 4.59 (d, J = 7.10 Hz, 2H), 4.00 (s, 1 H), 3.96 (s, 1H), 2.16 (m, 2H), 2.10 (m, 2H), 2.05 (s, 3H), 1.75 (d, J = 9.43 Hz, 3H), 1.70 (s, 3H); <sup>13</sup>C-NMR (400 MHz, CDCl<sub>3</sub>) δ 171.2, 141.5, 132.2, 130.0, 118.9, 61.3, 52.4, 38.7, 26.2, 24.1, 16.5, 14.2



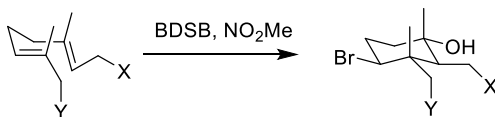
Under an inert atmosphere, stir NaSO<sub>2</sub>Ph (3.37 g, 19 mmoles, 2.5 eq) in DMSO (105 mL, 0.1 M) until complete dissolution. Add bromide substrate **47** (2.09 g, 7.6 mmoles, 1 eq)

slowly and stir resulting solution at room temperature for 1 hour. To stop reaction, add water, extract desired product into DCM, wash with brine (2x), dry over magnesium sulfate, filter, concentrate and purify. Purification with flash column chromatography provided **46** in 95% yield.  $R_f = 0.16$  (20% EtOAc/Hexane, resolved with UV and vanillin stain) )  $^1\text{H-NMR}$  (500 MHz,  $\text{CDCl}_3$ )  $\delta$  7.85 (d,  $J = 7.68$  Hz, 2H), 7.63 (t,  $J = 7.24$  Hz, 1H), 7.54 (t,  $J = 7.44$  Hz, 2H), 5.18 (t,  $J = 6.88$  Hz, 1H), 4.97 (t,  $J = 6.86$  Hz, 1H), 4.49 (d,  $J = 7.00$  Hz, 2H), 3.66 (s, 2H), 2.03 (m, 5H), 1.83 (m, 2), 1.76 (s, 3H), 1.64 (s, 3H), 1.57 (m, 1H);  $^{13}\text{C-NMR}$  (400 MHz,  $\text{CDCl}_3$ )  $\delta$  171.1, 141.2, 138.4, 135.4, 133.5, 128.9, 128.9, 128.5, 123.7, 118.8, 66.1, 61.2, 38.4, 26.4, 21.0, 16.7, 16.4.



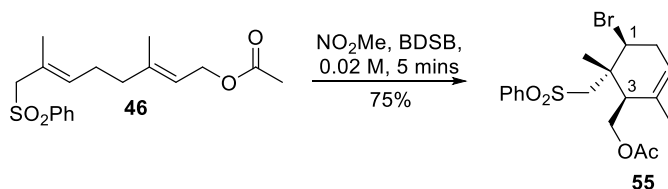
Under an inert atmosphere to a flask at  $-30^\circ\text{C}$ , add  $\text{Et}_2\text{S}$  (1.2 mL, 11 mmol, 1.1 eq) and  $\text{SbCl}_5$  (12 mL, 12 mmol, 1 eq, 1 M in DCM) to a solution of  $\text{Br}_2$  (0.5 mL, 10 mmol, 1 eq) in dry 1,2- DCE (30 mL, 0.33 M). Stir for 30 minutes then gently warm until complete dissolution is observed ( $30\text{--}40^\circ\text{C}$ ). Slowly cool solution to  $-20^\circ\text{C}$ . Decant solvent keeping product (light orange plates). Rinse plates with cold DCM and remove excess solvent under vacuum. Store under inert atmosphere at  $-20^\circ\text{C}$ . Melting point =  $100^\circ\text{C}$

#### BDSB Cyclization Study (Table 4)

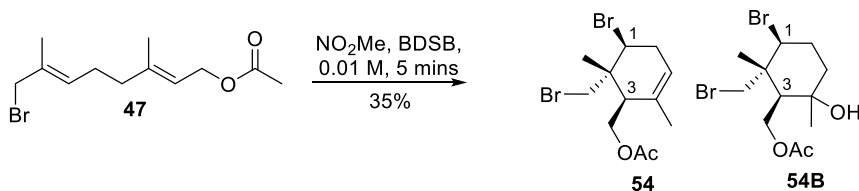


**General BDSB Cyclization Procedure:** Under an inert atmosphere. Make a solution of BDSB (0.6 mmol, 1.1 eq) in freshly distilled  $\text{NO}_2\text{Me}$  (15 mL, 0.04 M) cooled to  $0^\circ\text{C}$ . Make another solution of cyclization substrate (0.5 mmol, 1 eq) in  $\text{NO}_2\text{Me}$  (15 mL, 0.03 M) cooled to  $0^\circ\text{C}$ . Quickly add BDSB/ $\text{NO}_2\text{Me}$  solution to cyclization substrate/ $\text{NO}_2\text{Me}$

solution and stir for 5 minutes. Quench reaction with 5% Na<sub>2</sub>SO<sub>3</sub> (aq): 5% Na<sub>2</sub>SO<sub>3</sub> (aq) (1:1) and stir for 15 minutes. Pour resulting mixture into water and extract with DCM. Combined organic layers dried over magnesium sulfate, filtered, concentrated and purified via flash column chromatography. \*Concentration varied by altering the amount of nitromethane used in the cyclization substrate nitromethane solution.



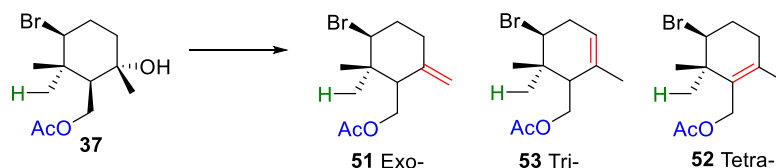
<sup>1</sup>H-NMR (500 MHz, CDCl<sub>3</sub>) δ 7.80 (d, J = 8.36 Hz, 2H), 7.61 (t, J = 7.36 Hz, 1H), 7.51 (t, J = 7.80 Hz, 2H), 5.05 (t, J = 7.12 Hz, 1H), 4.51 (dd, J = 3.64 Hz, 12.20 Hz, 1H), 4.28 (dd, J = 8.80 Hz, 12.20 Hz, 1H), 4.08 (m, 1H), 3.69 (s, 2H), 2.2 (m, broad 1H), 2.07 (m, 5H), 1.74 (m, 4H), 1.65 (s, 1H), 1.48 (m, 1H), 1.34 (m, 1H), 1.26 (s, 2H); <sup>13</sup>C-NMR (500 MHz, CDCl<sub>3</sub>) δ 171.28, 170.5, 138.2, 138.1, 135.3, 134.8, 133.6, 133.5, 128.9, 128.8, 128.3, 124.9, 123.8, 75.2, 73.1, 72.2, 66.2, 65.9, 65.3, 60.5, 40.5, 38.4, 29.5, 26.6, 24.5, 23.7, 23.5, 22.0, 20.8, 16.6, 16.5



<sup>1</sup>H-NMR (500 MHz, CDCl<sub>3</sub>) δ 5.51 (t, J = 7.12 Hz, 1H), 4.58 (dd, J = 3.85 Hz, 12.20 Hz, 1H), 4.50 & 3.83 (dd, J = 2.55 Hz, 11.60 Hz, dd, J = 2.52 Hz, 8.22 Hz, 1H), 4.32 (dd, J = 8.65 Hz, 12.20 Hz, 1H), 4.15 (m, 1H), 3.99 (s, 2H), 2.35-2.12 (m, 4H), 2.09 (s, 3H), 2.05-2.01 (m, 1H), 1.89-1.77 (m, 2H), 1.75-1.66 (m, 6H), 1.63-1.58 (m, 1H), 1.34 (s, 11H) <sup>13</sup>C-NMR (500 MHz, CDCl<sub>3</sub>) δ 171.4, 170.6, 133.0, 132.7, 132.4, 129.6, 128.5, 75.8, 73.4,

72.6, 66.3, 65.3, 60.8, 52.0, 41.2, 40.8, 38.6, 26.9, 24.5, 24.2, 24.0, 21.8, 20.8, 14.6, 14.1, 14.0 HRMS (ESI) m/z: Calcd. For C<sub>12</sub>H<sub>20</sub>Br<sub>2</sub>O<sub>3</sub> 371.98; Found 372.3

### Selective Elimination Study (Table 5)



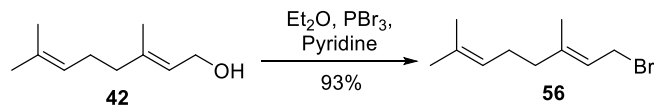
**Swern Oxidation:** Under an inert atmosphere. Make a solution of dry DMSO (0.11 mL, 1.68 mmol, 4.8 eq) in dry DCM (3.6 mL, 0.45 M) and get solution to -78° C. In another flask make a solution of (COCl)<sub>2</sub> (0.10 g, 0.84 mmol, 2.4 eq) in dry DCM (0.9 mL, 0.9 M). Add oxalyl chloride to cooled flask slowly, temperature should not rise above -60° C. Stir the resulting mixture for 10 minutes then add solution of cyclized substrate, **37**, (0.100 g, 0.35 mmol, 1 eq) in dry DCM (3.7 mL, 0.09 M). After stirring for 20 minutes TEA (0.23 mL, 1.75 mmol, 5 eq) was added and stirred for an additional 15 minutes. Gently bring the flask to room temperature over a period of 1.5 hours. Once the flask is at room temperature concentrate the contents then dissolve the residue in diethyl ether, filter the contents, concentrate and purify. Purification using flash column chromatography provided the elimination product R<sub>f</sub> = 0.75 (20% EtOAc/Hexane, resolved with vanillin stain)

**Swern Elimination:** Under an inert atmosphere. Make a solution of dry DMSO (0.33 mL, 4.75 mmol, 9.5 eq) in dry DCM (1.9 mL, 2.5 M) and get solution to -60° C. In another flask make a solution of (COCl)<sub>2</sub> (0.22 mL, 2.65 mmol, 5.3 eq) in dry DCM (5 mL, 0.53 M). Add oxalyl chloride to cooled flask slowly, temperature should not rise above -60° C. Stir the resulting mixture for 5 minutes then add solution of cyclized substrate (146 mg, 0.5 mmol, 1 eq) in dry DCM (1 mL, 0.5 M). After stirring for 45 minutes TEA (1.67 mL, 12 mmol, 24 eq) was added and stirred for an additional 10 minutes. Gently bring the

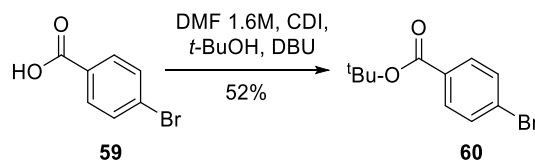
flask to room temperature over a period of 1.5 hours. Once the flask is at room temperature water was added and extracted with diethyl ether. Combined ether extracts were then washed with water (2x),  $\text{NaHCO}_3$  and water. The organic layer was then dried over sodium sulfate, concentrated and purified. Purification using flash column chromatography provided the elimination product  $R_f = 0.75$  (20% EtOAc/Hexane, resolved with vanillin stain)

**Ambrlyst-15 dry Elimination:** Under an inert atmosphere. Ambrlyst-15 dry resin added to flask along with cyclized substrate (0.102 g, 0.35 mmol, 1 eq) and DCM (20 mL, 0.02 M). Upon reaction completion flask contents filtered, concentrated and purified. Purification using flash column chromatography provided the elimination product  $R_f = 0.75$  (20% EtOAc/Hexane, resolved with vanillin stain)

### 3.2 Aryl- Allyl Cross-Coupling



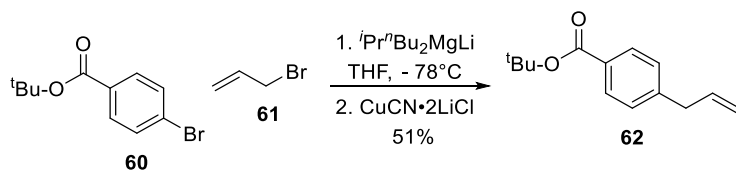
Under an inert atmosphere. A solution of geraniol (5.39 g, 35 mmoles, 1 eq) and pyridine (0.22 mL, 2.8 mmoles, 0.08 eq) in diethyl ether (44 mL, 0.8 M) was made and the resulting solution was stirred at 0°C. PBr<sub>3</sub> (17.5 mL, 17.5 mmoles, 0.5 eq, 1M solution in DCM) was then added slowly over a period of 15 minutes and the resulting solution was then stirred for an additional 15 minutes. Upon reaction completion, the resulting yellow mixture was then decanted into ice cold water and solid washed with hexane, adding the hexane wash to ice cold water. Further extraction from cold water was accomplished with diethyl ether and the combined organic layers were then washed with brine (6x) and dried over magnesium sulfate. The product was carried forward without any additional purification. **56** was formed in 93% yield: R<sub>f</sub> = 0.78 (100% Hexane, resolved with vanillin stain) <sup>1</sup>H-NMR (400 MHz, CDCl<sub>3</sub>) δ 5.52 (dt, J = 1.04 Hz, 8.44 Hz, 1H), 5.06 (m, 1H), 4.01 (d, J = 8.44 Hz, 2H), 2.07 (m, 4H), 1.72 (s, 3H), 1.67 (s, 3H), 1.59 (s, 3H) ; <sup>13</sup>C-NMR (400 MHz, CDCl<sub>3</sub>) δ 143.56, 131.97, 123.54, 120.55, 39.54, 29.66, 26.21, 25.70, 17.72, 15.97



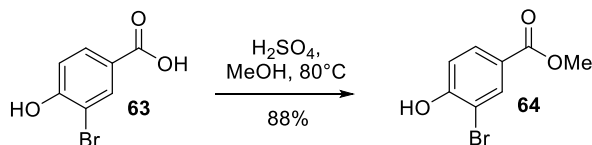
Under an inert atmosphere. A solution was made of **59** (2.02 g, 10 mmoles, 1 eq) and carbonyl diimidazole (CDI, 2.43 g, 15 mmoles, 1.5 eq) in DMF (6.0 mL, 1.6 M). The mixture was then heated to 43° C for 3 hours then treated with tert-butanol (2.85 mL, 30 mmoles, 3 eq) and DBU (1.5 mL, 10 mmoles, 1 eq) and stirred for 48 hours. Upon reaction completion, the solution was diluted with diethyl ether and the organic layer washed with



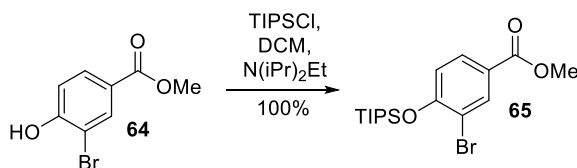
1 M HCl, water, saturated K<sub>2</sub>CO<sub>3</sub> (aq), dried over sodium sulfate, filtered, concentrated and purified. Purification using flash column chromatography provided tert-butyl 4-bromobenzoate in 52% yield: R<sub>f</sub> = 0.66 (20% EtOAc/Hexane, resolved with UV) <sup>1</sup>H-NMR (400 MHz, CDCl<sub>3</sub>) δ 7.83 (d, J = 8.56 Hz, 2H), 7.54 (d, J = 8.52 Hz, 2H), 1.58 (s, 9H); <sup>13</sup>C-NMR (400 MHz, CDCl<sub>3</sub>) δ 165.00, 131.47, 130.99, 130.91, 127.42, 81.47, 28.15



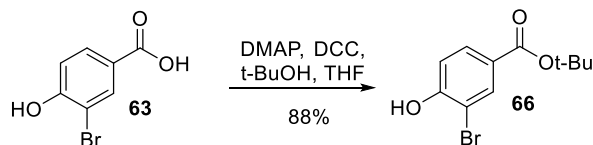
Under an inert atmosphere to a flask cooled to 0° C a solution of isopropylmagnesium bromide (1.2 mL, 1.2 mmol, 1.2 eq, 1 M solution in THF) in THF (2 mL, 0.6 M) was made. n-Butyl lithium (0.96 mL, 2.4 mmol, 2.4 eq, 2.3 M solution in hexanes) was added to reaction vessel and stirred for 10 minutes. The flask was then brought to -78° C and a solution of **60** (0.25 g, 1 mmol, 1 eq) in THF (2 mL, 0.5 M) was added dropwise and stirred for 1 hour. CuCN·2LiCN (0.3 mL, 0.3 mmol, 0.3 eq, 1 M solution in THF) was then added to the reaction vessel followed by **61** (0.48 g, 4 mmol, 4 eq). The solution was then stirred for 0.5 hour and quenched with saturated NH<sub>4</sub>Cl (aq) and the flask was gently brought to room temperature. After addition of a small amount of water to break-up the emulsion, the aqueous layer was extracted with hexane, combined organic extracts dried over sodium sulfate, filtered, concentrated and purified. Purification using flash column chromatography provided **62** in 51% yield: R<sub>f</sub> = 0.56 (20% EtOAc/Hexane, resolved with UV) <sup>1</sup>H-NMR (500 MHz, CDCl<sub>3</sub>) δ 7.92 (d, J = 8.25 Hz, 2H), 7.22 (d, J = 8.35 Hz, 2H), 5.94 (dtq, J = 27.06 Hz, 6.67 Hz, 6.58 Hz, 1H), 5.07 (d, J = 8.10 Hz, 2H), 3.42 (d, J = 6.65 Hz, 2H), 1.59 (s, 9H); <sup>13</sup>C-NMR (500 MHz, CDCl<sub>3</sub>) δ 165.60, 144.71, 136.39, 129.76, 129.42, 128.27, 116.23, 80.56, 65.69, 39.94, 28.01



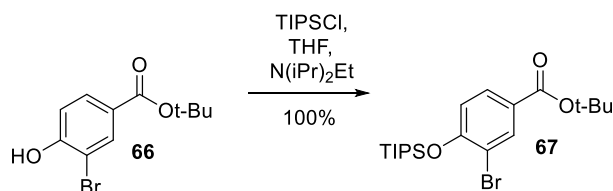
A solution was made of **63** (2.17 g, 10 mmol, 1 eq) in methanol (12.9 mL, 0.8 M). Sulfuric acid (0.1 mL, 2 mmol, 0.2 eq) was added to the reaction vessel and the contents then stirred for 16.5 hours. Upon completion, the solution was concentrated and the residue dissolved in ethyl acetate, washed with saturated  $\text{NaHCO}_3$  (aq, 3x), brine, dried over sodium sulfate, filtered, concentrated and purified. Purification using flash column chromatography provided **64** in 88% yield:  $R_f = 0.62$  (50% EtOAc/Hexane, resolved with UV)  $^1\text{H-NMR}$  (400 MHz,  $\text{CDCl}_3$ )  $\delta$  8.19 (d,  $J = 1.96$  Hz, 1H), 7.92 (dd,  $J = 10.52$  Hz, 6.56 Hz, 1H), 7.05 (d,  $J = 8.52$  Hz, 1H), 5.94 (s, 1H), 3.89 (s, 3H);  $^{13}\text{C-NMR}$  (400 MHz,  $\text{CDCl}_3$ )  $\delta$  165.59, 156.15, 133.92, 131.04, 124.07, 115.78, 110.09, 52.21



Under an inert atmosphere. A solution of the **64** (1.61 g, 7 mmol, 1 eq) in DCM (35 mL, 0.2 M) was made by gently heating to 40-50° C to facilitate complete dissolution. TIPSCl (1.79 mL, 8.4 mmol, 1.2 eq) and  $\text{N}(\text{iPr})_2\text{Et}$  (3.65 mL, 21 mmol, 3 eq) were then added to the reaction vessel and the resulting solution stirred for 3.5 hours at room temperature. Upon completion, the solution was washed with saturated  $\text{NH}_4\text{Cl}$  (aq),  $\text{NaHCO}_3$ , brine, dried over magnesium sulfate, filtered, concentrated and purified. Purification using flash column chromatography provided **65** in 100% yield:  $R_f = 0.5$  (20% EtOAc/Hexane, resolved with UV)  $^1\text{H-NMR}$  (400 MHz,  $\text{CDCl}_3$ )  $\delta$  8.22 (d,  $J = 2.08$  Hz, 1H), 7.86 (dd,  $J = 2.10$  Hz, 8.50 Hz, 1H), 6.90 (d,  $J = 8.52$ , 1H), 3.88 (s, 3H), 1.38-1.30 (m, 3H), 1.13 (d,  $J = 7.40$  Hz, 18H);  $^{13}\text{C-NMR}$  (400 MHz,  $\text{CDCl}_3$ )  $\delta$  165.8, 157.1, 135.1, 130.1, 123.9, 118.9, 114.9, 52.1, 17.9, 12.9

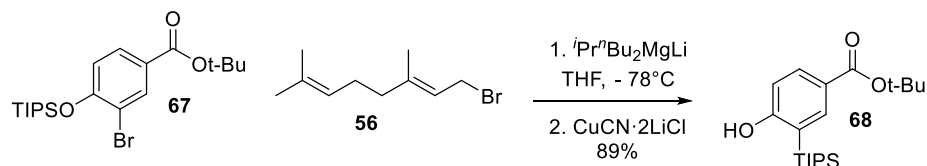


Under an inert atmosphere, a solution of **63** (2.17 g, 10 mmol, 1 eq) and DMAP (0.06 g, 0.5 mmol, 0.05 eq) in tert-butanol (63 mL, 0.16 M) was made. A solution of DCC (2.47 g, 12 mmol, 1.2 eq) in THF (21 mL, 0.47 M) was then added to the reaction vessel and the resulting mixture stirred for 12 hours. The contents of the flask were then concentrated under reduced pressure and the residue dissolved in diethyl ether (211 mL, 0.05 M) and stirred with oxalic acid (2.7 g, 30 mmol, 3 eq). The resulting mixture was then filtered through a short pad of silica. The filtrate was then washed with saturated NaHCO<sub>3</sub> (aq), water, brine, dried over sodium sulfate, filtered, concentrated and purified. Purification using flash column chromatography provided **66** in 88% yield: *R*<sub>f</sub> = 0.35 (20% EtOAc/Hexane, resolved with UV) <sup>1</sup>H-NMR (400 MHz, CDCl<sub>3</sub>) δ 8.11 (d, *J* = 2.00 Hz, 1H), 7.86 (dd, *J* = 2.02 Hz, 8.50 Hz, 1H), 7.02 (d, *J* = 8.52 Hz, 1H), 5.95 (s, 1H), 1.57 (s, 9H); <sup>13</sup>C-NMR (400 MHz, CDCl<sub>3</sub>) δ 164.29, 155.74, 133.71, 130.85, 125.92, 115.56, 109.90, 81.36, 28.19

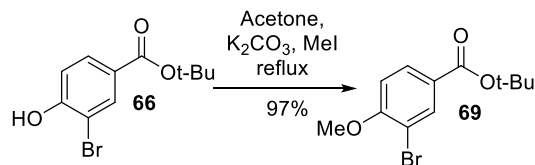


Under an inert atmosphere. A solution of the substrate (2.32 g, 8.5 mmol, 1 eq) in THF (42.5 mL, 0.2 M) was made. TIPSCl (1.96 g, 10.2 mmol, 1.2 eq) and N(iPr)<sub>2</sub>Et (3.29 g, 25.5 mmol, 3 eq) were then added to the reaction vessel and the resulting solution stirred for 5 hours at room temperature. Upon completion, the solution was washed with saturated NH<sub>4</sub>Cl (aq), NaHCO<sub>3</sub>, brine, dried over magnesium sulfate, filtered, concentrated and purified. Purification using flash column chromatography provided tert-butyl 3-bromo-4-

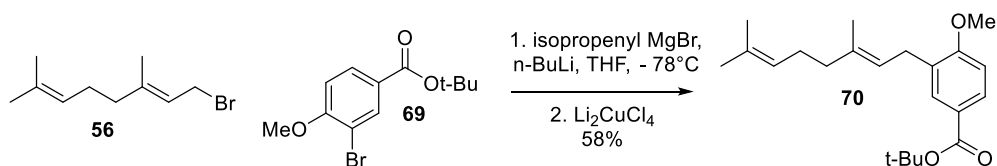
((triisopropylsilyl)oxy)benzoate in 100% yield:  $R_f = 0.8$  (20% EtOAc/Hexane, resolved with UV)  $^1\text{H-NMR}$  (400 MHz,  $\text{CDCl}_3$ )  $\delta$  8.14 (d,  $J = 2.16$  Hz, 1H), 7.80 (dd,  $J = 2.16$  Hz, 8.52 Hz, 1H), 6.87 (d,  $J = 8.52$  Hz, 1H), 1.56 (s, 9H), 1.33 (m, 3H), 1.13 (d,  $J = 7.36$  Hz, 18H);  $^{13}\text{C-NMR}$  (400 MHz,  $\text{CDCl}_3$ )  $\delta$  165.7, 157.1, 135.1, 130.1, 123.9, 118.9, 114.9, 52.1, 17.9, 12.9



Under an inert atmosphere to a flask cooled to  $0^\circ\text{C}$  a solution of isopropylmagnesium bromide (0.6 mL, 0.6 mmol, 1.2 eq) in THF (0.6 M) was made. n-Butyl lithium (0.5 mL, 1.2 mmol, 2.4 eq) was added to reaction vessel and stirred for 10 minutes. The flask was then brought to  $-78^\circ\text{C}$  and a solution of **67** (0.212 g, 0.5 mmol, 1 eq) in THF (2 mL, 0.5 M) was added dropwise and stirred for 1 hour.  $\text{CuCN}\cdot 2\text{LiCN}$  (0.15 mL, 0.15 mmol, 0.3 eq, 1 M solution in THF) was then added to the reaction vessel followed by geranyl bromide (0.43 g, 2 mmol, 4 eq). The solution was then stirred for 0.5 hour and quench with saturated  $\text{NH}_4\text{Cl}$  (aq) and the flask was gently brought to room temperature. After addition of a small amount of water to break-up the emulsion, the aqueous layer was extracted with hexane, combined organic extracts dried over sodium sulfate, filtered, concentrated and purified. Purification using flash column chromatography provided tert-butyl 4-hydroxy-3-(triisopropylsilyl)benzoate in 89% yield:  $R_f = 0.44$  (5% EtOAc/Hexane, resolved with UV)  $^1\text{H-NMR}$  (400 MHz,  $\text{CDCl}_3$ )  $\delta$  8.10 (d, 1H), 7.87 (dd, 1H), 6.70 (d, 1H), 5.55 (s, 1H), 1.57 (s, 9H), 1.54-1.48 (m, 3H), 1.10 (d, 18H)



Under an inert atmosphere, a solution was made consisting of **66** (1.50 g, 5.5 mmol, 1 eq), potassium carbonate (3.80 g, 27.5 mmol, 5 eq), and methyl iodide (8.36 mL, 55 mmol, 10 eq) in acetone (22 mL, 0.25 M). The resulting solution was stirred at reflux for 6 hours. Upon reaction completion, the mixture was cooled, filtered, concentrated and purified. Purification using flash column chromatography provided **69** in 97% yield:  $R_f = 0.52$  (20% EtOAc/Hexane, resolved with UV)  $^1\text{H-NMR}$  (400 MHz,  $\text{CDCl}_3$ )  $\delta$  8.15 (d,  $J = 2.10$  Hz, 1H), 7.93 (dd,  $J = 2.10$  Hz, 8.60 Hz, 1H), 6.89 (d,  $J = 8.65$  Hz, 1H), 3.94 (s, 3H), 1.57 (s, 9H);  $^{13}\text{C-NMR}$  (400 MHz,  $\text{CDCl}_3$ )  $\delta$  164.22, 158.88, 134.44, 130.22, 125.49, 110.67, 81.04, 56.22, 28.02



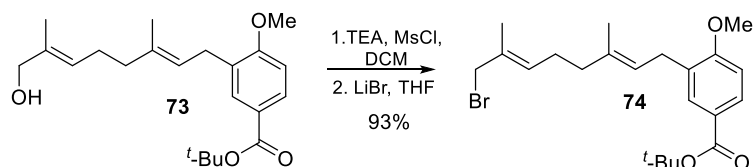
**Optimized:** Under an inert atmosphere to a flask cooled to  $0^\circ\text{C}$  a solution of isopropylmagnesium bromide (15.6 mL, 7.8 mmol, 1.2 eq) in THF (0.3 M) was made. n-Butyl lithium (6.78 mL, 15.6 mmol, 2.4 eq) was added to reaction vessel and stirred for 10 minutes. The flask was then brought to  $-78^\circ\text{C}$  and a solution of **69** (1.86 g, 6.5 mmol, 1 eq) in THF (1 M) was added dropwise and stirred for 1 hour.  $\text{Li}_2\text{CuCl}_4$  (19.5 mL, 1.95 mmol, 0.3 eq, 1 M solution in THF) was then added to the reaction vessel followed by **56** (5.16 mL, 26 mmol, 4 eq). The solution was then stirred for 0.5 hour and quench with saturated  $\text{NH}_4\text{Cl}$  (aq) and the flask was gently brought to room temperature. After addition of a small amount of water to break-up the emulsion, the aqueous layer was extracted with hexane, combined organic extracts dried over sodium sulfate, filtered, concentrated and purified. Purification using flash column chromatography in sequence

(1<sup>st</sup> column: 3% EtOAc/Hexane; 2<sup>nd</sup> column: 1% Et<sub>2</sub>O/Petroleum ether) provided **70** in 53% yield:  $R_f$  = 0.48 (10% Et<sub>2</sub>O/Hexane, resolved with UV and vanillin stain) <sup>1</sup>H-NMR (500 MHz, CDCl<sub>3</sub>)  $\delta$  7.84 (dd,  $J$  = 2.27 Hz, 8.52 Hz, 1H) 7.77 (d,  $J$  = 2.15, 1H), 6.83 (d,  $J$  = 8.60 Hz, 1H), 5.31 (dt,  $J$  = 1.25 Hz, 7.30 Hz, 1H), 5.11 (tt,  $J$  = 1.37 Hz, 10.26 Hz, 1H), 3.87 (s, 3H), 3.33 (d,  $J$  = 7.25 Hz, 2H), 2.11 (m, 2H), 2.04 (m, 2H), 1.70 (s, 3H), 1.66 (s, 3H), 1.59 (s, 3H), 1.57 (s, 9H); <sup>13</sup>C-NMR (500 MHz, CDCl<sub>3</sub>)  $\delta$  165.7, 160.5, 136.3, 131.1, 130.4, 129.6, 128.9, 124.1, 123.8, 121.5, 109.1, 80.1, 55.3, 39.6, 28.0, 26.6, 25.5, 17.5, 15.9

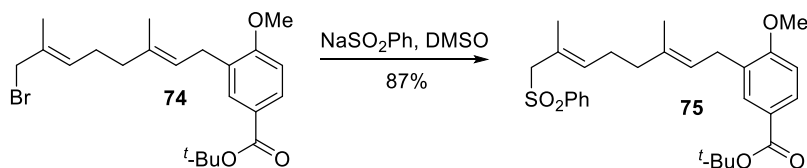


Salicylic acid (30 mg, 0.22 mmoles, 0.1 eq), SeO<sub>2</sub> (7 mg, 0.06 mmoles, 0.03 eq) then DCM (3.3 mL, 0.62 M) was added to a flask at room temperature. TBHP (0.75 mL, 5.5 mmoles, 2.5 eq, 70% in H<sub>2</sub>O) was added to the resulting solution and stirred for 15 minutes. **70** (0.75 g, 2.2 mmoles, 1 eq) was then added and the mixture was stirred for 20 hours. Flask contents was then concentrated under reduced pressure below 30°C. The residue was then diluted in Et<sub>2</sub>O and the organic layer was then washed with 10% KOH (3x), H<sub>2</sub>O (3x), and brine (1x). The ether layer was then dried over magnesium sulfate, filtered and concentrated. Purification using chromatography provided tert-butyl 3-((2E,6E)-8-hydroxy-3,7-dimethylocta-2,6-dien-1-yl)-4-methoxybenzoate in 24% yield:  $R_f$  = 0.23 (20% EtOAc/Hexane, resolved with vanillin stain) <sup>1</sup>H-NMR (500 MHz, CDCl<sub>3</sub>)  $\delta$  7.83 (dd,  $J$  = 2.20 Hz, 8.50 Hz, 1H), 7.77 (d,  $J$  = 2.20 Hz, 1H), 6.82 (d,  $J$  = 8.60 Hz, 1H), 5.42 (dt,  $J$  = 1.32 Hz, 6.86 Hz, 1H), 5.32 (dt,  $J$  = 1.22 Hz, 7.36 Hz, 1H), 3.98 (d,  $J$  = 7.30 Hz, 2H), 3.87 (s, 3H), 3.33 (d, 2H), 2.20 (m, 2H), 2.12 (m, 2H), 1.77 (t, 1H), 1.69 (s, 3H), 1.64 (s, 3H), 1.58 (s, 1H), 1.57 (s, 9H); <sup>13</sup>C-NMR (500 MHz, CDCl<sub>3</sub>)  $\delta$  165.9, 160.5, 136.1, 134.9,

130.3, 129.5, 128.8, 125.0, 123.7, 121.7, 109.0, 80.3, 68.4, 55.3, 39.0, 28.0, 27.8, 25.6, 15.8, 13.5



Under an inert atmosphere, a solution of **73** (0.360 g, 1 mmole, 1 eq) in DCM (4.16 mL, 0.24 M) was prepared and then cooled to -40°C then add TEA (0.2787 mL, 2 mmoles, 2 eq). Add MsCl (0.1548 mL, 2 mmoles, 2 eq) dropwise then stir for 90 minutes. Get flask to -15 °C then add a solution of LiBr (0.2171 g, 2.5 mmoles, 2.5 eq) in THF (1 mL, 1 M) and stir the resulting solution overnight. Quench with saturated NH<sub>4</sub>Cl (aq), extract with DCM, dry over sodium sulfate, filter, and concentrate. Crude **74** was provided in 93% yield. R<sub>f</sub> = 0.8 (20% EtOAc/Hexane, resolved with UV and vanillin stain)

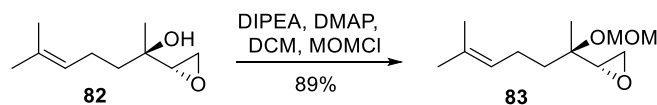


Under an inert atmosphere, stir NaSO<sub>2</sub>Ph (0.4104 g, 2.5 mmoles, 2.5 eq) in DMSO (10 mL, 0.1 M) until complete dissolution. Add **74** (0.4233 g, 1 mmole, 1 eq) slowly and stir resulting solution at room temperature overnight. To stop reaction, add water, extract desired product into DCM, wash with brine (2x), dry over magnesium sulfate, filter, concentrate and purify. Purification with flash column chromatography provided **75** in 87% yield. R<sub>f</sub> = 0.34 (20% EtOAc/Hexane, resolved with UV and vanillin stain) <sup>1</sup>H-NMR (500 MHz, CDCl<sub>3</sub>) δ 7.82 (d, J = 7.75 Hz, 3H), 7.71 (d, J = 1.95 Hz, 1H), 7.61 (t, J = 7.37 Hz, 1H), 7.50 (t, J = 7.75 Hz, 2H), 6.83 (t, J = 8.25 Hz, 1H), 5.18 (t, J = 7.25 Hz, 1H), 5.03 (t, J = 7.15 Hz, 1H), 3.87 (s, 2H), 3.72 (s, 1H), 3.28 (d, J = 7.30 Hz, 2H), 2.07 (t, J = 7.62 Hz, 2H), 1.87 (t, J = 7.55 Hz, 2H), 1.75 (d, 2H), 1.62 (s, 2H), 1.59 (s, 1H), 1.57 (s, 9H), 1.55

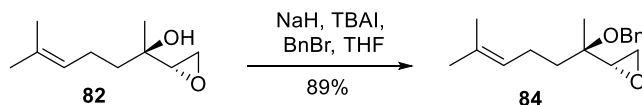
(s, 2H);  $^{13}\text{C}$ -NMR (500 MHz,  $\text{CDCl}_3$ )  $\delta$  165.7, 160.5, 138.1, 135.6, 135.4, 133.2, 130.3, 129.3, 128.9, 128.6, 128.3, 123.8, 123.2, 122.1, 109.0, 80.2, 65.9, 55.3, 38.4, 28.0, 27.9, 26.5, 16.4, 15.7



### 3.3 Linalool Fragment- Callophycolide A

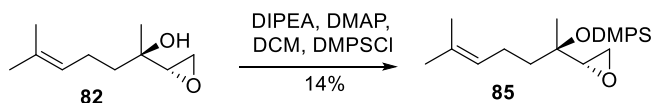


Under an inert atmosphere, a solution was prepared containing **82** (0.170 g, 1 mmole, 1 eq), DIPEA (0.52 mL, 3 mmole, 3 eq), and DMAP (8 mg, 0.07 mmole, 0.07 eq) in DCM (3.45 mL, 0.3 M). The resulting mixture was then cooled to 0° C and MOMCl (0.16 mL, 2.1 mmole, 2.1 eq) was added dropwise. The flask was then gently warmed to room temperature and the contents stirred for 16 hours. Upon completion, the contents were then poured into 10% citric acid (aq), extracted with DCM and then washed with water and brine. The resulting solution was then dried over sodium sulfate, filtered and concentrated under reduced pressure below 30° C. Purification using flash column chromatography provided **83** in 89% yield  $R_f = 0.8$  (30% EtOAc/Hexane resolved with vanillin and UV)  $^1\text{H-NMR}$  (500 MHz,  $\text{CDCl}_3$ )  $\delta$  5.10 (t,  $J = 6.96$  Hz, 1H), 4.79 (d,  $J = 7.28$  Hz, 1H), 4.67 (d,  $J = 7.28$  Hz, 1H), 3.37 (s, 3H), 2.97 (t,  $J = 3.30$  Hz, 1H), 2.75 (m, 1H), 2.70 (t,  $J = 4.56$  Hz, 1H), 2.10 (q,  $J = 8.00$  Hz, 2H), 1.68 (s, 3H), 1.61 (s, 3H), 1.21 (s, 3H) ;  $^{13}\text{C-NMR}$  (500 MHz,  $\text{CDCl}_3$ )  $\delta$  131.74, 124.17, 91.55, 76.70, 75.72, 57.20, 55.38, 44.0, 37.80, 25.69, 21.73, 19.85, 17.62



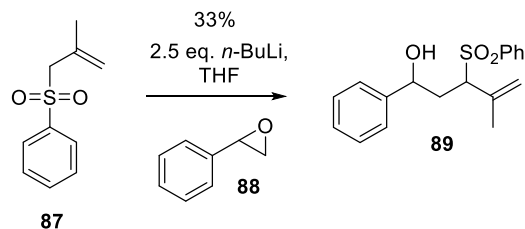
Under an inert atmosphere, a solution was prepared containing **82** (0.2979 g, 1.75 mmole, 1 eq) in THF (9 mL, 0.2 M) and then cooled to 0° C. NaH (0.28 g, 7 mmole, 4 eq) was then added to the reaction vessel and the solution gently warmed to room temperature. Recrystallized TBAI (96 mg, 0.26 mmole, 0.15 eq) and benzyl bromide (0.416 mL, 3.5 mmole, 2 eq) were then added to the flask and the contents were stirred for 22 hours. To quench the reaction, cool the flask to 0° C then add water slowly. The mixture was then

extracted with diethyl ether, dried over sodium sulfate, filtered, concentrated under reduced pressure below 30° C and purified. Purification using flash column chromatography provided **84** in 89% yield  $R_f = 0.65$  (20% EtOAc/Hexane resolved with vanillin and UV)  $^1\text{H-NMR}$  (500 MHz,  $\text{CDCl}_3$ )  $\delta$  7.35 (m, 5H), 5.10 (tquint,  $J = 10.69$  Hz, 1.41 Hz, 1H), 4.64 (dd,  $J = 11.85$  Hz, 52.72 Hz, 2H), 3.70 (dddd,  $J = 4.50$  Hz, 6.07 Hz, 11.20 Hz, 50.37 Hz, 2H), 3.02 (dd,  $J = 4.50$  Hz, 6.05 Hz, 1H), 2.10 (q,  $J = 7.67$  Hz, 2H), 1.67 (s, 3H), 1.64 (m, 1H), 1.60 (s, 3H), 1.50 (m, 1H), 1.25 (s, 3H);  $^{13}\text{C-NMR}$  (500 MHz,  $\text{CDCl}_3$ )  $\delta$  137.7, 131.9, 128.2, 127.5, 127.5, 123.2, 73.0, 68.7, 61.1, 59.8, 38.2, 25.5, 23.4, 17.4, 16.6



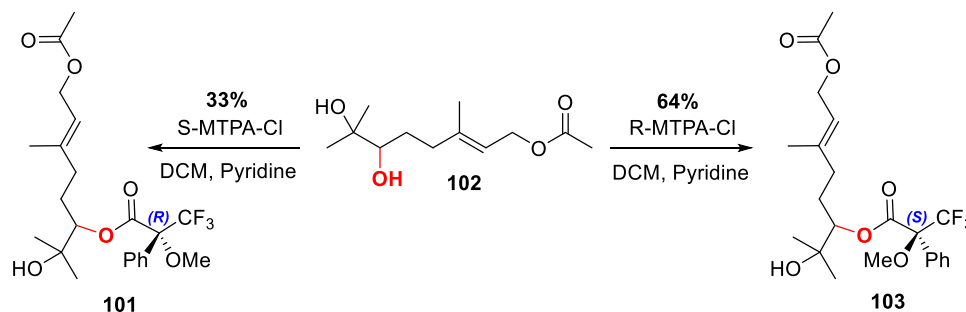
Under an inert atmosphere, a solution was prepared containing **82** (170 mg, 1 mmole, 1 eq), DIPEA (0.52 mL, 3 mmoles, 3 eq), and DMAP (8 mg, 0.07 mmoles, 0.07 eq) in DCM (3.44 mL, 0.3 M). The resulting mixture was then cooled to 0° C and DMPSCI (0.35 mL, 2.1 mmoles, 2.1 eq) was added dropwise. The flask was then gently warmed to room temperature and the contents stirred for 16 hours. Upon completion, the contents were then poured into 10% citric acid (aq), extracted with DCM and then washed with water and brine. The resulting solution was dried over sodium sulfate, filtered and concentrated under reduced pressure below 30° C. Purification using flash column chromatography **85** in 14% yield  $R_f = 0.27$  (20% EtOAc/Hexane resolved with vanillin and UV)  $^1\text{H-NMR}$  (500 MHz,  $\text{CDCl}_3$ )  $\delta$  7.61 (m, 2H), 7.37 (m, 3H), 5.10 (tquint,  $J = 10.72$  Hz, 1.40 Hz, 1H), 2.88 (dd,  $J = 2.72$  Hz, 3.96 Hz, 1H), 2.71 (dd,  $J = 2.72$  Hz, 5.36 Hz, 1H), 2.61 (dd,  $J = 3.96$  Hz, 5.36 Hz, 1H), 2.12 (m, 2H), 1.68 (m, 4H), 1.60 (m, 5H), 1.21 (s, 3H), 0.45 (d,  $J = 3.16$  Hz, 1H), 0.40 (d,  $J = 3.16$  Hz, 4H), 0.34 (d,  $J = 3.24$  Hz, 1H);  $^{13}\text{C-NMR}$  (500 MHz,  $\text{CDCl}_3$ )  $\delta$  140.0, 133.2, 131.5, 129.2, 127.6, 124.3, 73.9, 57.9, 44.3, 41.1, 25.7, 24.4, 22.1, 17.6, 1.2, 1.1

### 3.4 Sulfone Stabilized Anionic Epoxide Ring Opening

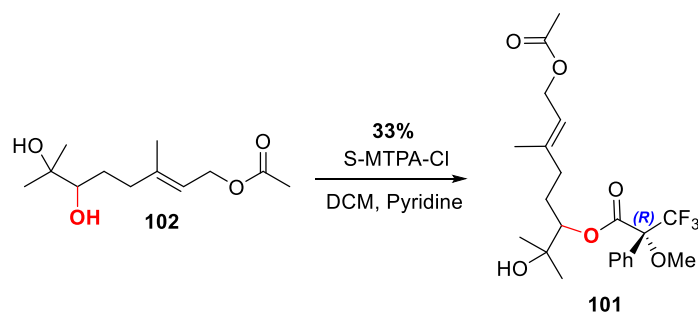


**General Procedure for Sulfone Stabilized Anionic Epoxide Ring Opening:** Under an inert atmosphere at 0° C, a solution was prepared of the **87** (1 eq) in THF (0.25 M). *n*-Butyl lithium (2.5 eq) was added to the solution, the flask gently warmed to room temperature and the resulting solution stirred for 1 hour. The flask was then cooled to -78° C and the epoxide (1 eq) was then added to the reaction vessel and the flask gently warmed to room temperature over a period of 4 hours. The solution was then stirred for 12- 24 hours. Upon completion, the solution was cooled to -78° C and quenched with the addition of 10% NaHSO<sub>4</sub> (aq). After gently warming the flask to room temperature, the solution was diluted with diethyl ether, washed with 10% NaHSO<sub>4</sub> (aq), dried over magnesium sulfate, filtered, concentrated and purified. Purification using flash column chromatography provided **89** in 33% yield. *R*<sub>f</sub> = 0.5 (50% EtOAc/Hexane, resolved with vanillin stain and UV)

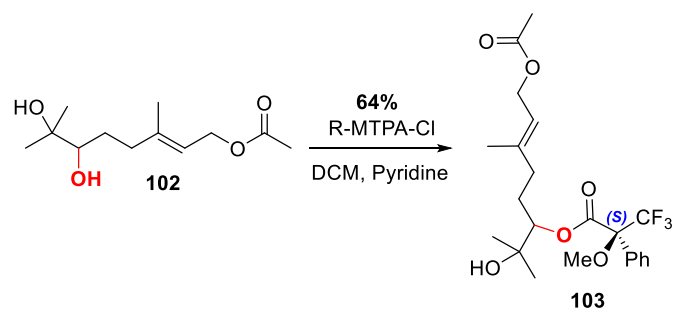
### 3.5 Pyran Formation- Bromophycolides P, Q, and U



**General Mosher ester procedure:** Under an inert atmosphere. A solution was made with **102** (92 mg, 0.4 mmols, 1 eq) and pyridine (0.10 mL, 1.24 mmols, 3.1 eq) in DCM (6.25 mL, 0.06 M). The Mosher acid chloride (0.191 g, 0.76 mmols, 1.9 eq) was then added to the solution and stirred for 2 hours at room temperature. The contents were then poured into a separatory funnel with diethyl ether and water. The aqueous layer was further extracted with diethyl ether and combined organic fractions dried over sodium sulfate, filtered, concentrated, and purified. Purification using flash column chromatography provided **101** in 33% yield  $R_f = 0.63$  (50% EtOAc/Hexane, resolved with vanillin stain); **103** in 64% yield  $R_f = 0.63$  (50% EtOAc/Hexane, resolved with vanillin stain)



$^1\text{H-NMR}$  (400 MHz,  $\text{CDCl}_3$ )  $\delta$  7.59 (m, 2H), 7.41 (m, 3H), 5.29 (dt,  $J = 1.22$  Hz, 7.04 Hz, 1H), 4.97 (dd,  $J = 2.24$  Hz, 9.88 Hz, 1H), 4.57 (d,  $J = 7.04$  Hz, 1H), 3.55 (s, 4H), 3.21 (br, 1H), 2.05 (s, 3H), 2.01 (t,  $J = 7.96$  Hz, 2H), 1.86 (m, 1H), 1.69 (m, 1H), 1.65 (s, 3H), 1.17 (s, 3H), 1.13 (s, 3H);  $^{13}\text{C-NMR}$  (400 MHz,  $\text{CDCl}_3$ )  $\delta$  171.37, 166.42, 140.75, 131.96, 129.77, 129.75, 128.54, 128.49, 127.45, 119.19, 82.32, 72.52, 61.29, 55.47, 35.88, 28.12, 26.04, 24.66, 21.05, 16.42



$^1\text{H-NMR}$  (400 MHz,  $\text{CDCl}_3$ )  $\delta$  7.62 (m, 2H), 7.40 (m, 3H), 5.24 (dt,  $J = 1.24$  Hz, 7.06 Hz, 1H), 4.97 (dd,  $J = 2.18$  Hz, 10.14 Hz, 1H), 4.54 (d,  $J = 7.08$  Hz, 2H), 3.56 (d,  $J = 1.20$  Hz, 3H) 2.04 (s, 3H), 1.91 (t,  $J = 7.94$  Hz, 2H), 1.74 (m, 1H), 1.65 (m, 2H), 1.62 (m, 3H), 1.21 (s, 3H), 1.15 (s, 3H) ;  $^{13}\text{C-NMR}$  (400 MHz,  $\text{CDCl}_3$ )  $\delta$  171.12, 166.93, 140.74, 132.06, 129.70, 128.46, 127.62, 119.06, 82.18, 72.57, 61.20, 55.50, 35.57, 28.18, 26.85, 23.95, 21.04, 16.39

## **APPENDIX A- NMR DATA**

Figure 38 HNMR of 38

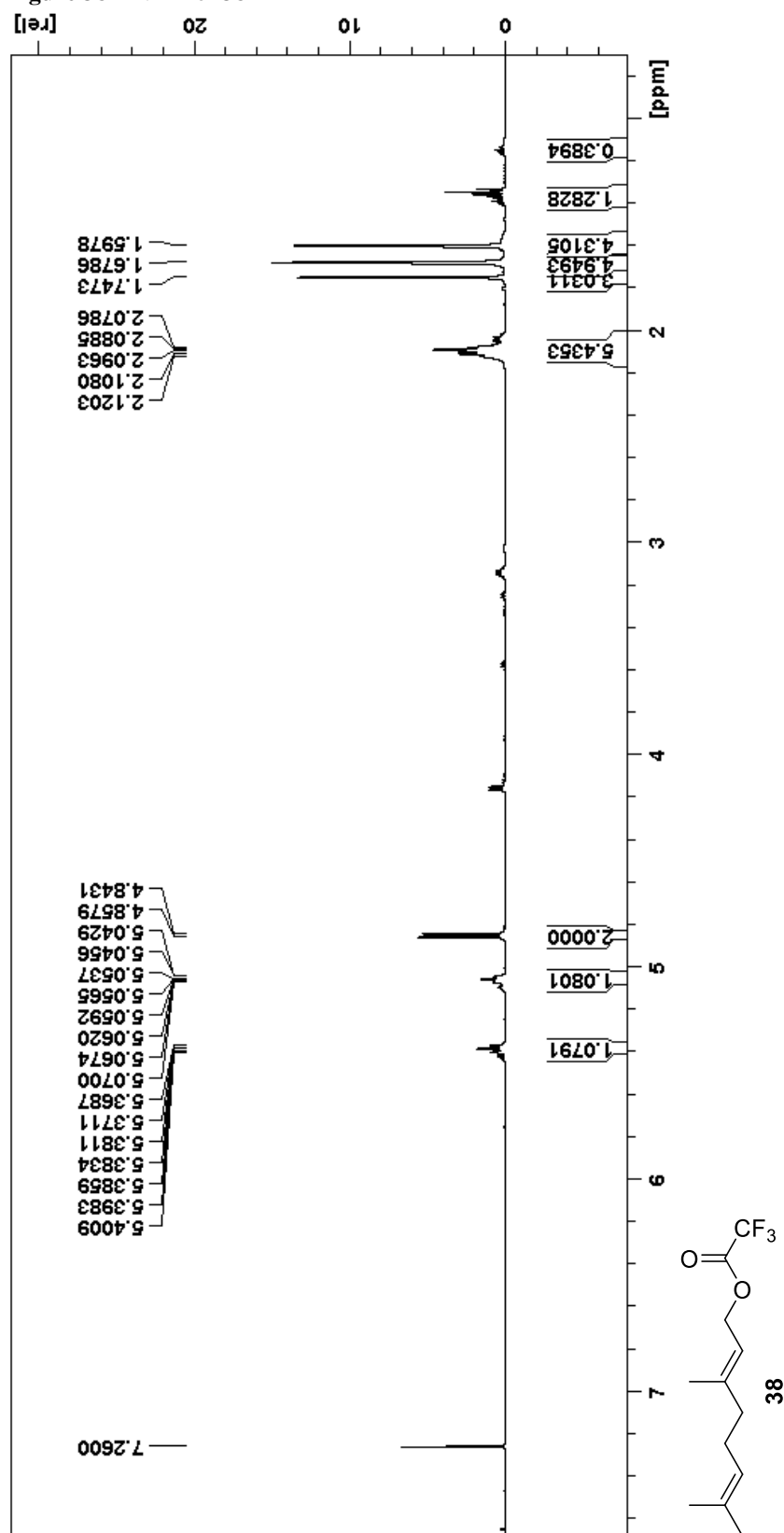


Figure 39 HNMR of 36

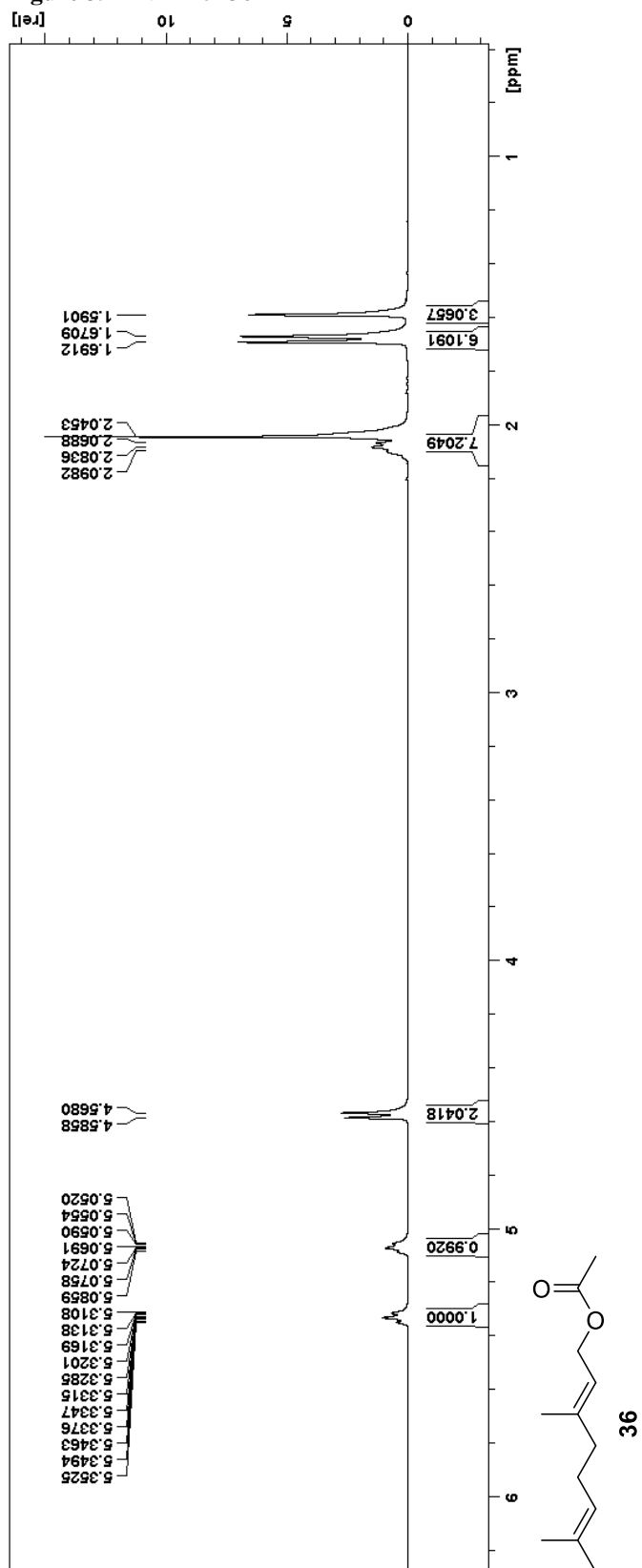




Figure 40 HNMR of 43

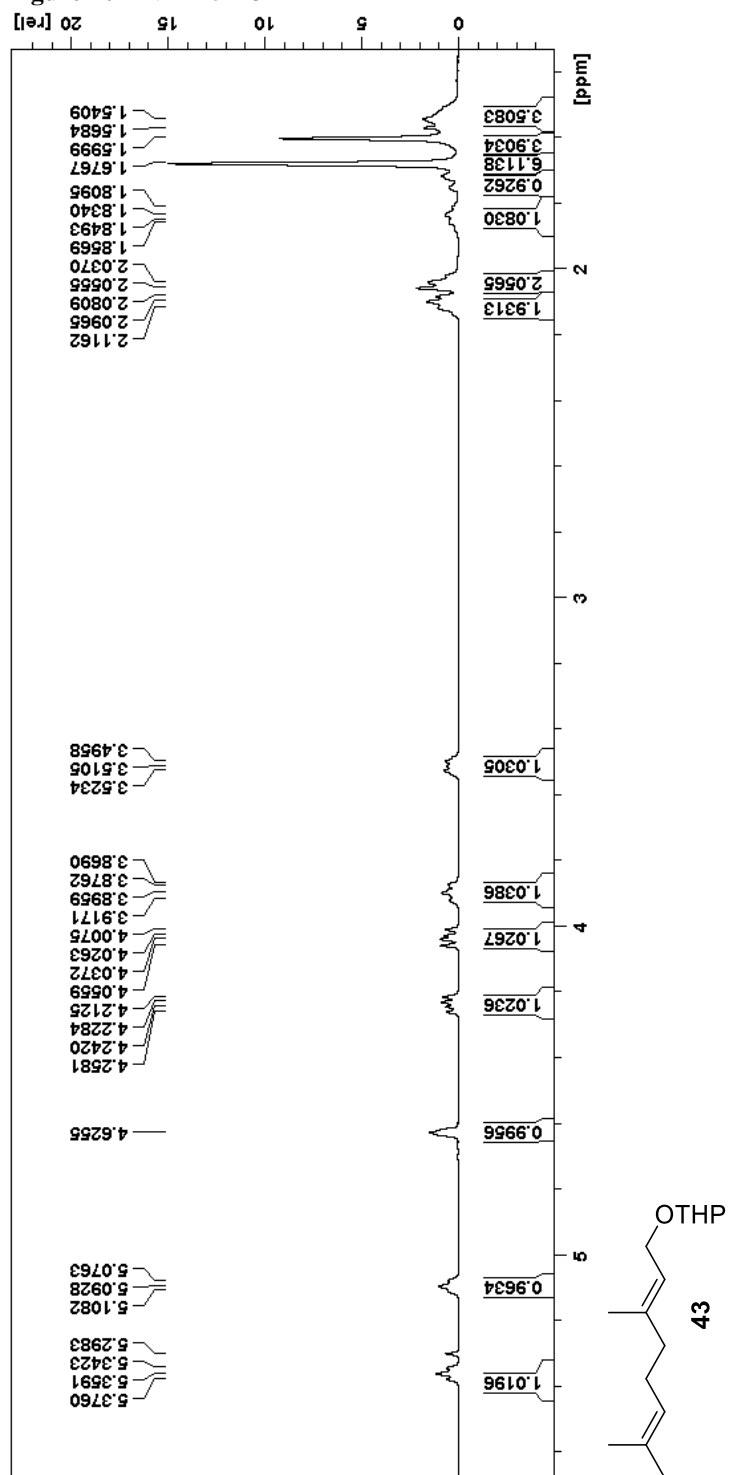


Figure 41 HNMR of 44

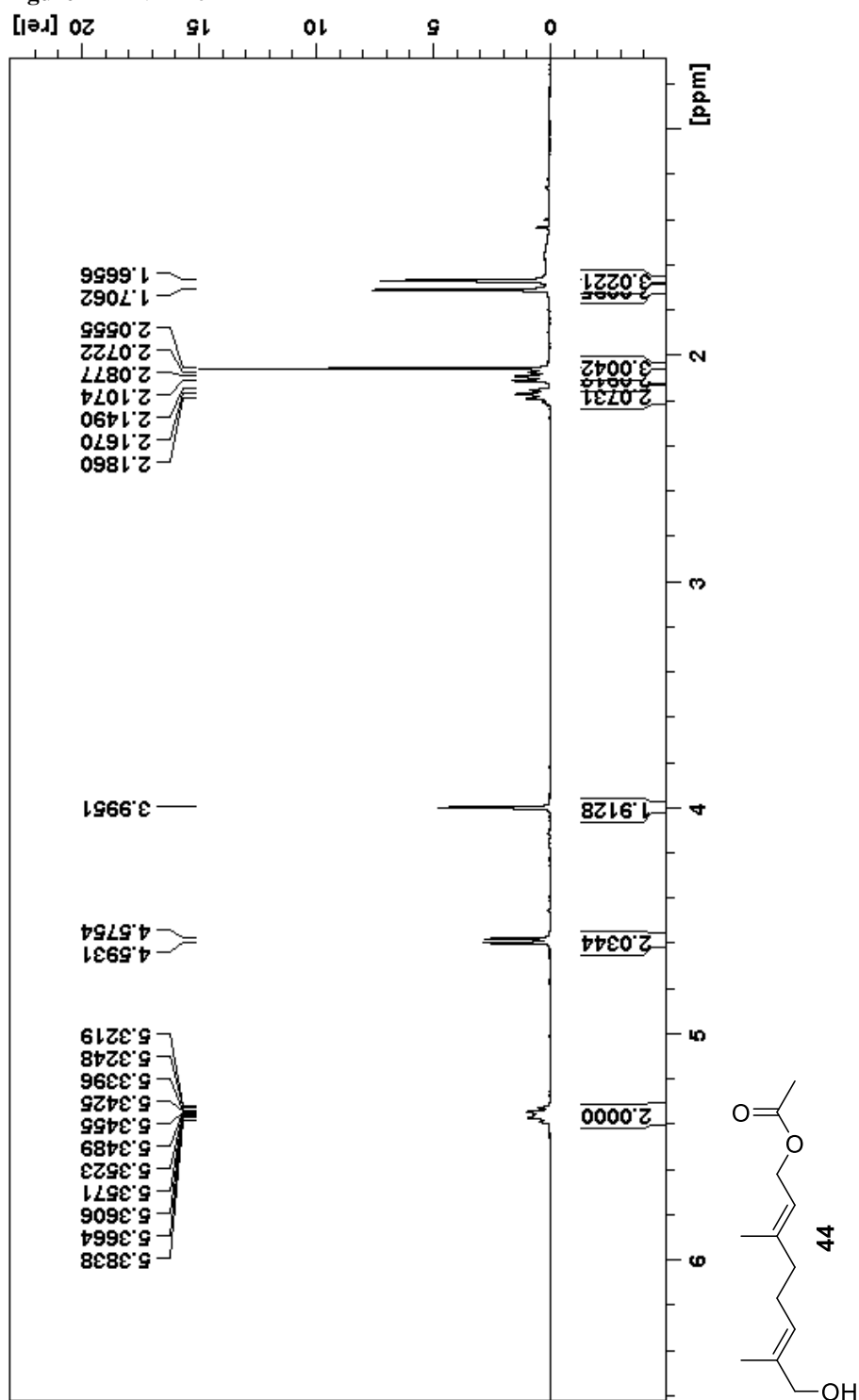


Figure 42 HNMR of 47

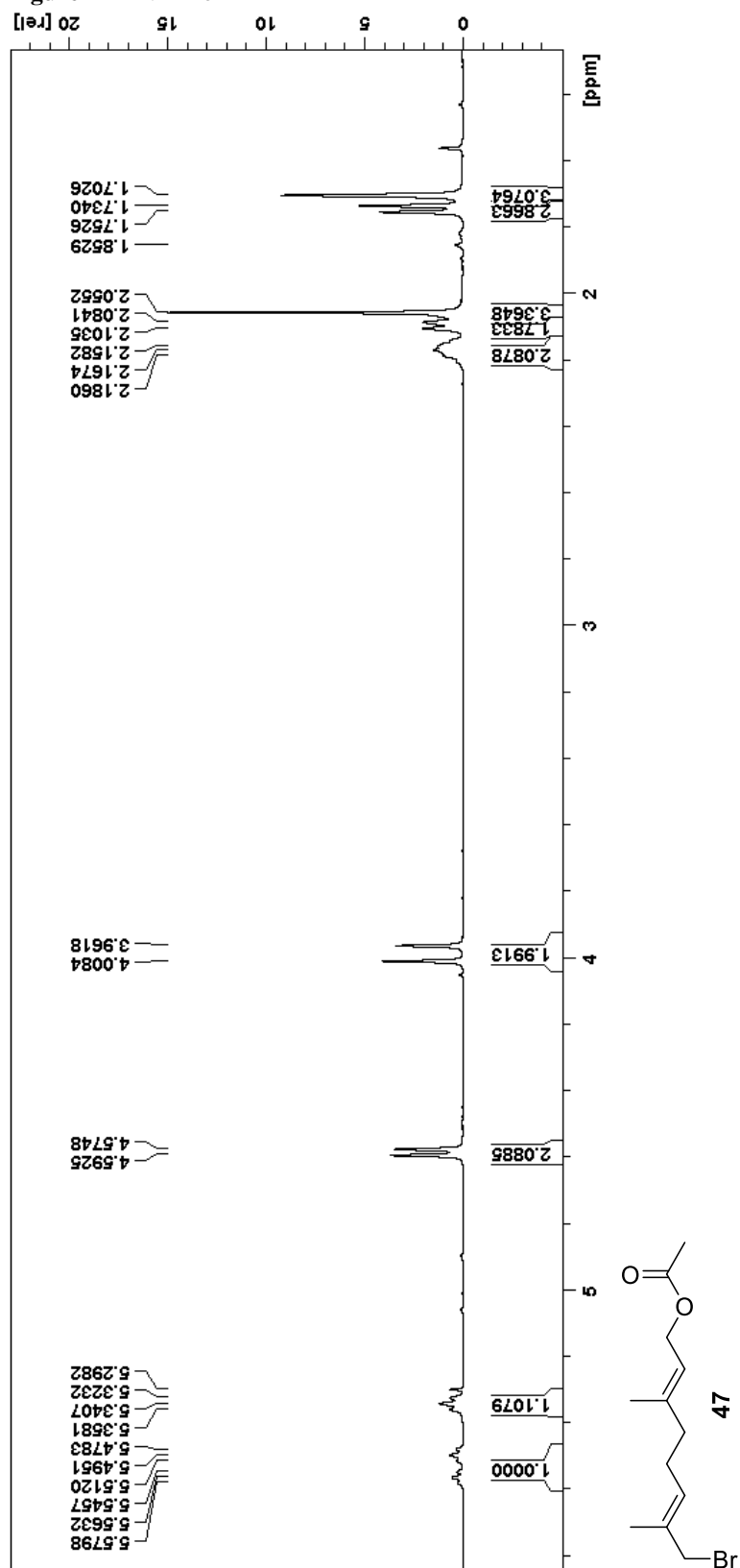


Figure 43 CNMR of 47

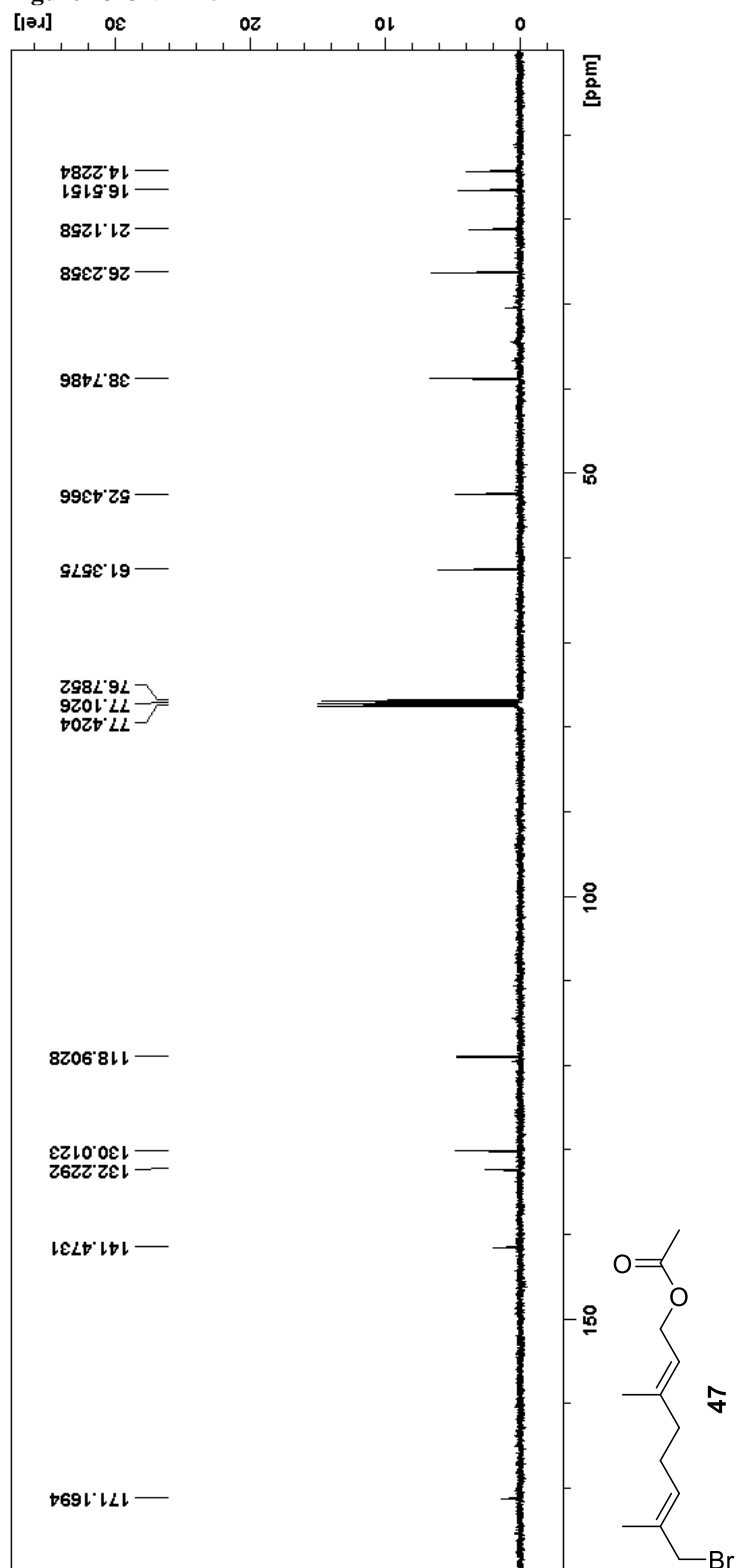


Figure 44 HNMR of 46

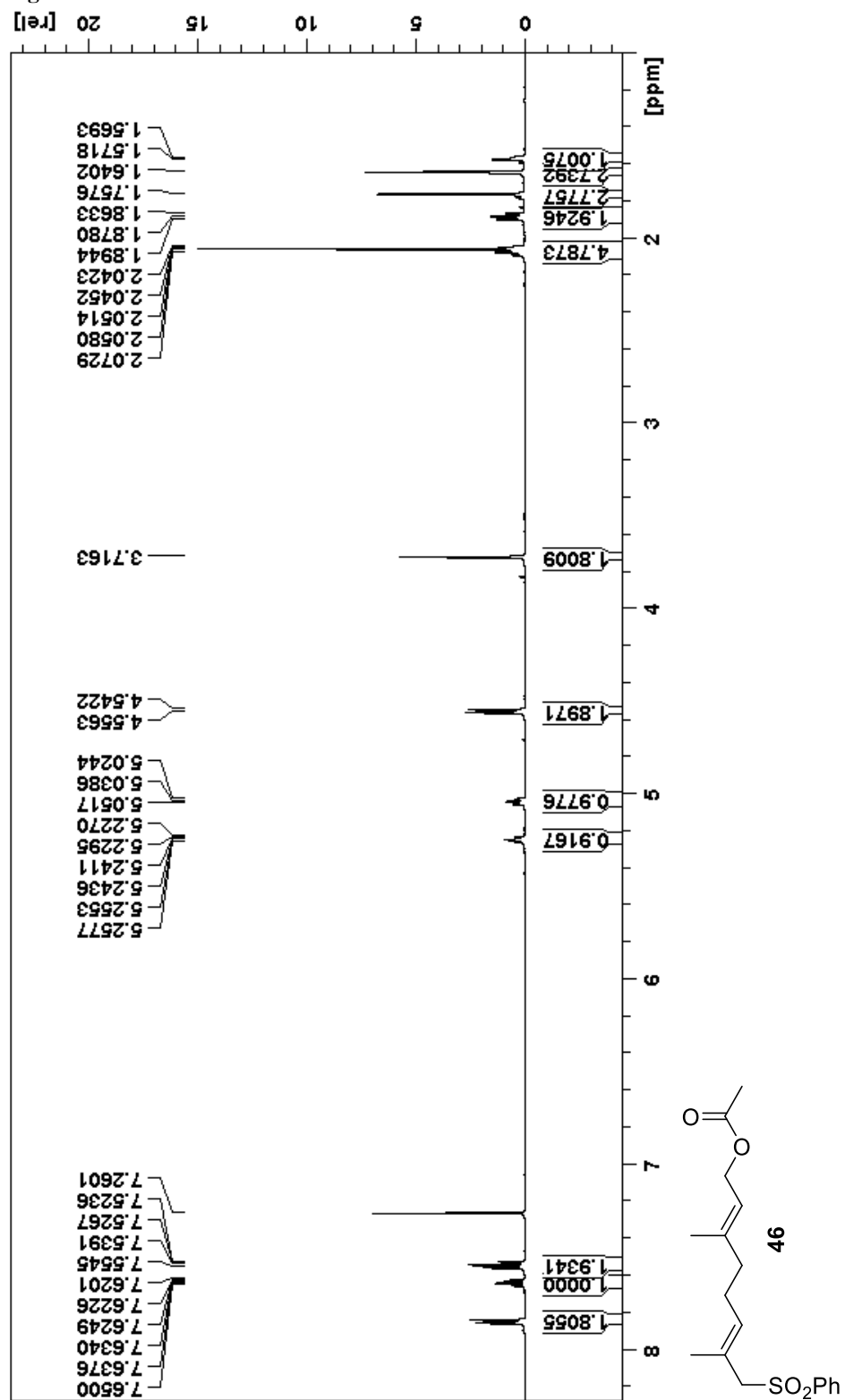


Figure 45 CNMR of 46

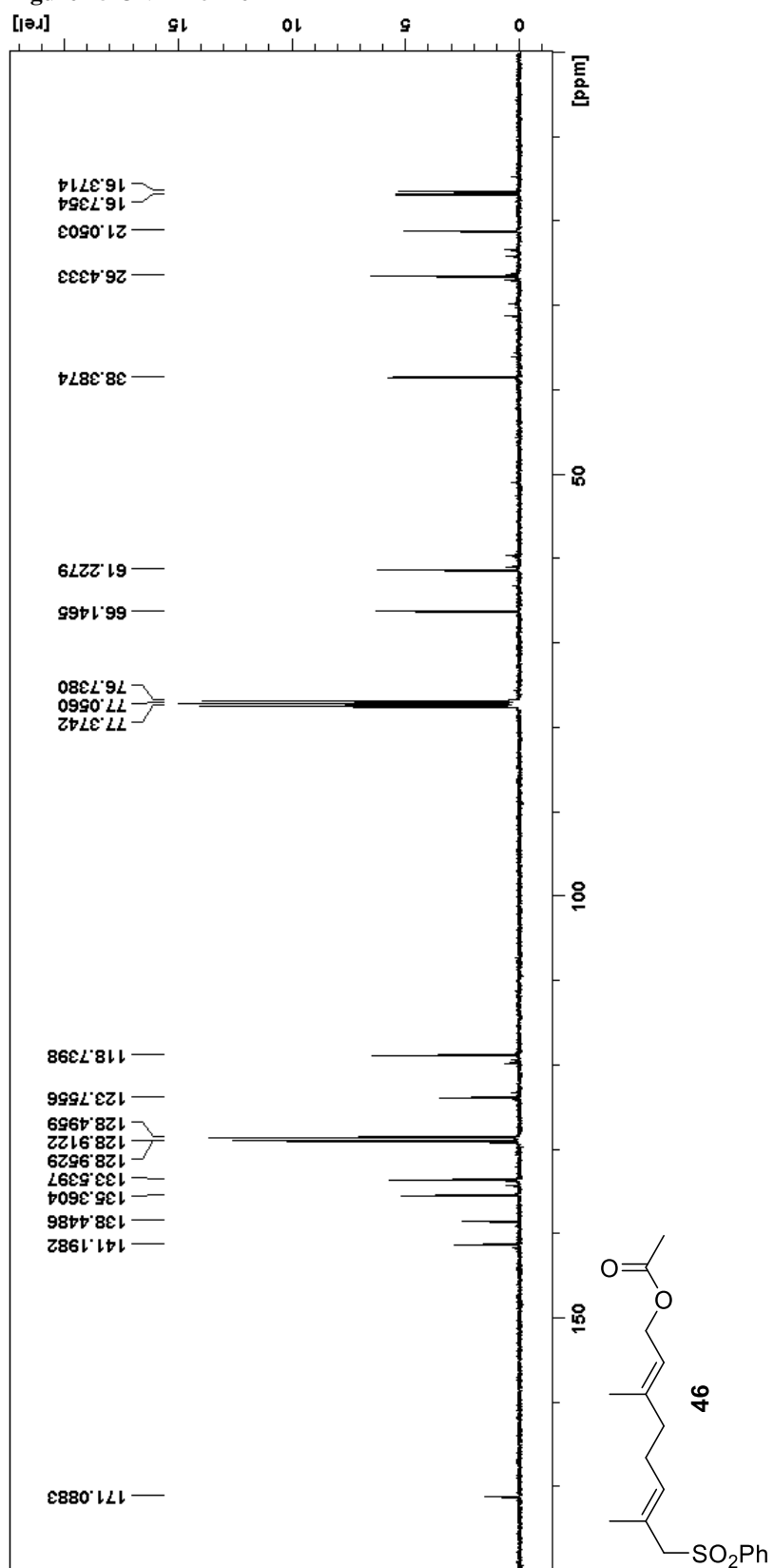


Figure 46 HNMR of 55

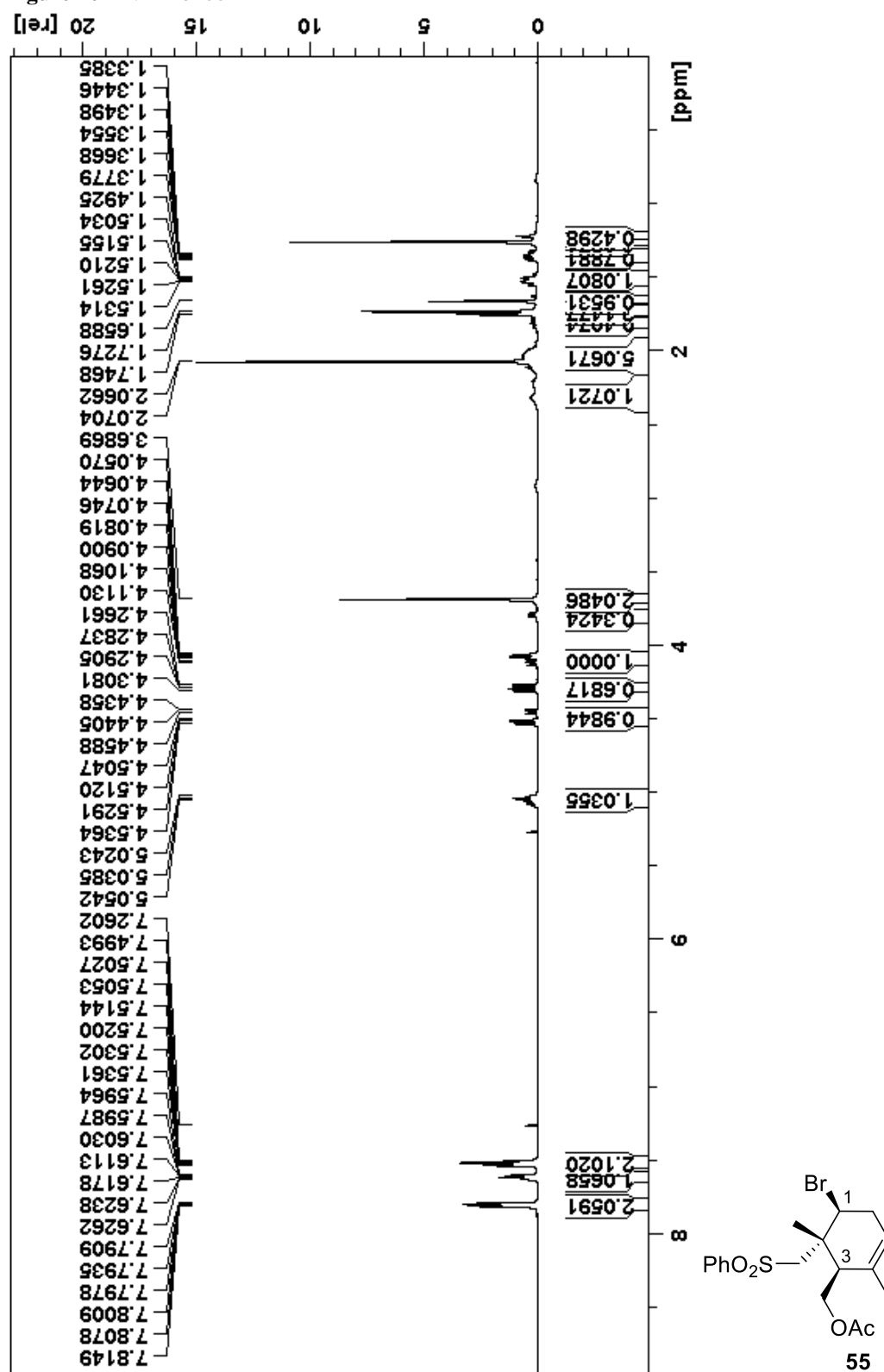


Figure 47 CNMR of 55

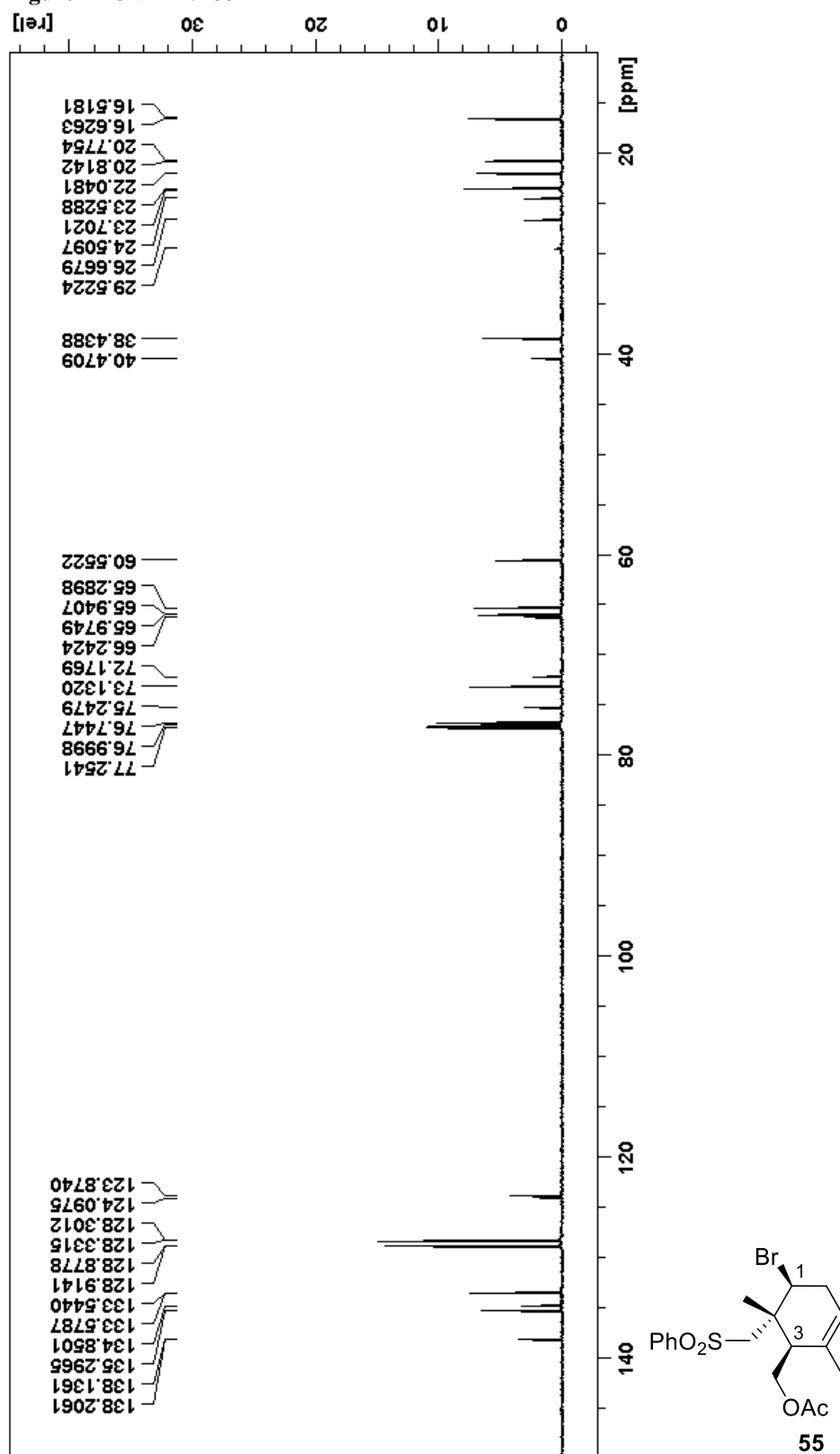




Figure 48 HNMR of 54

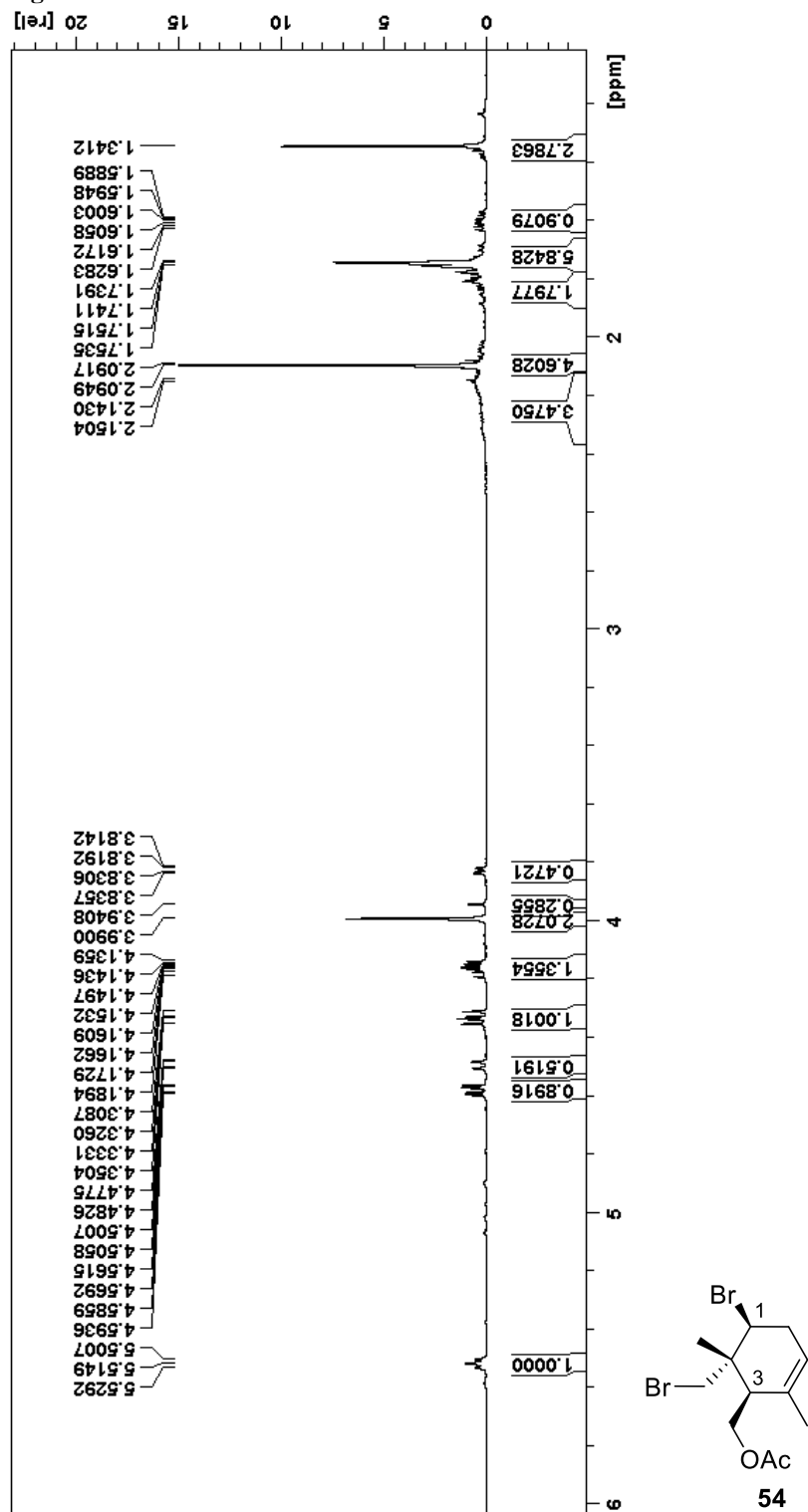


Figure 49 CNMR of 54

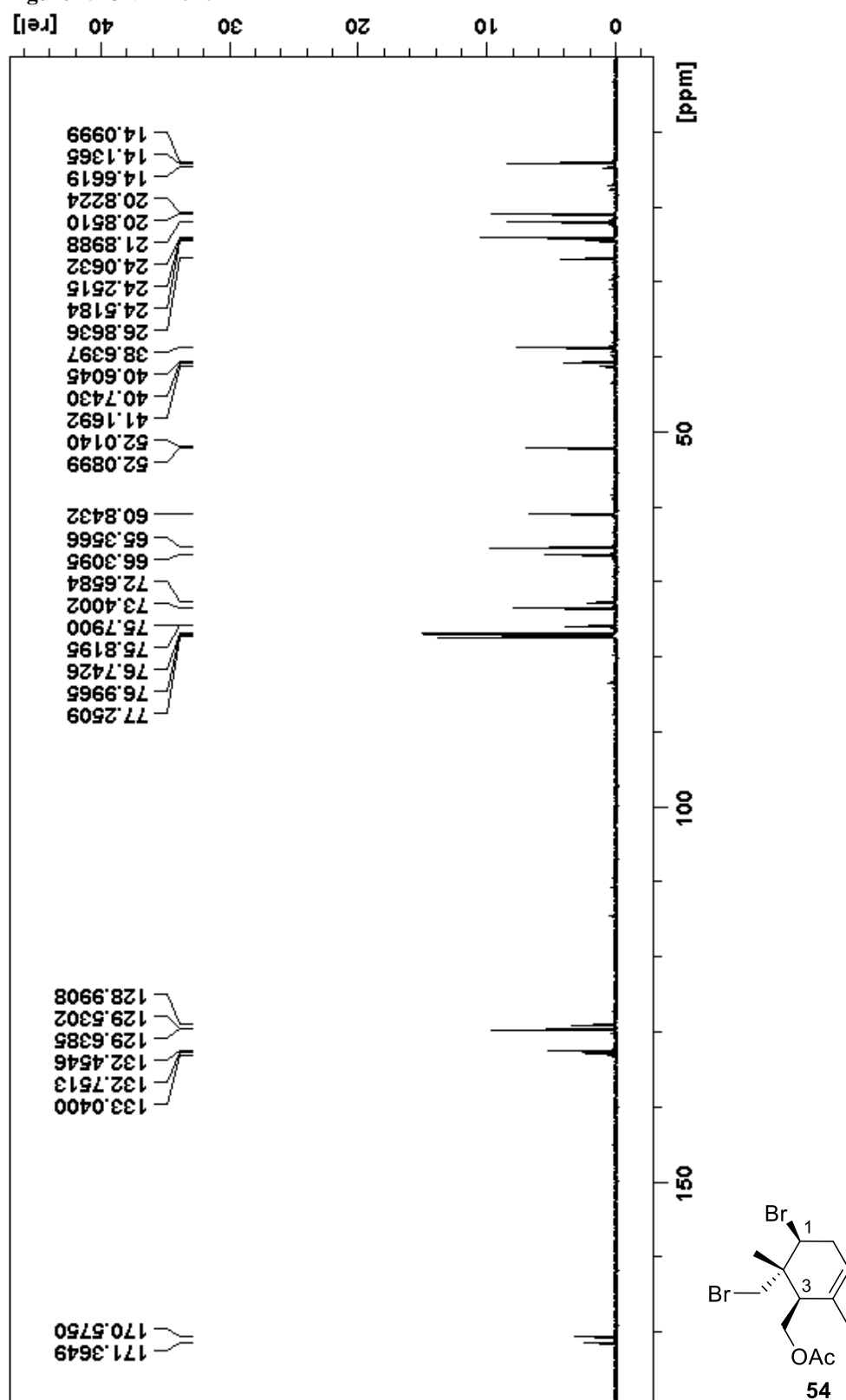


Figure 50 HNMR of 56

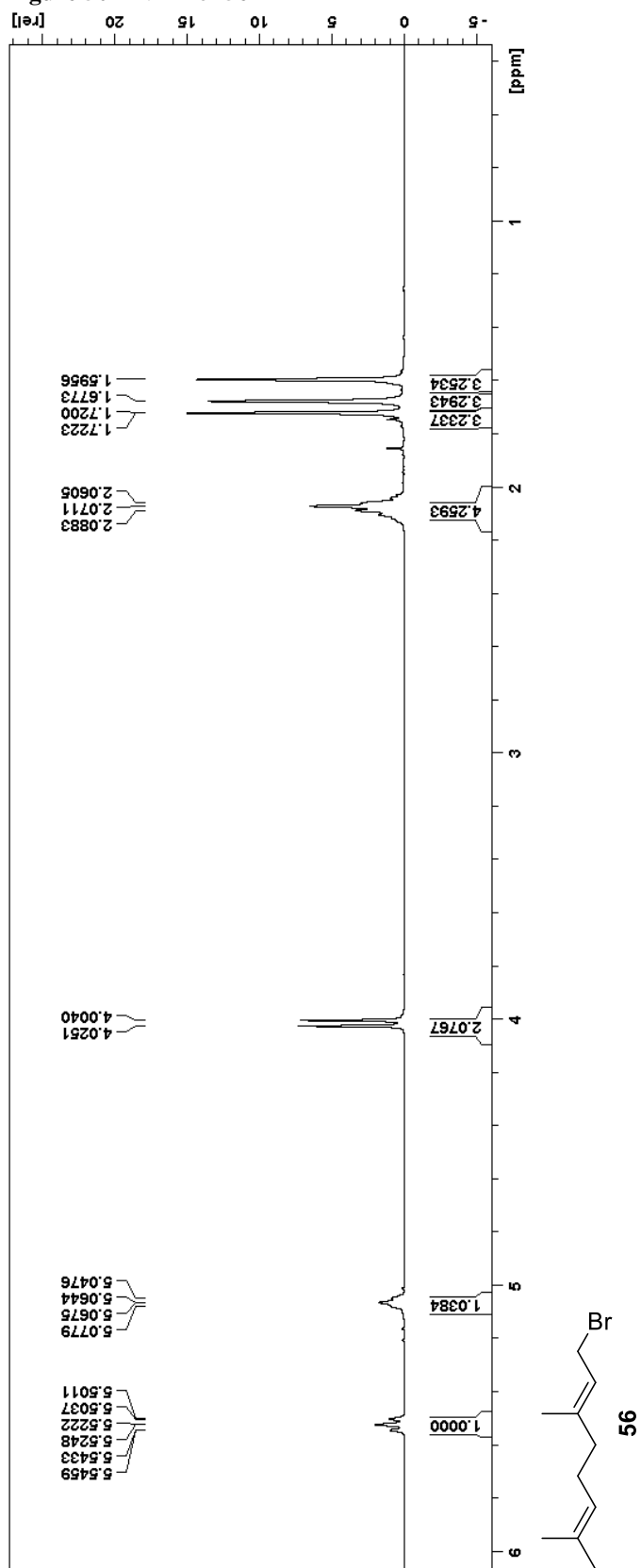


Figure 51 CNMR of 56

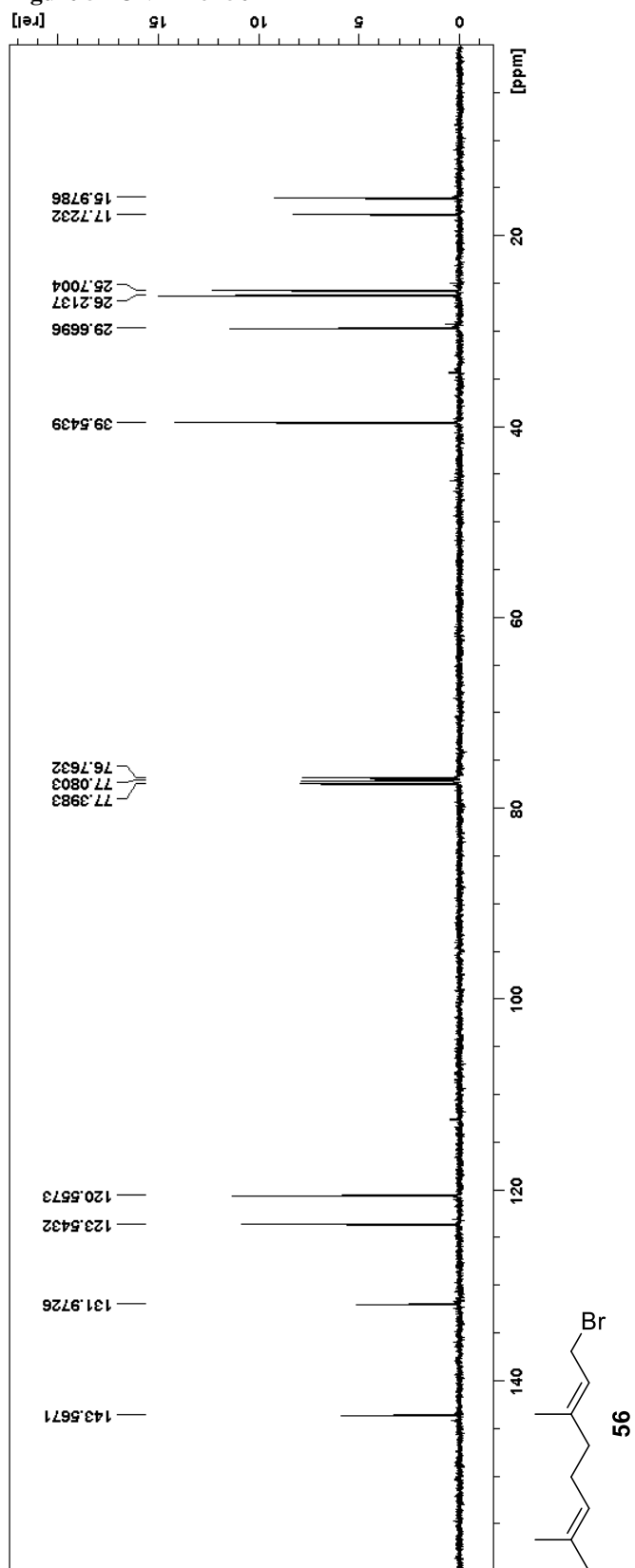


Figure 52 HNMR of 60

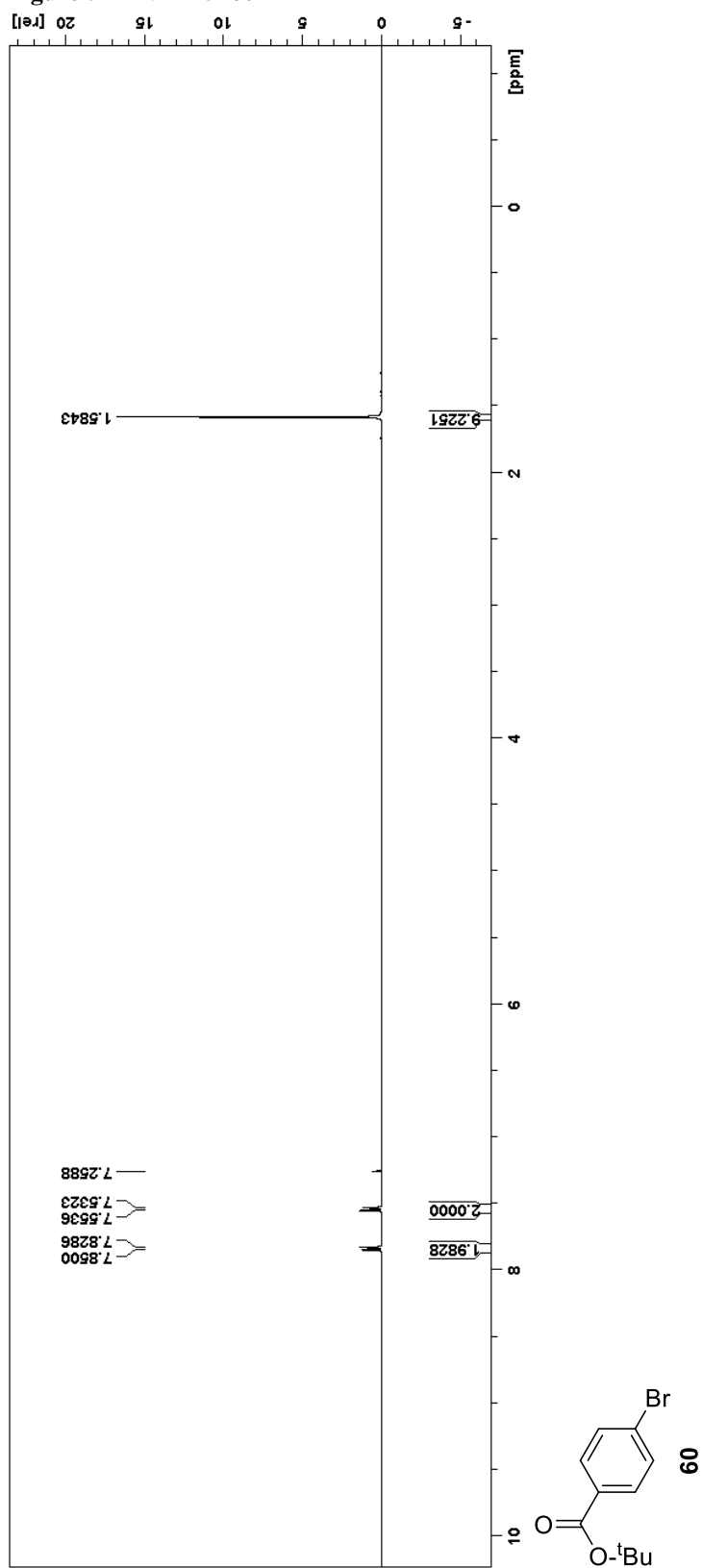


Figure 53 CNMR of 60

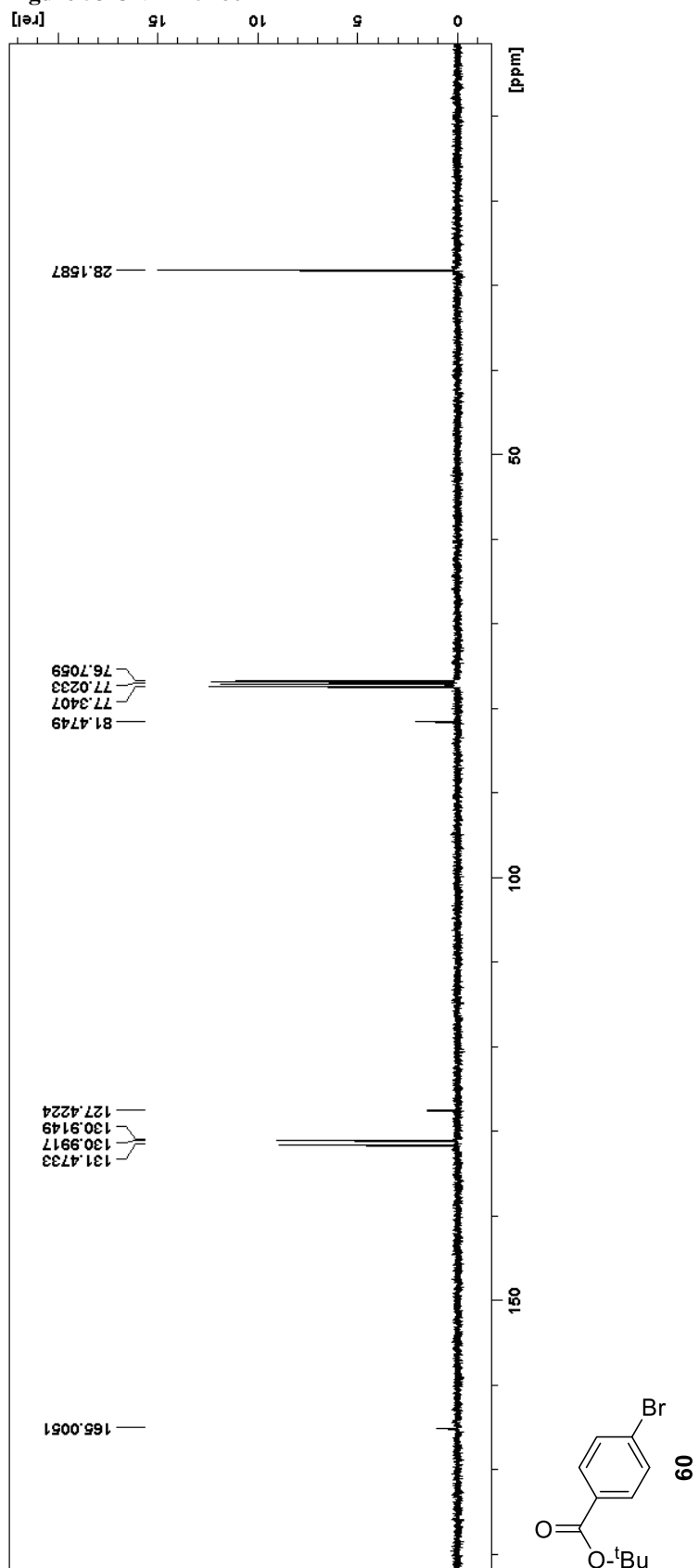


Figure 54 HNMR of 62

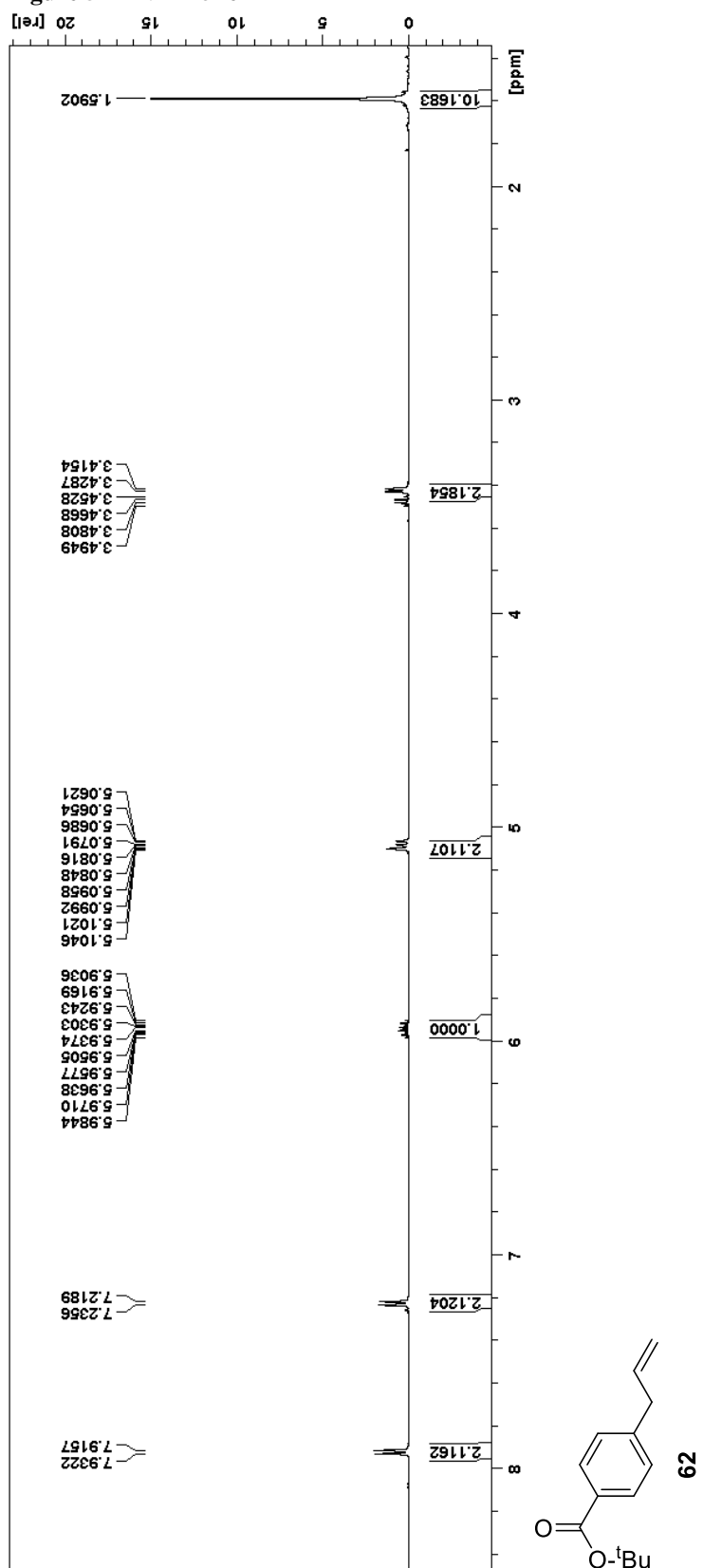


Figure S5 CNMR of 62

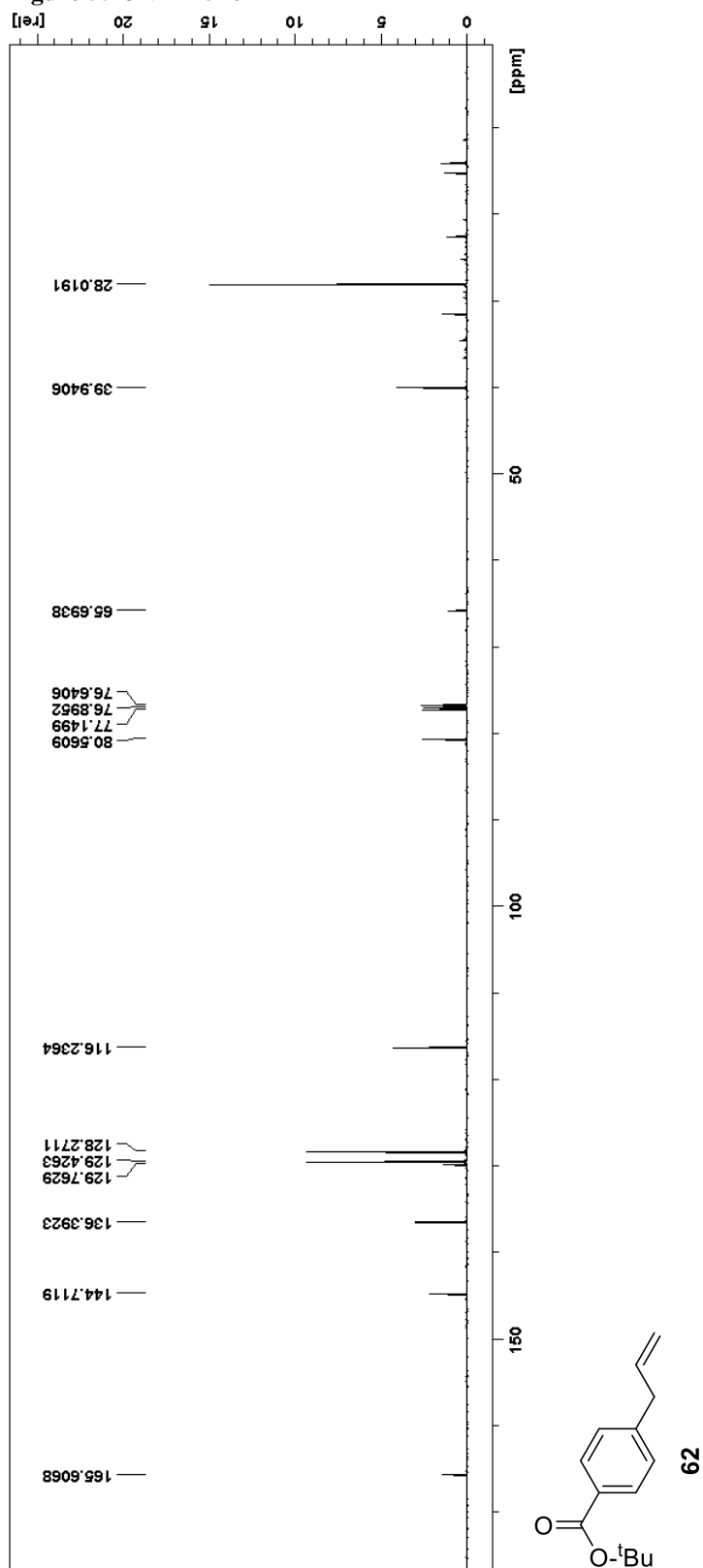




Figure S6 HNMR of 64

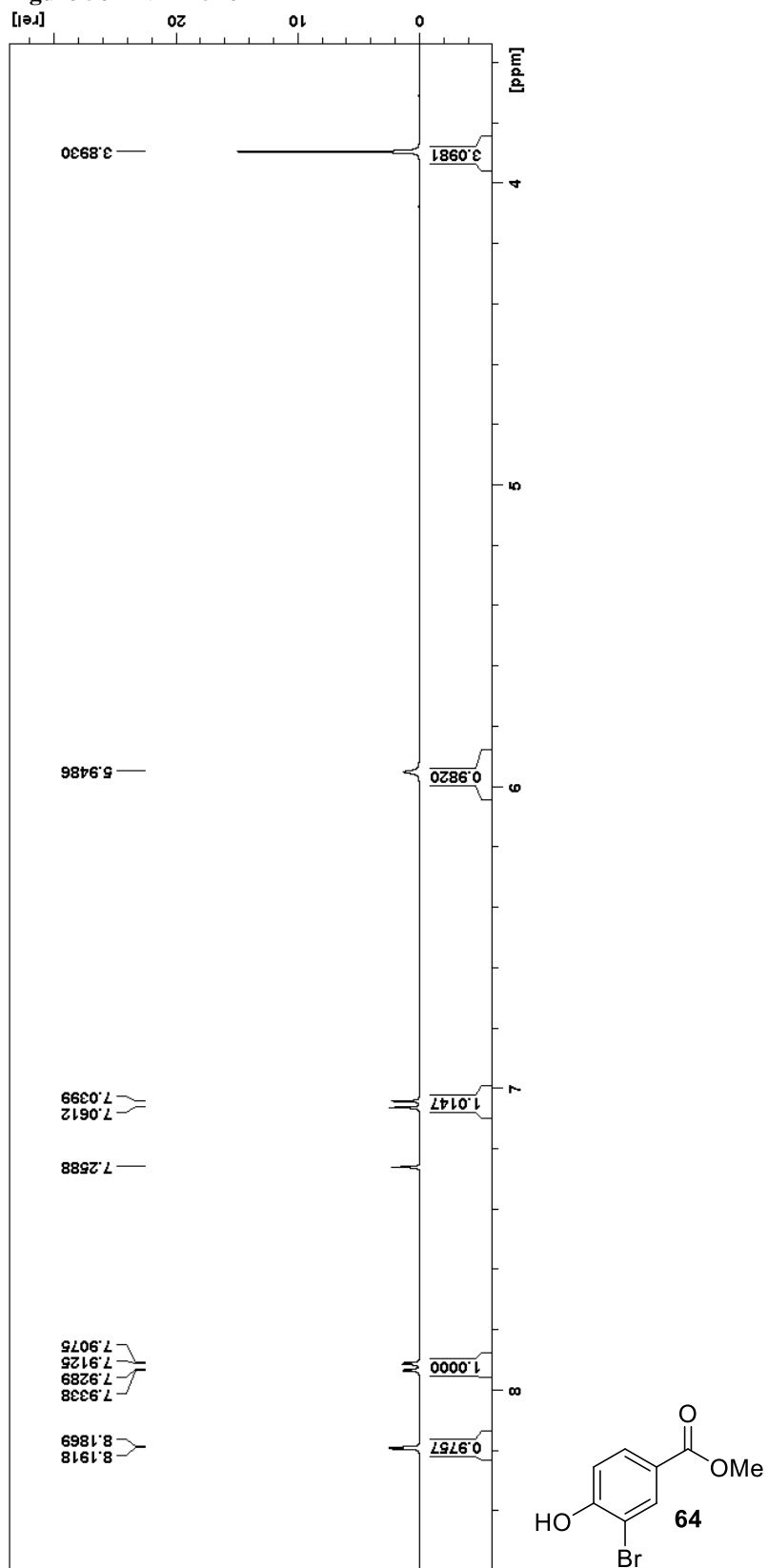


Figure 57 CNMR of 64

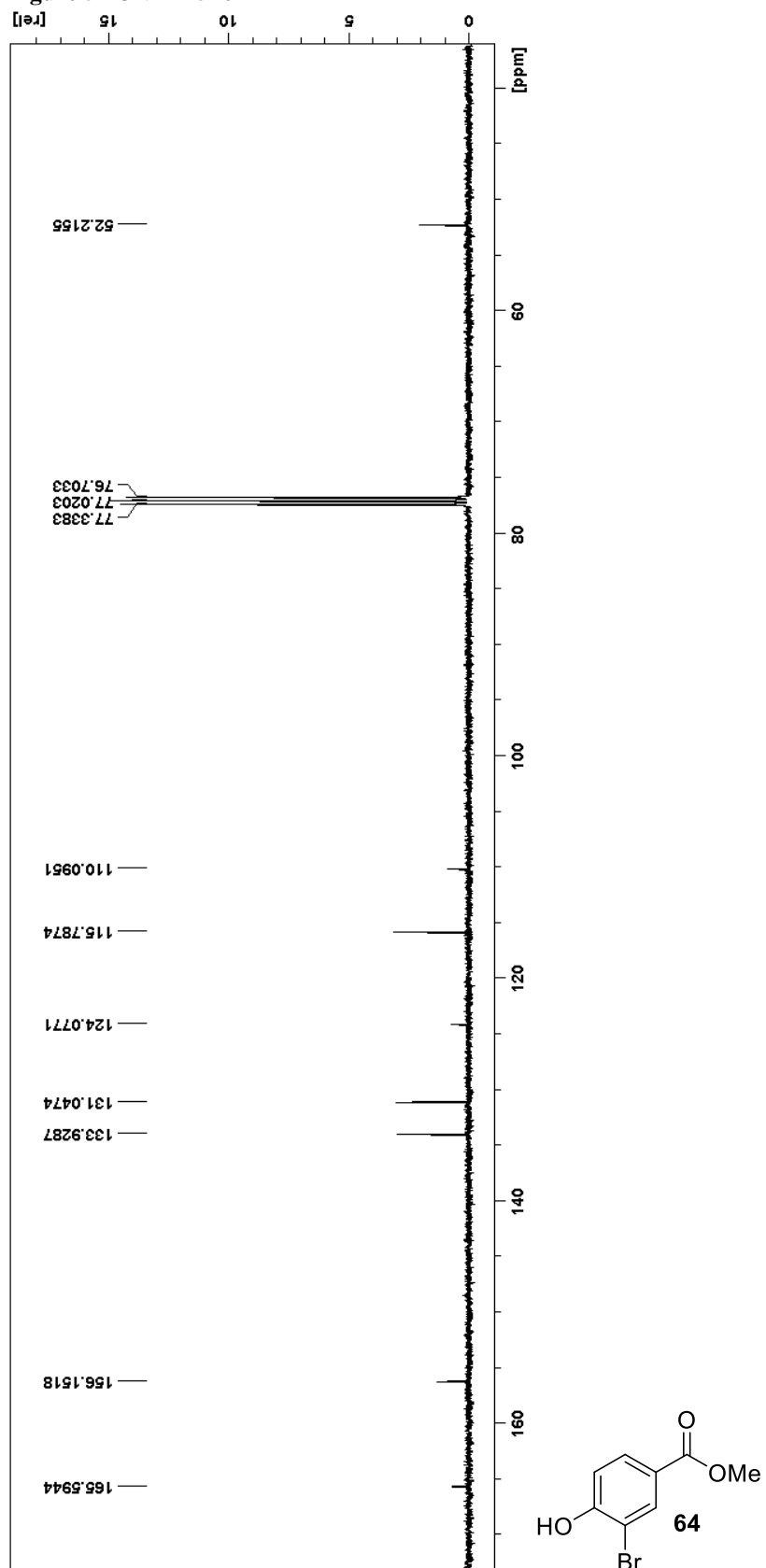


Figure 58 HNMR of 65

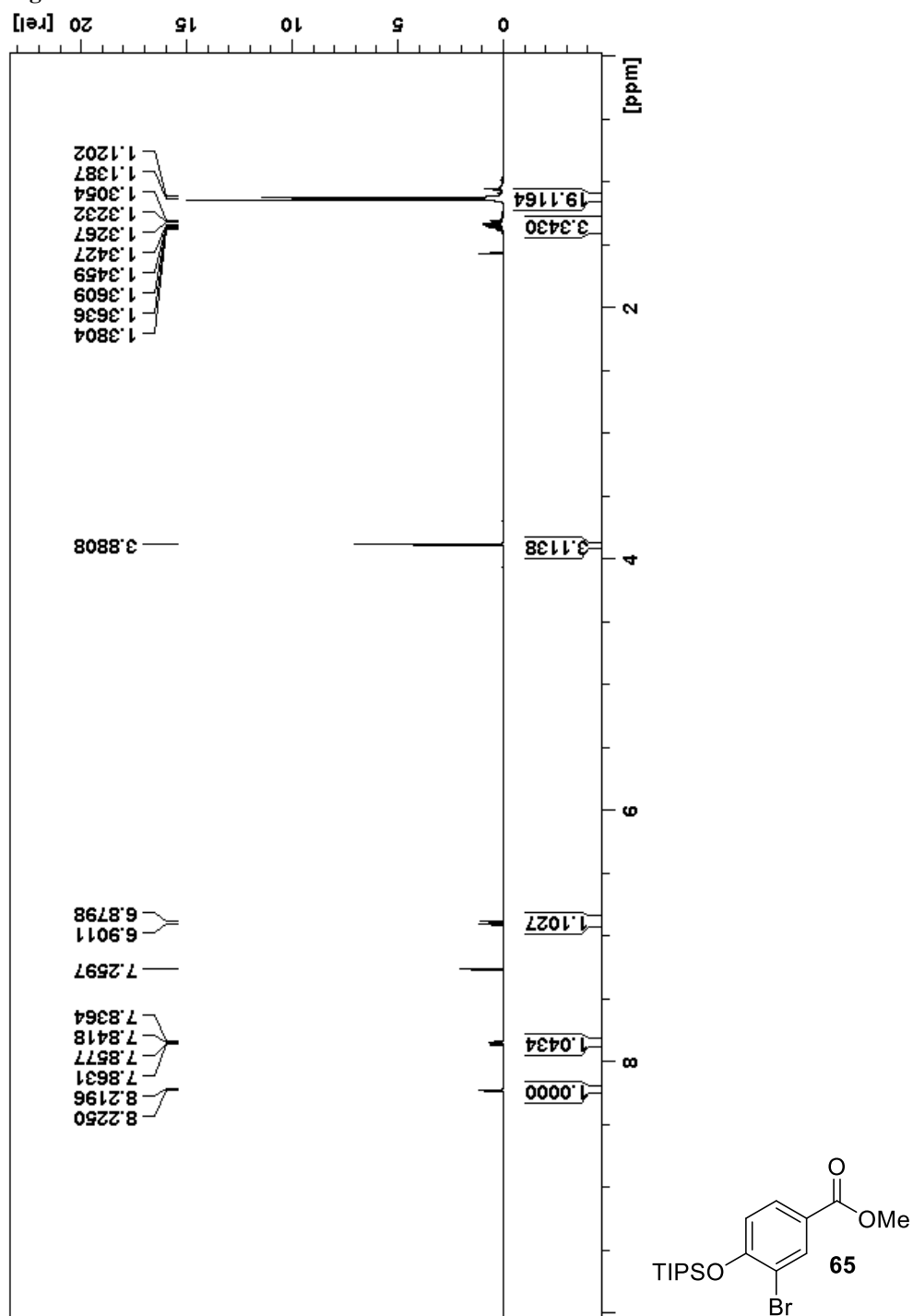


Figure 59 CNMR of 65

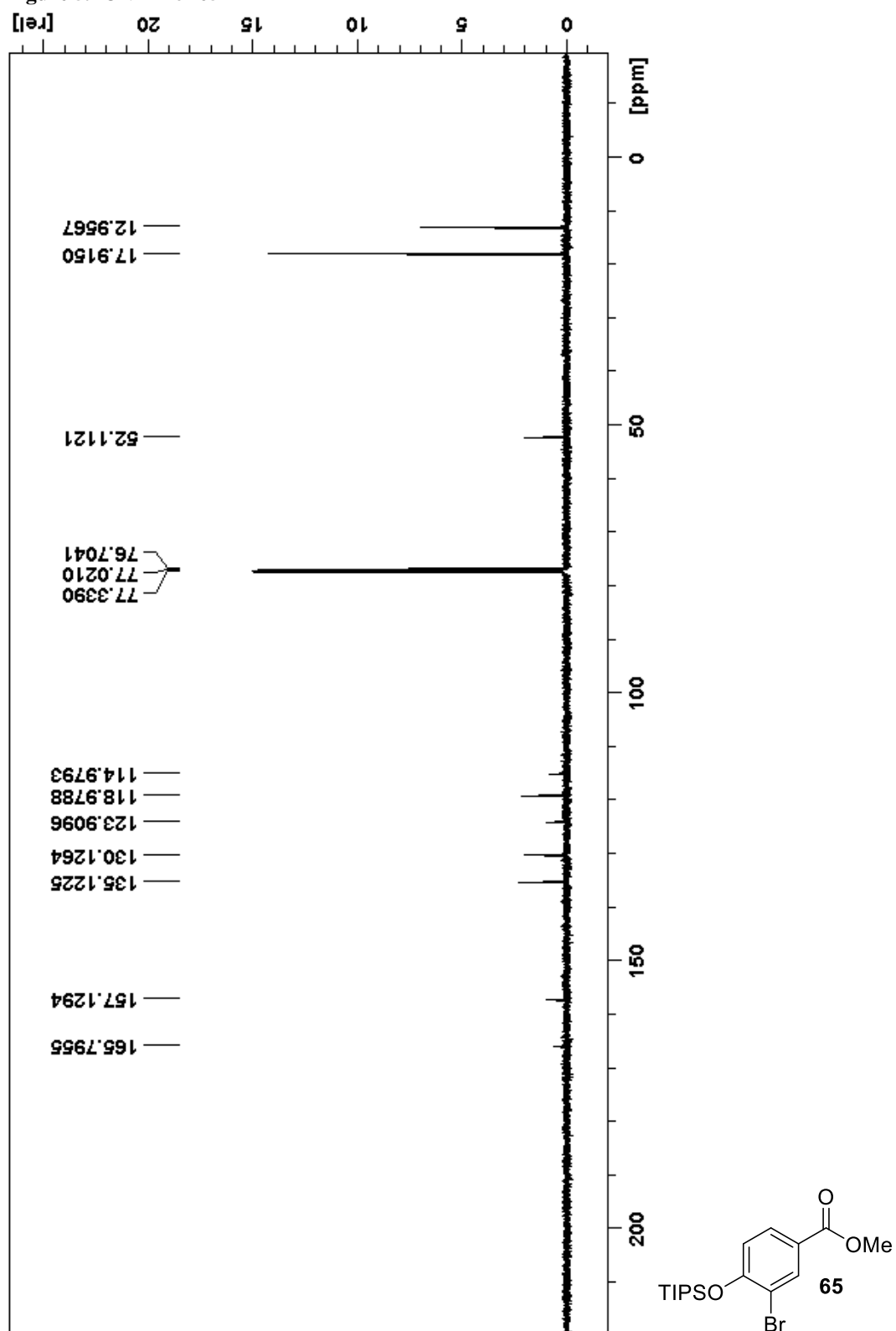


Figure 60 HNMR of 66

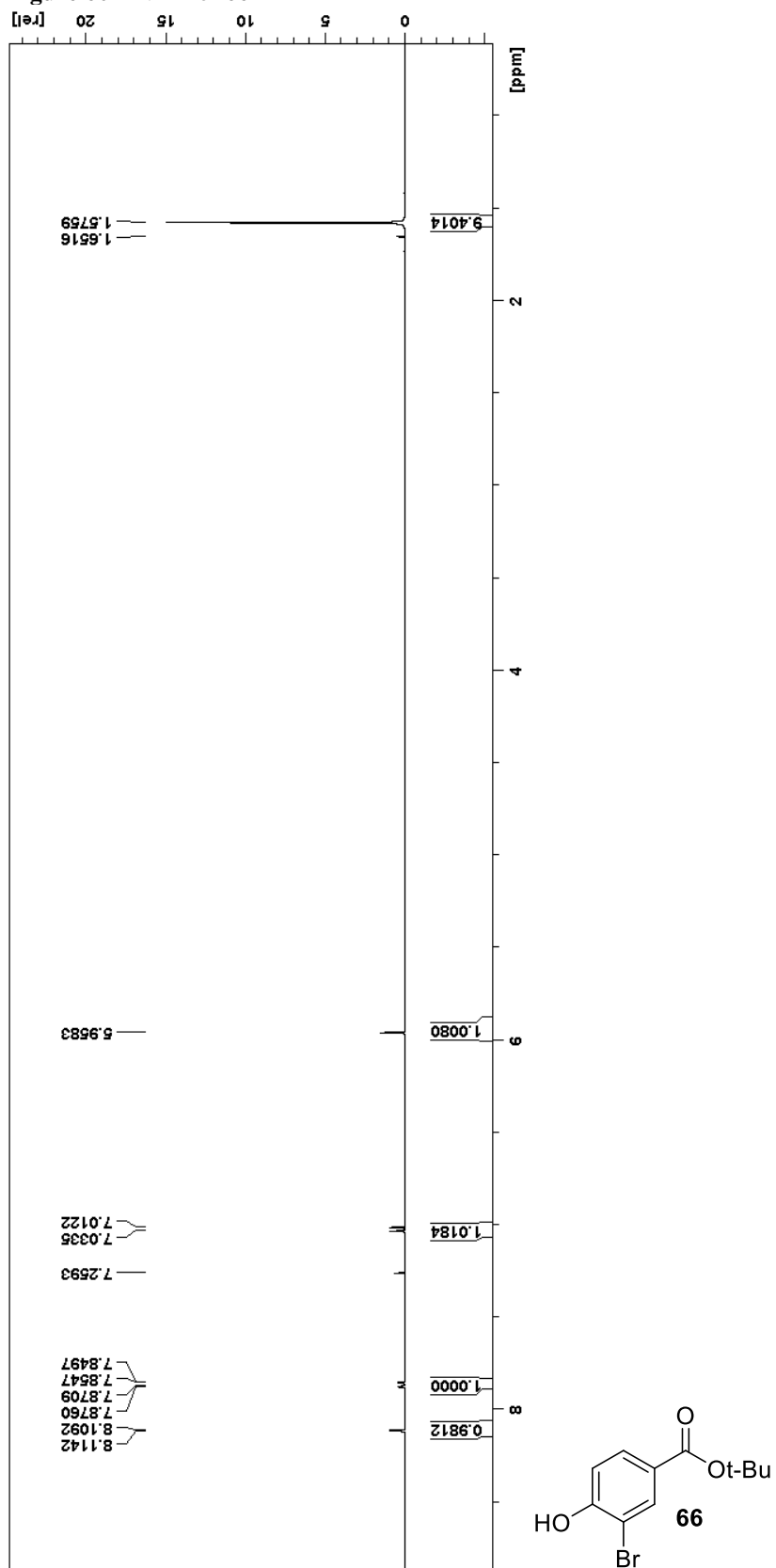


Figure 61 CNMR of 66

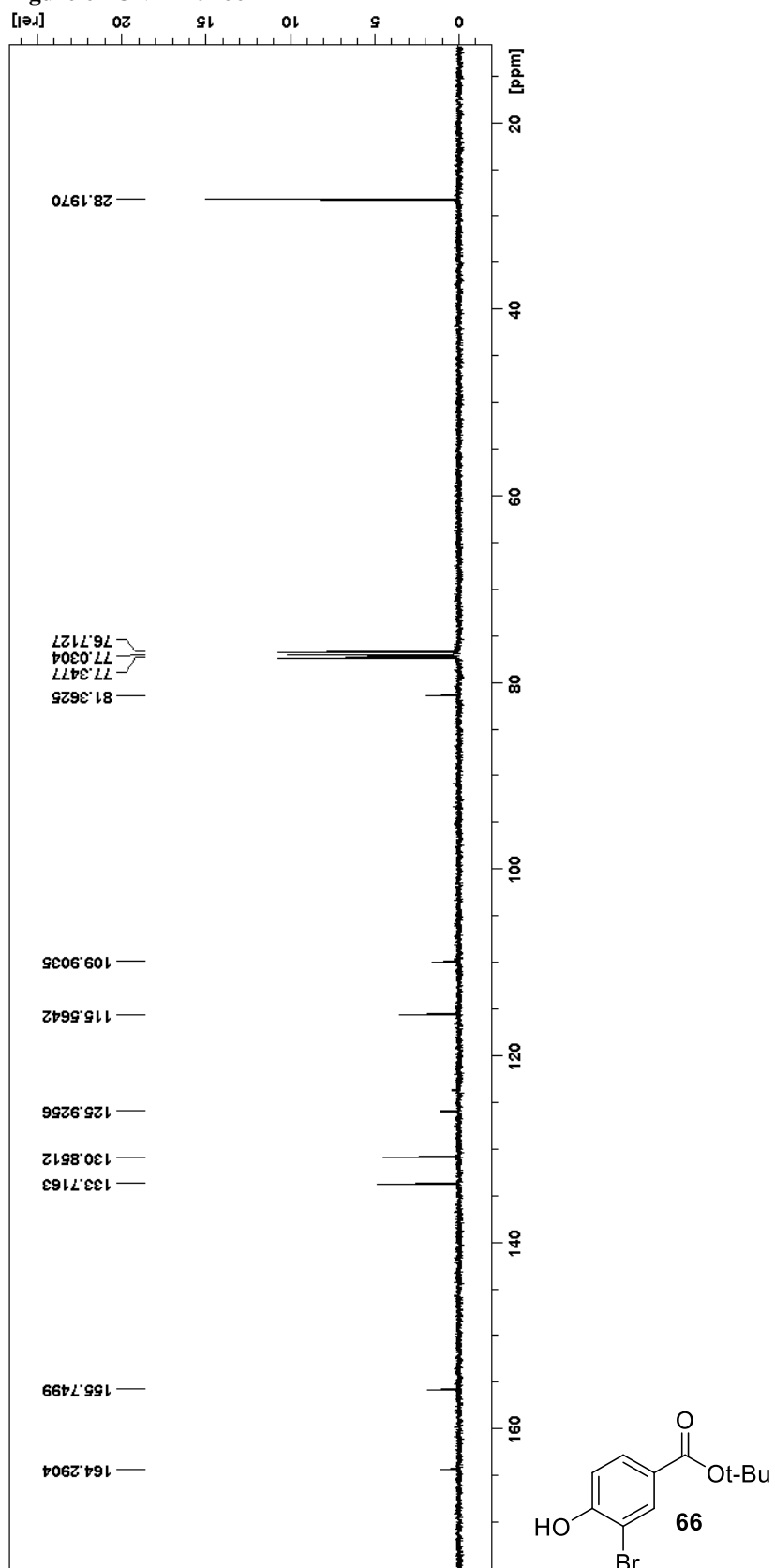


Figure 62 HNMR of 67

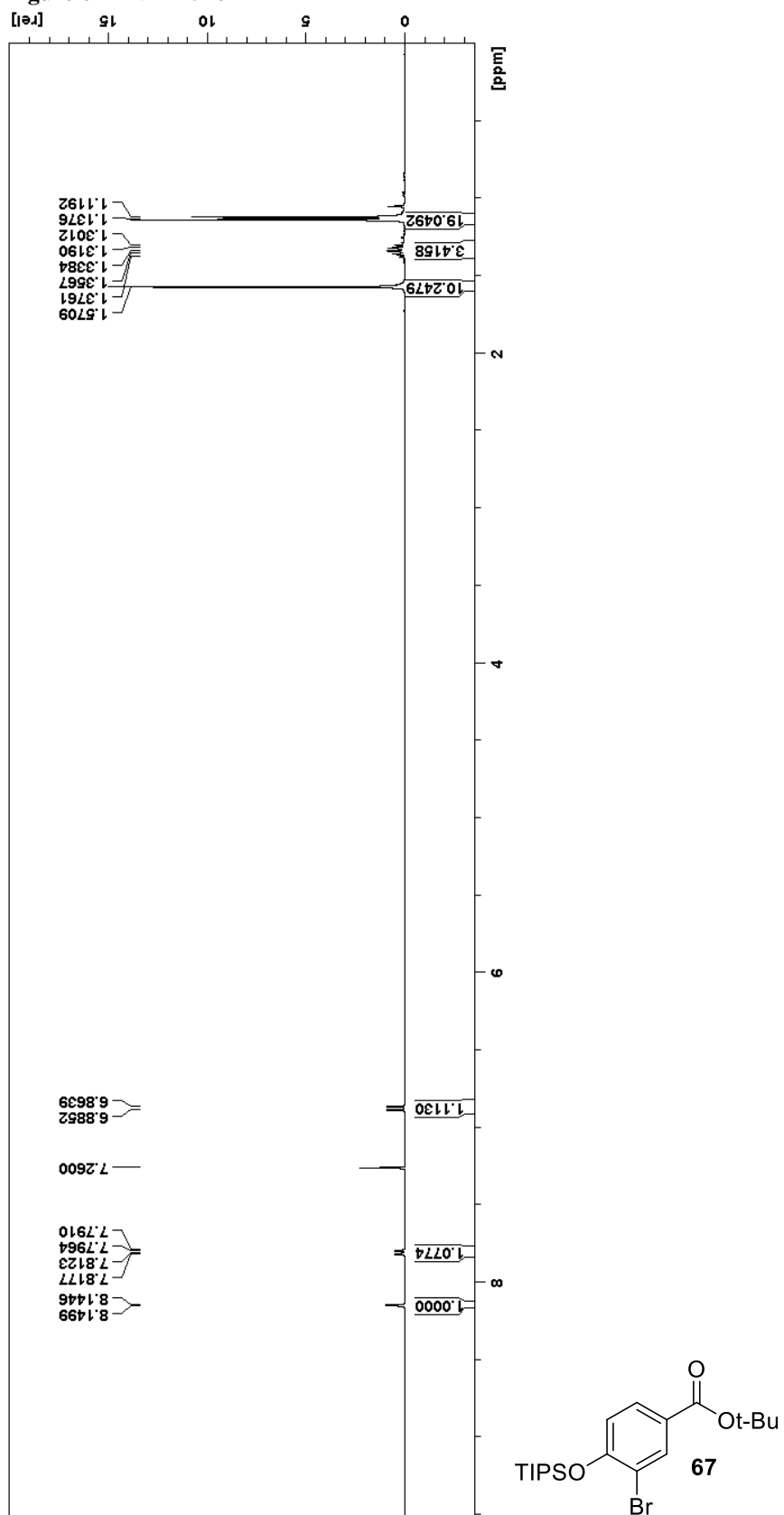


Figure 63 CNMR of 67

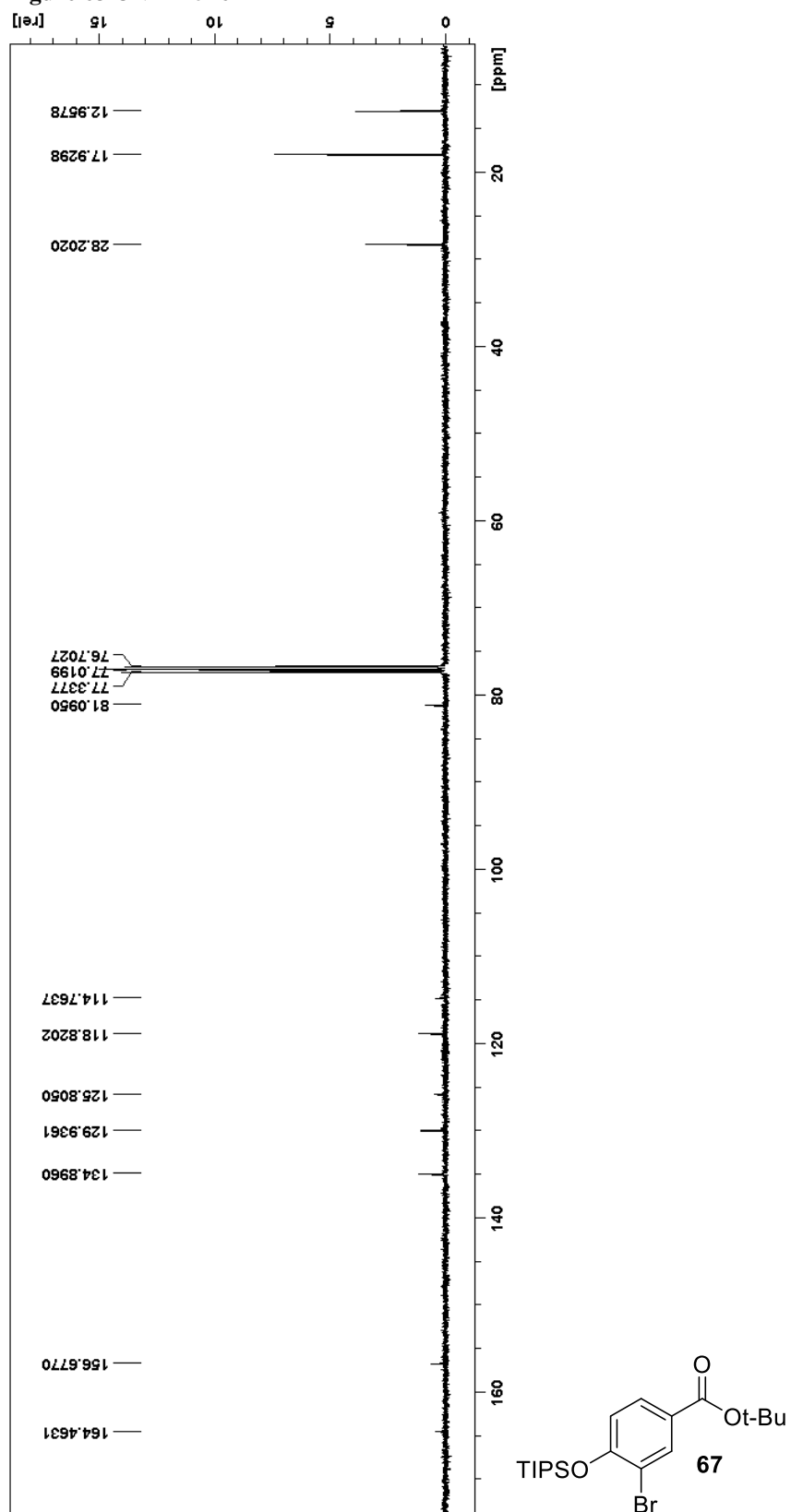




Figure 64 HNMR of 68

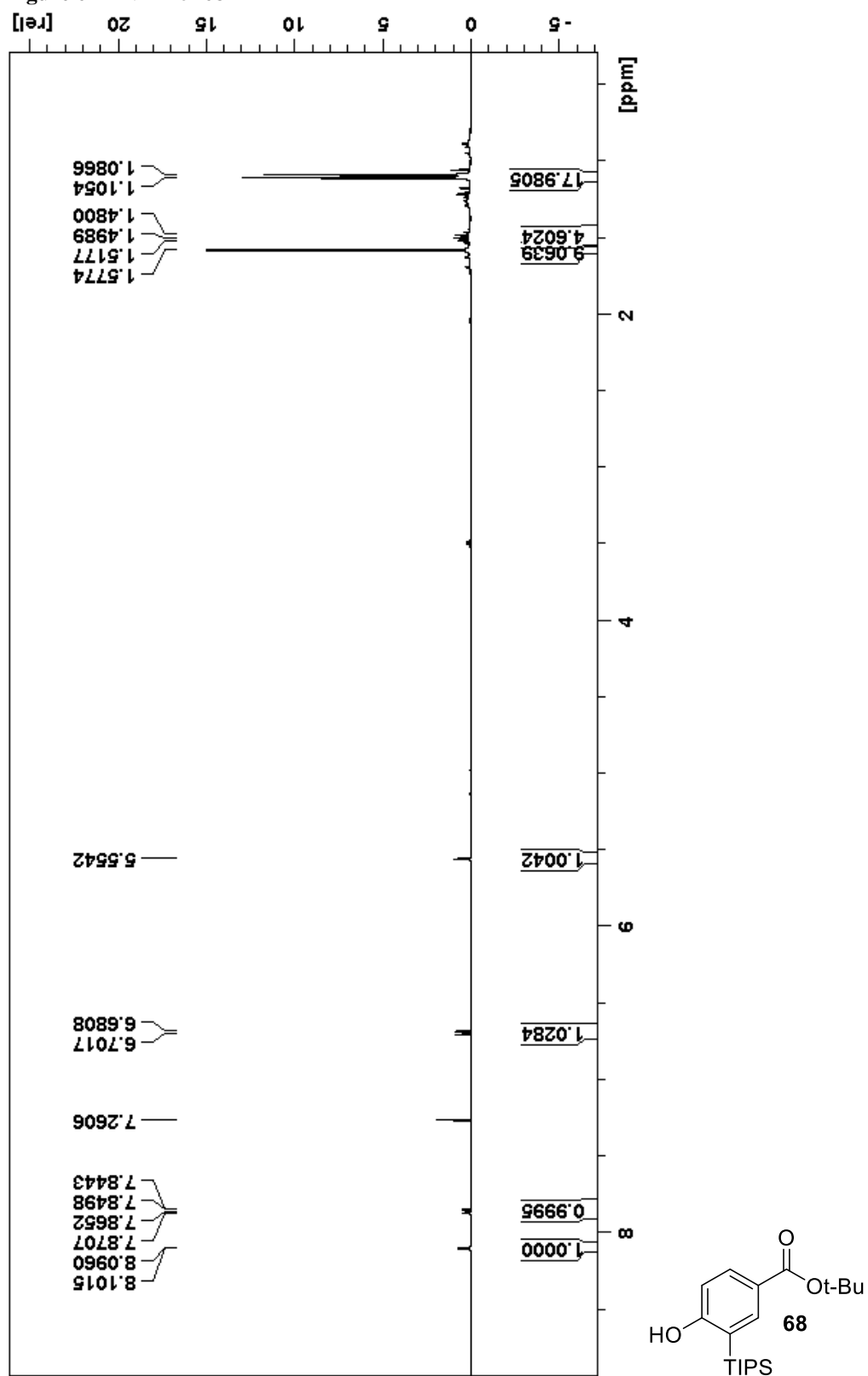


Figure 65 HNMR of 69

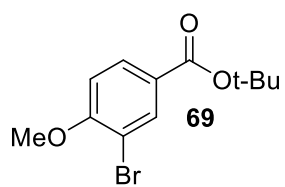
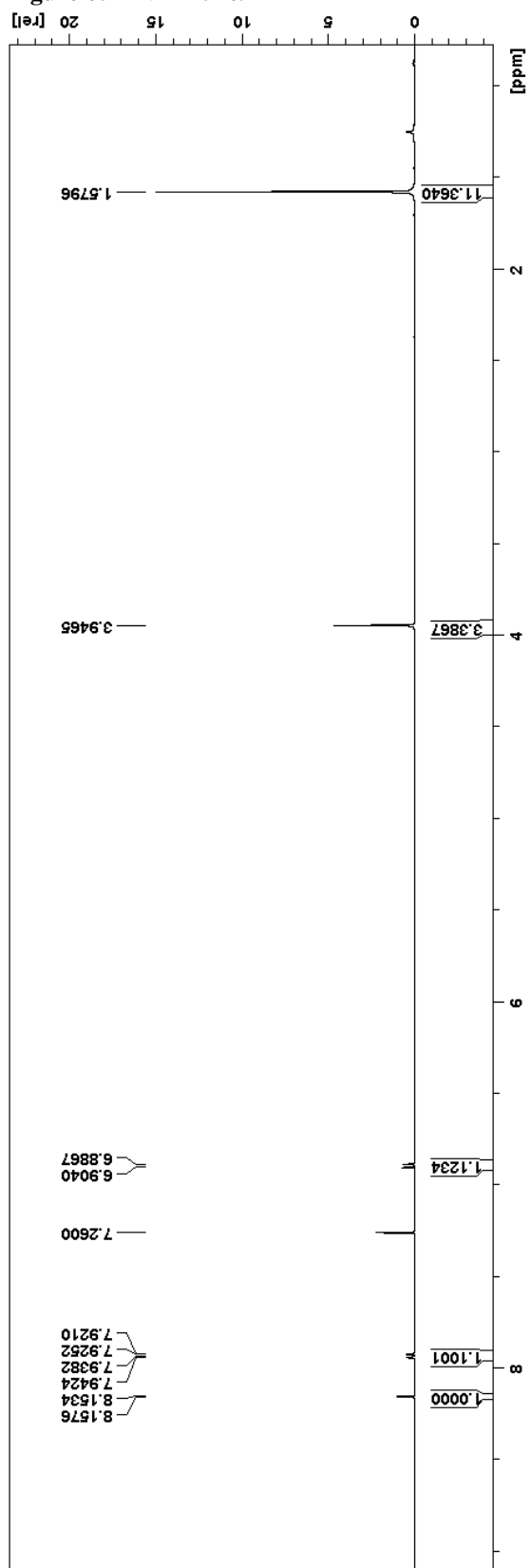


Figure 66 CNMR of 69

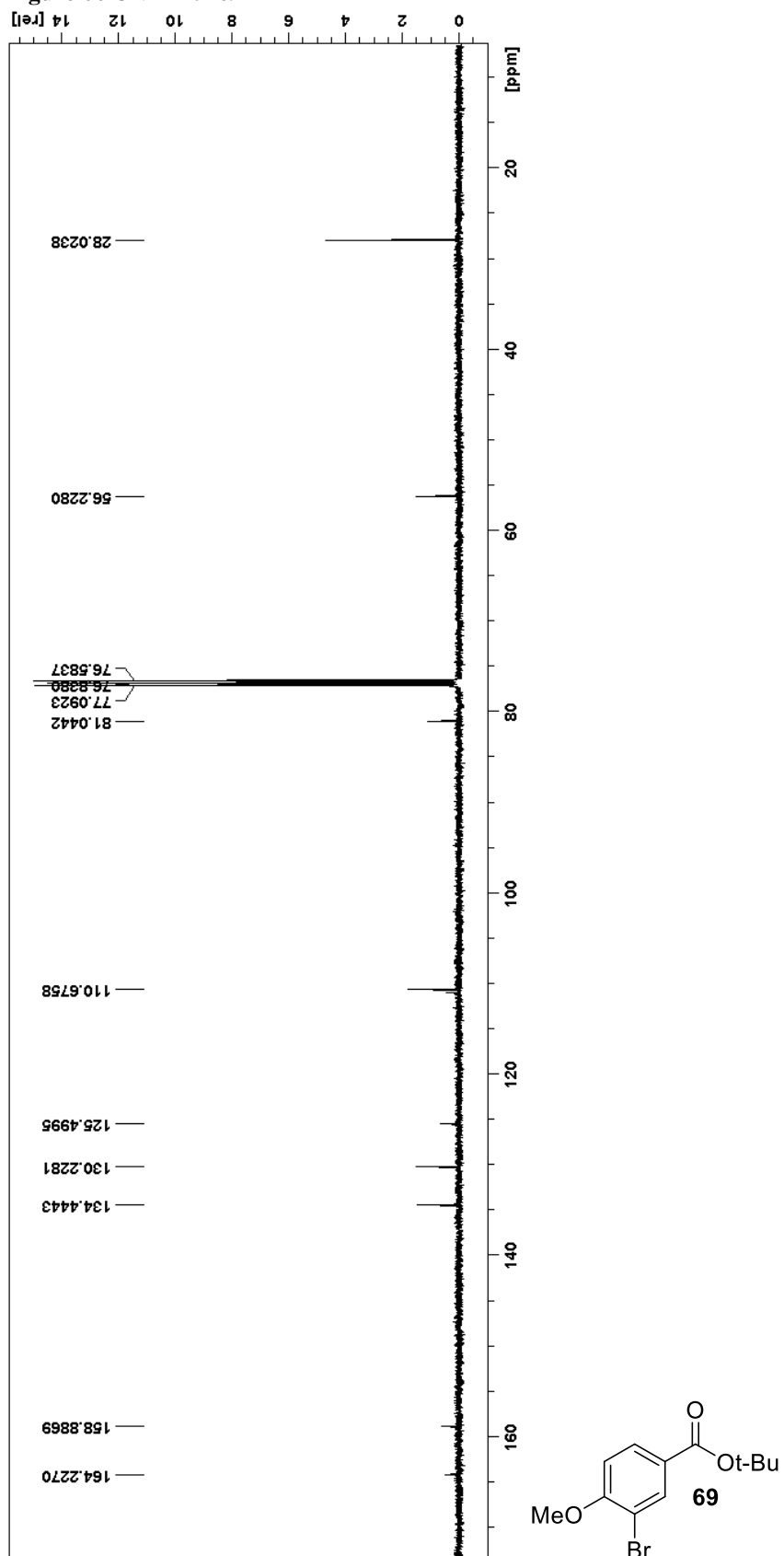


Figure 67 HNMR of 70

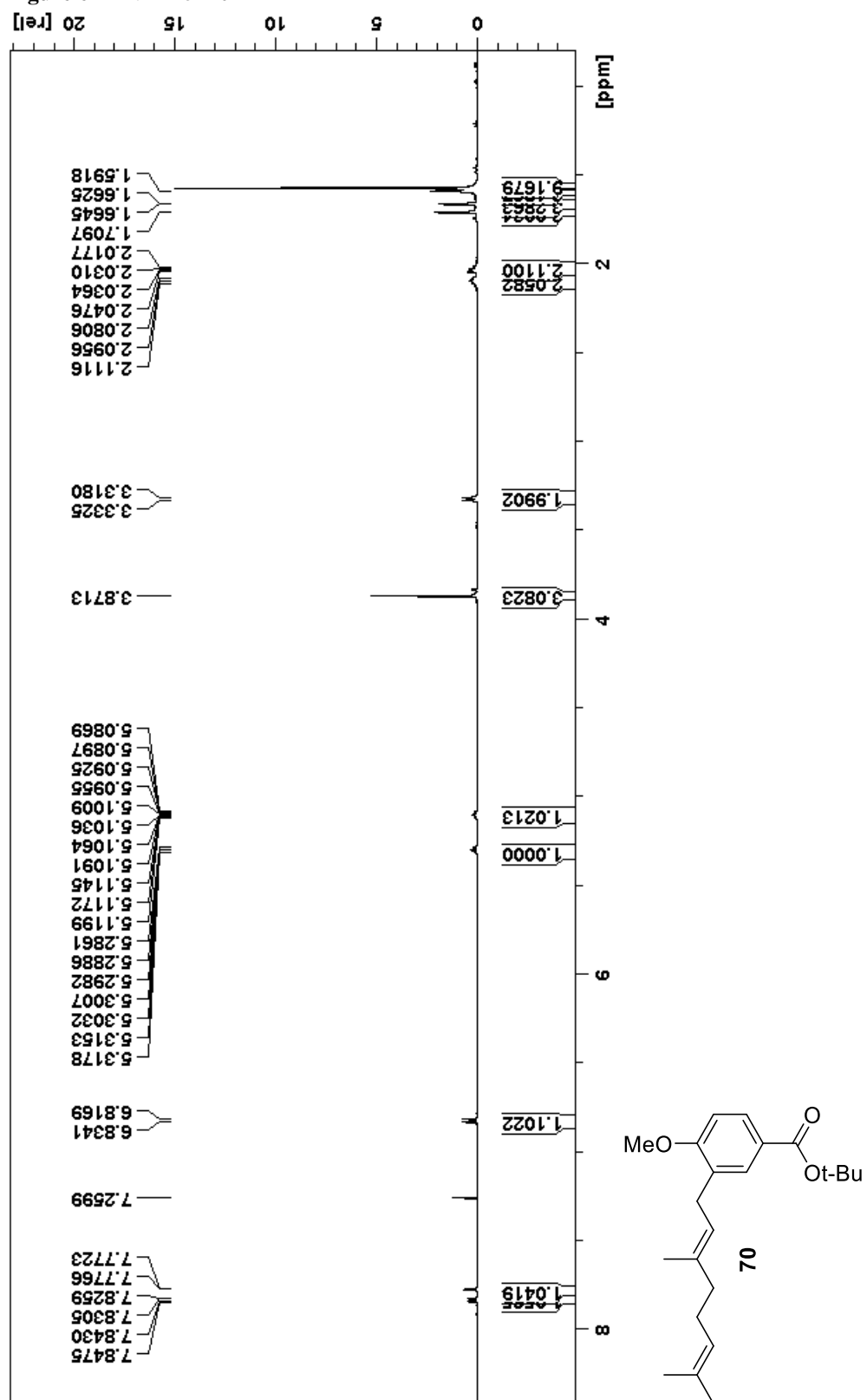


Figure 68 CNMR of 70

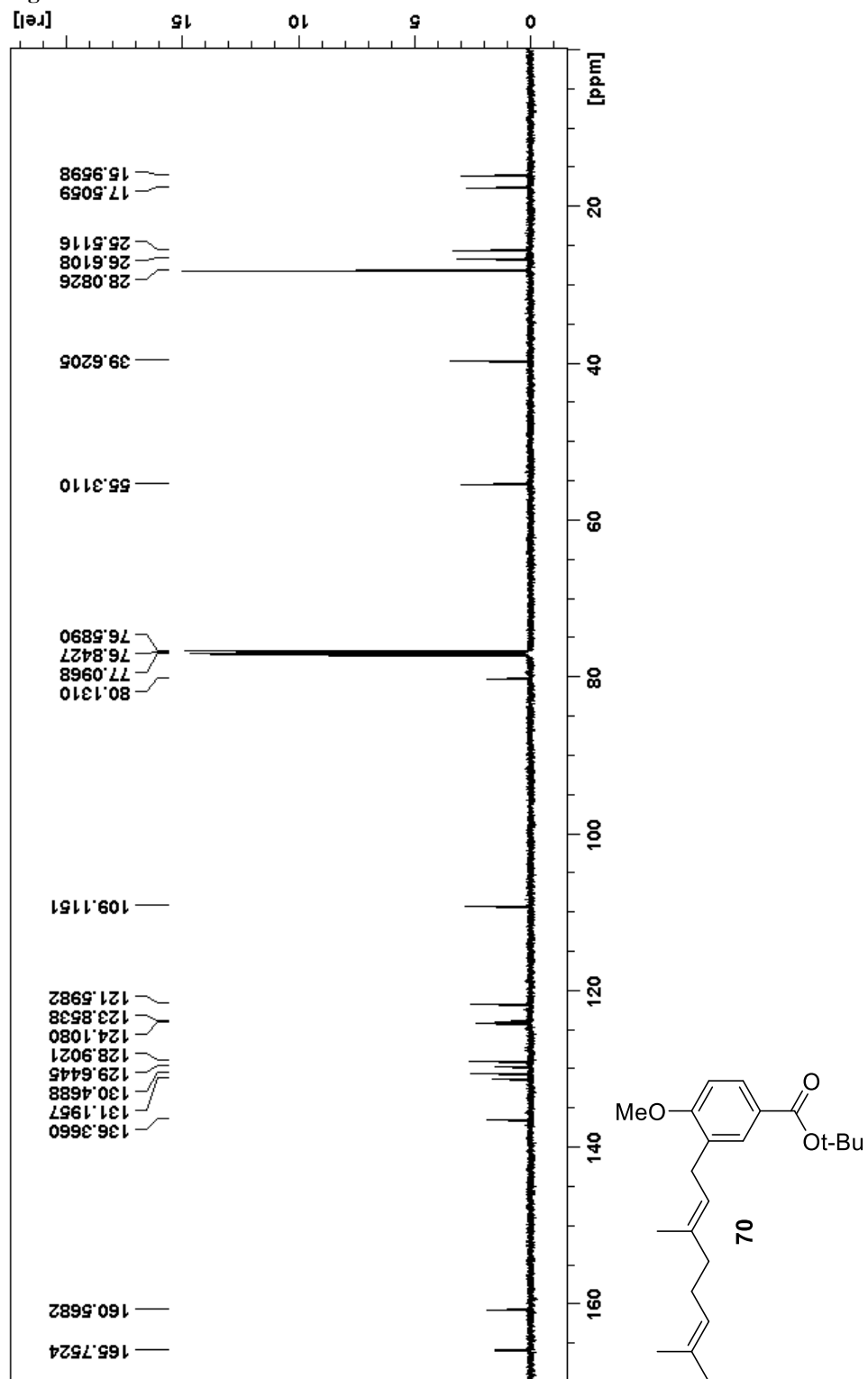


Figure 69 HNMR of 73

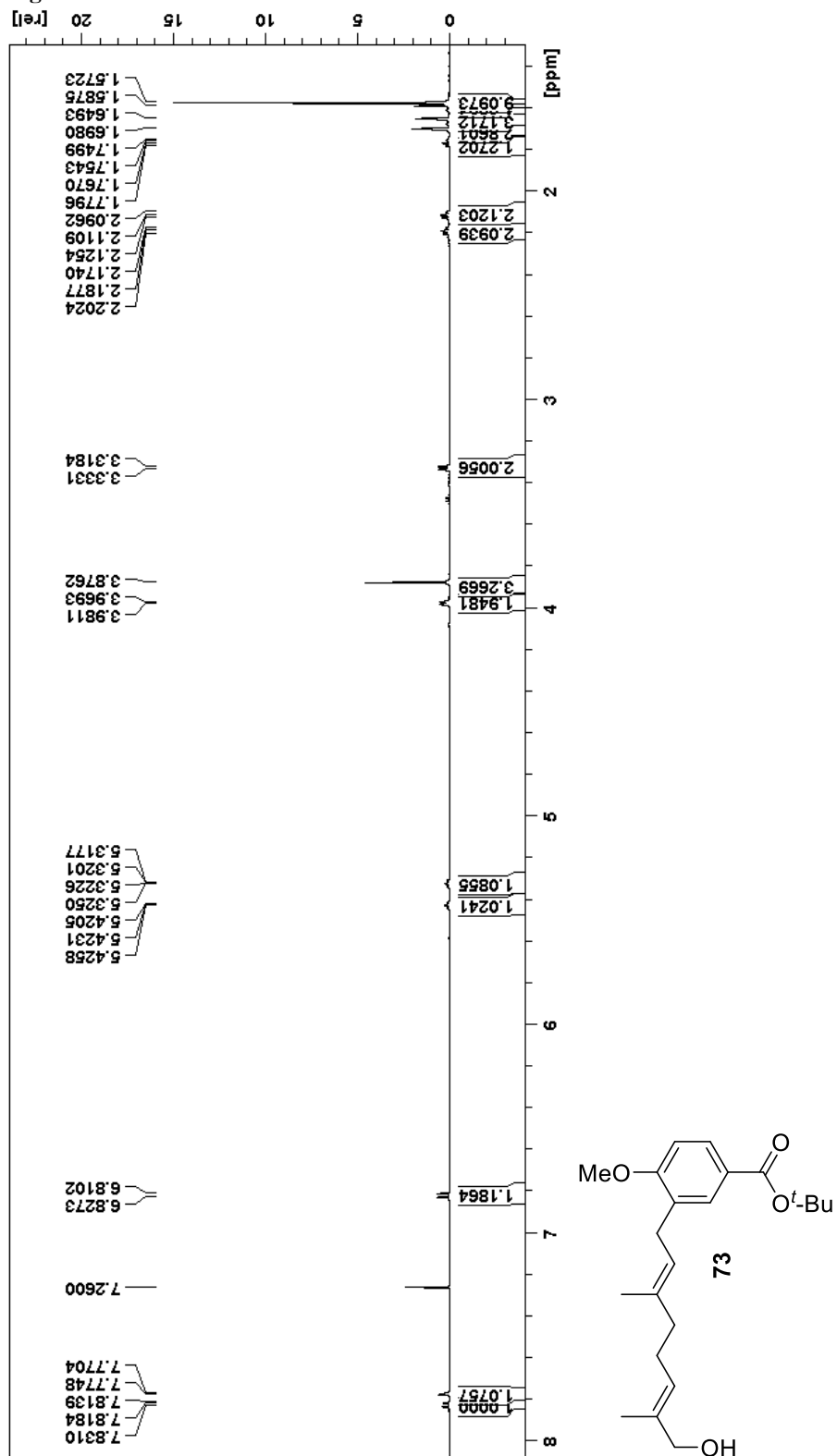


Figure 70 CNMR of 73

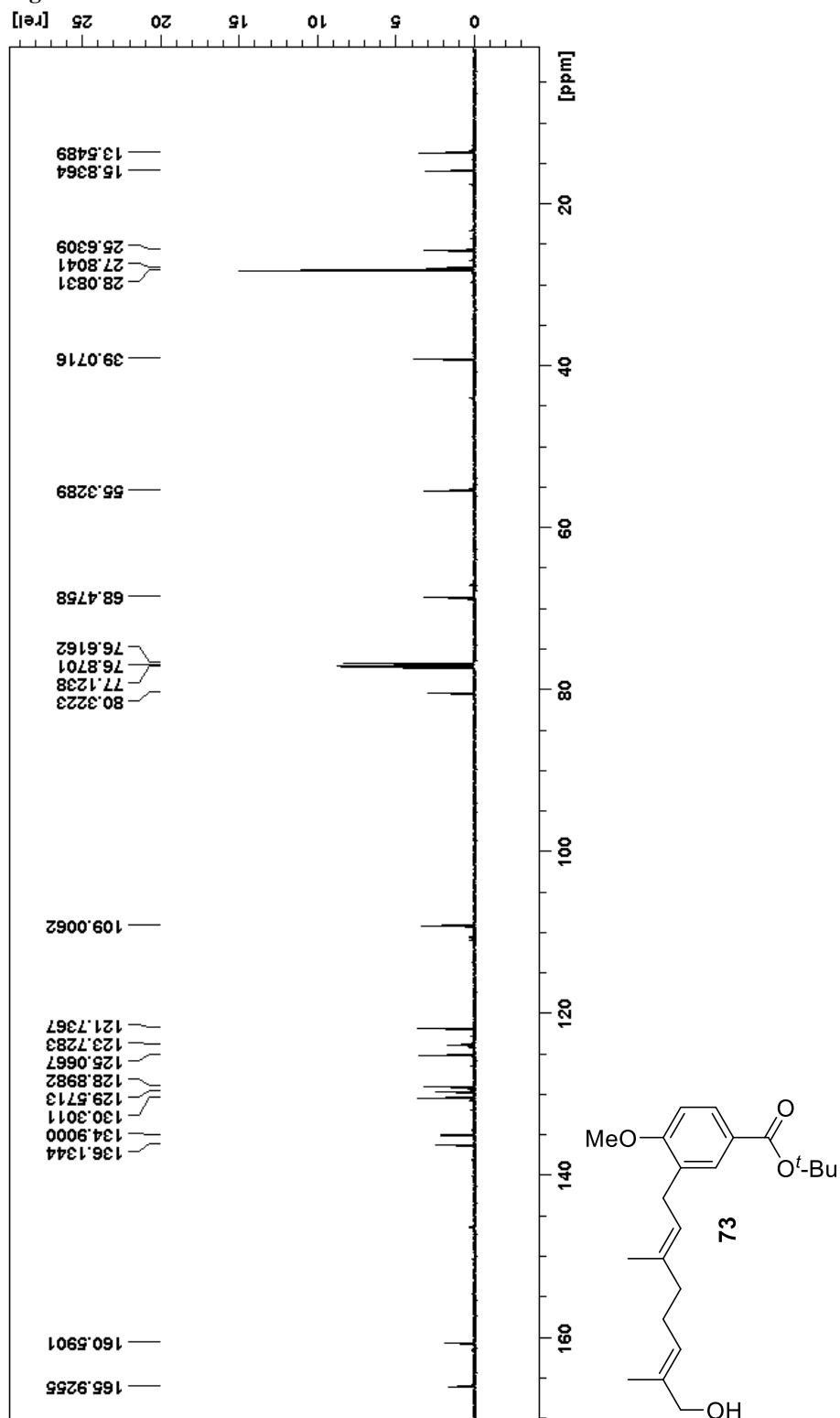


Figure 71 HNMR of 75

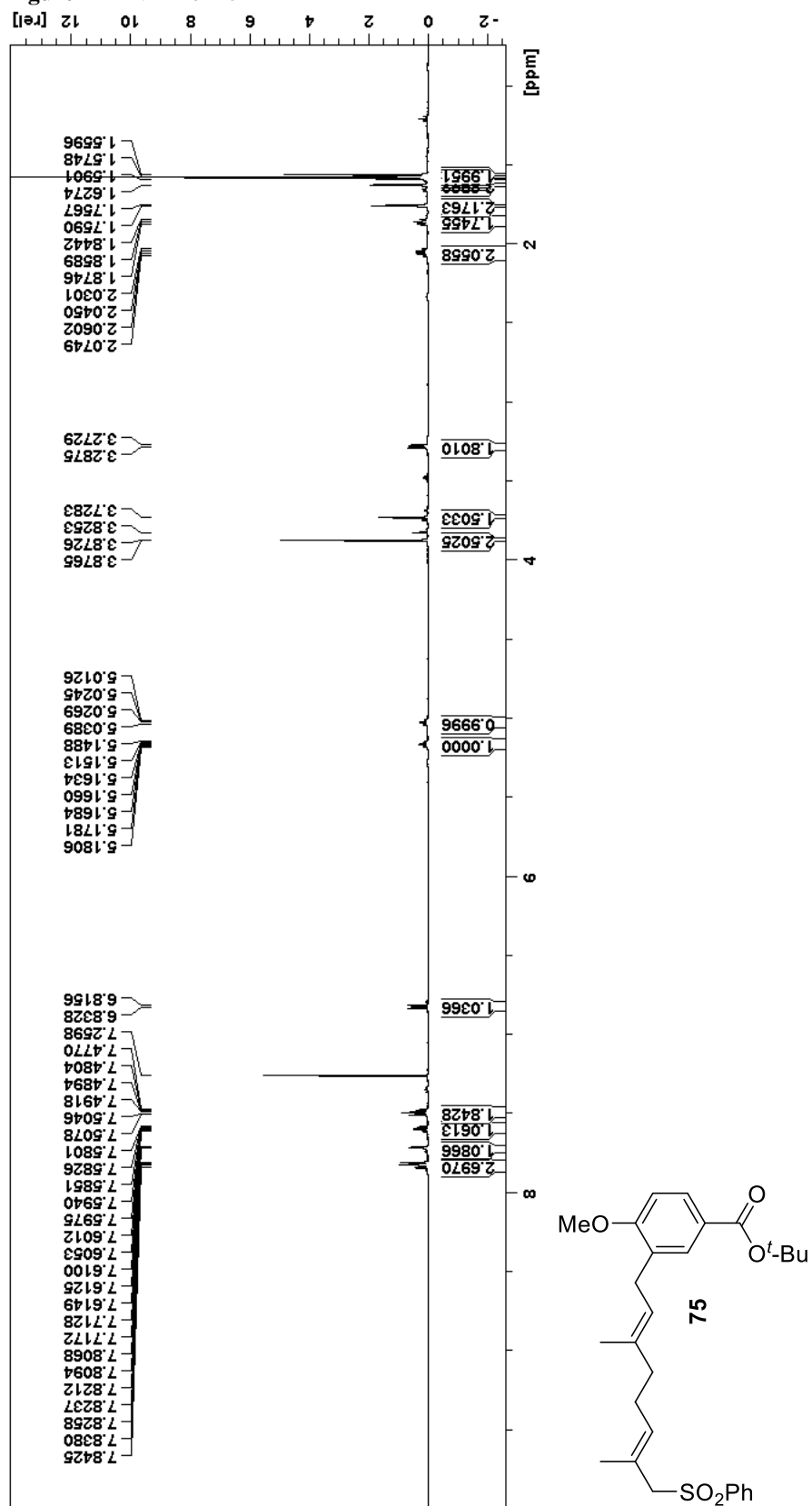






Figure 73 HNMR of 83

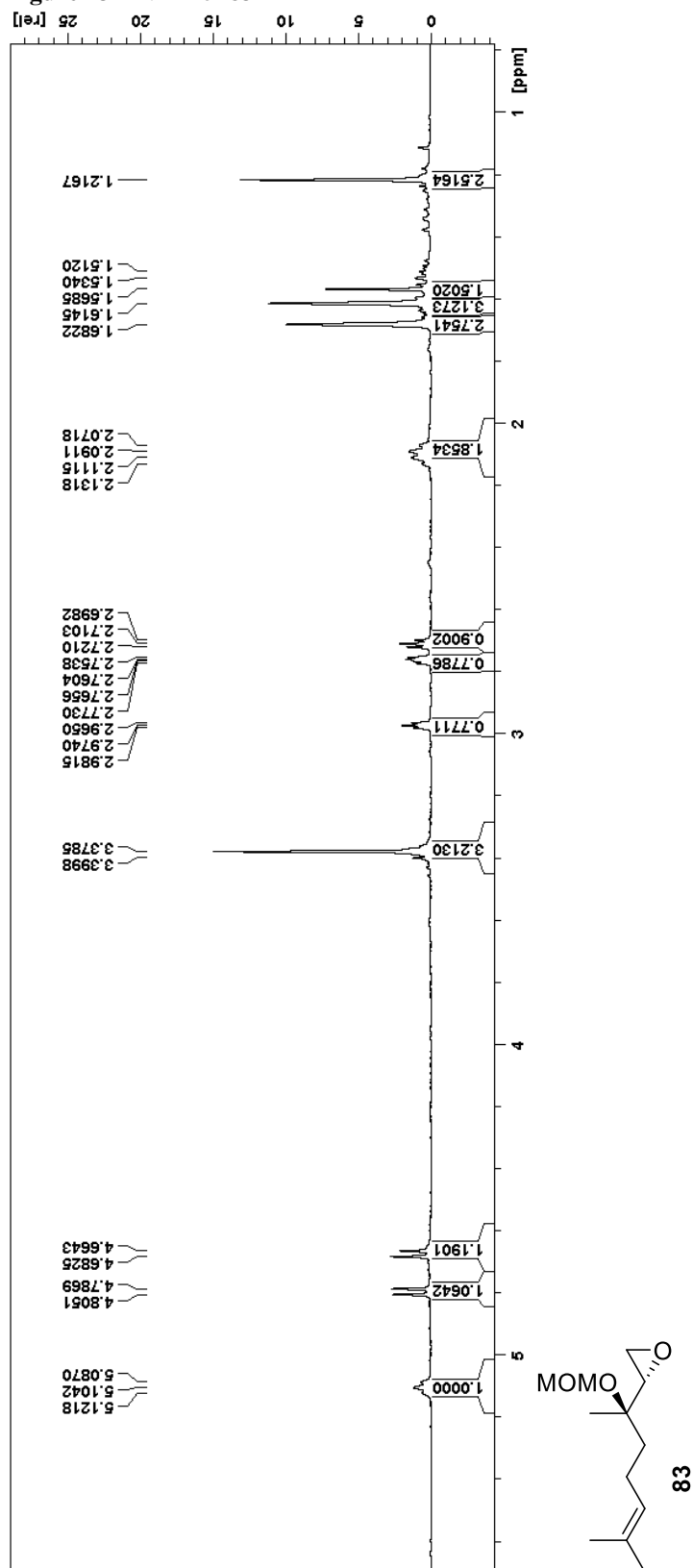


Figure 74 CNMR of 83

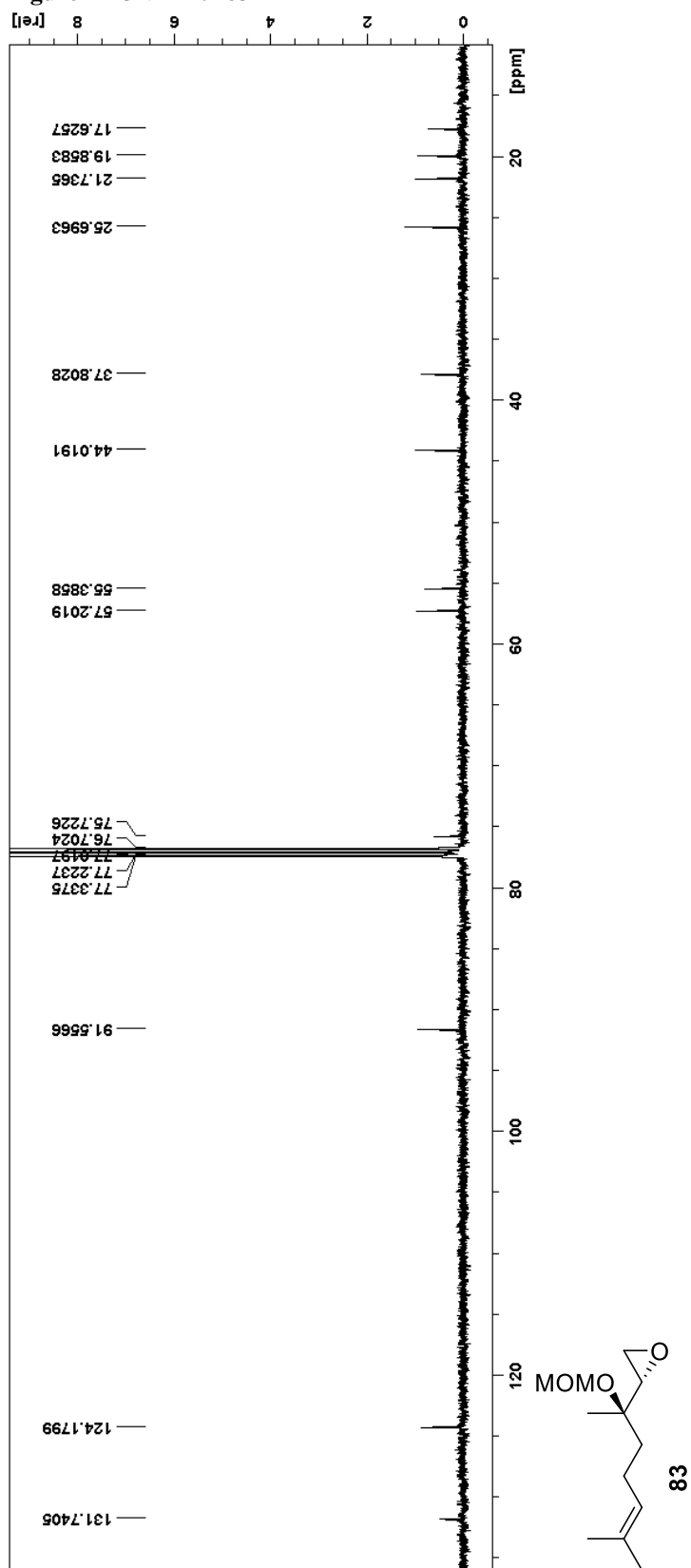


Figure 75 HNMR of 84

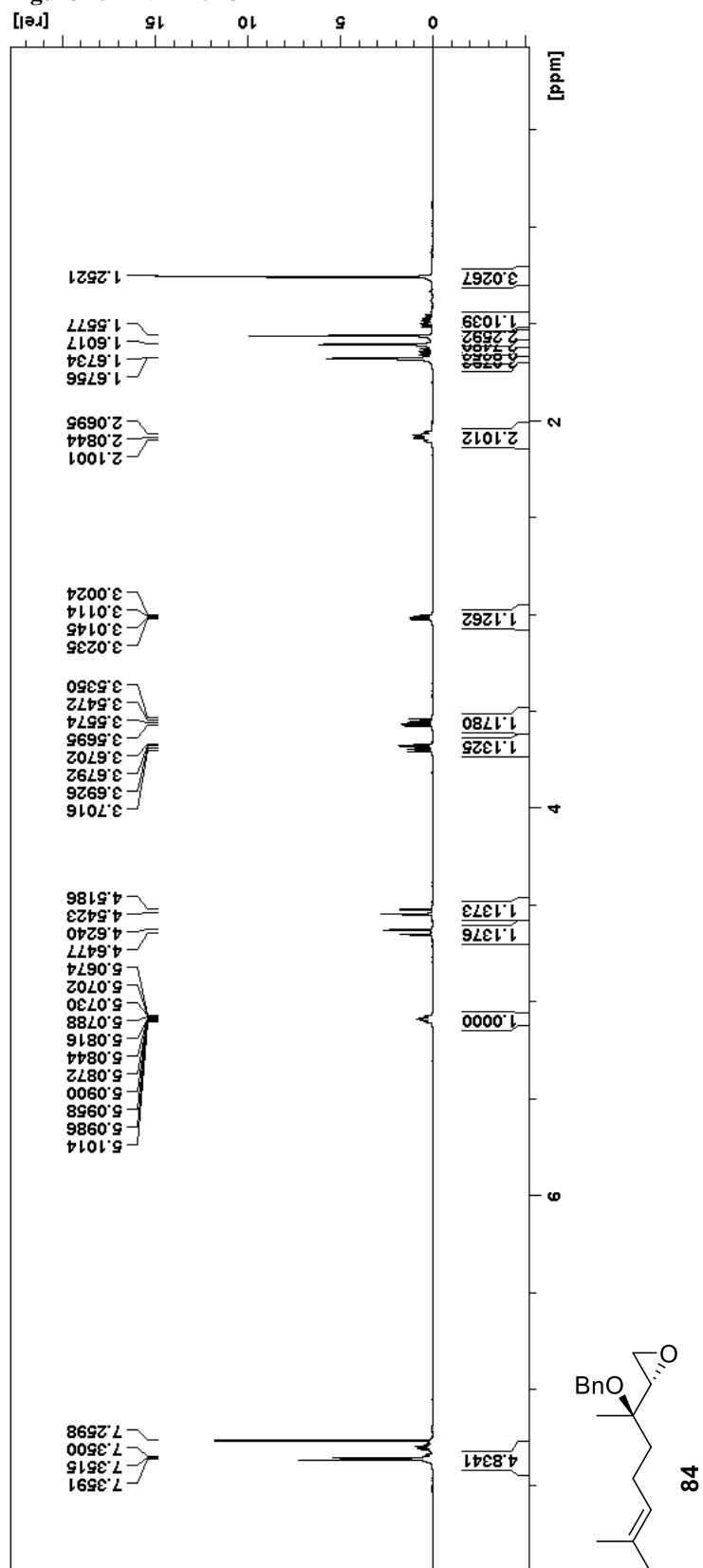


Figure 76 CNMR of 84

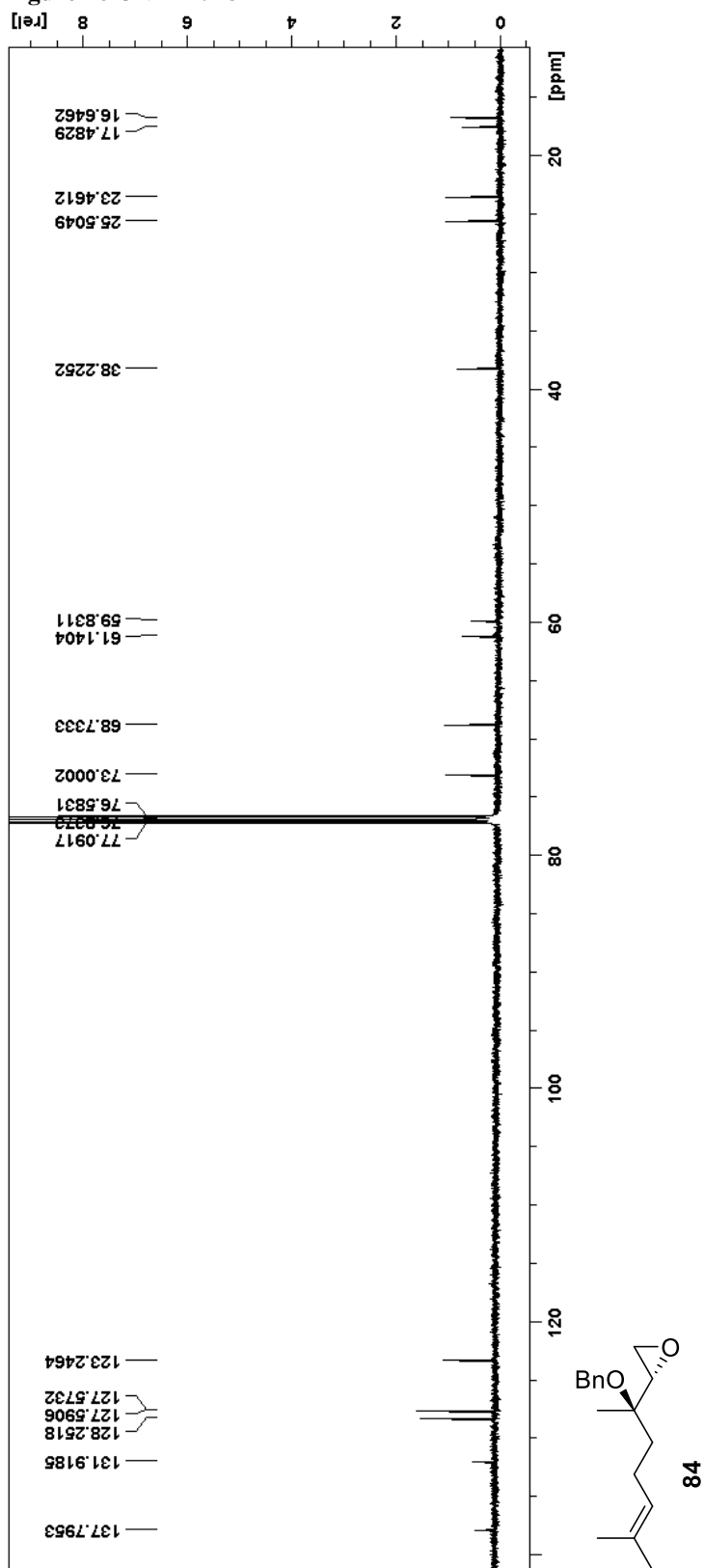


Figure 77 HNMR of 85

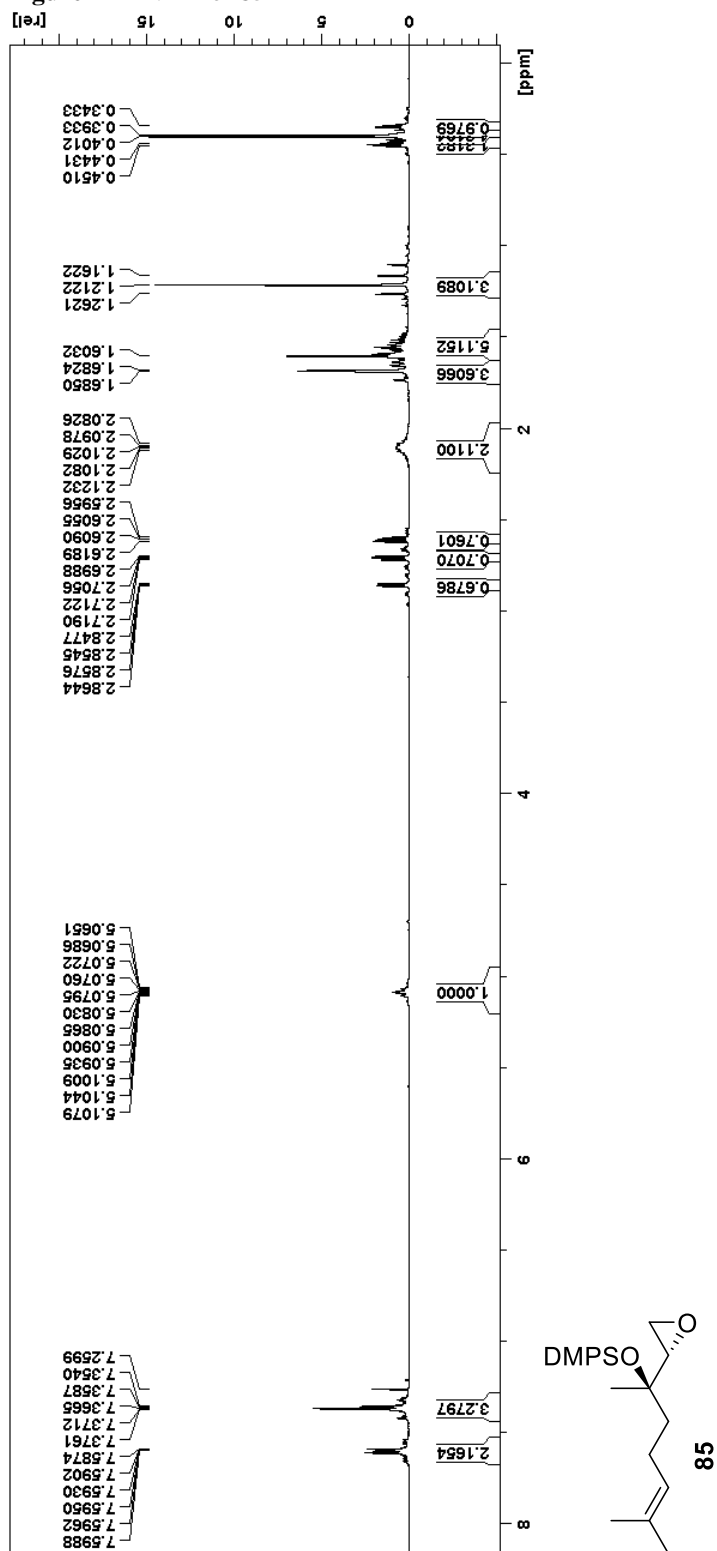
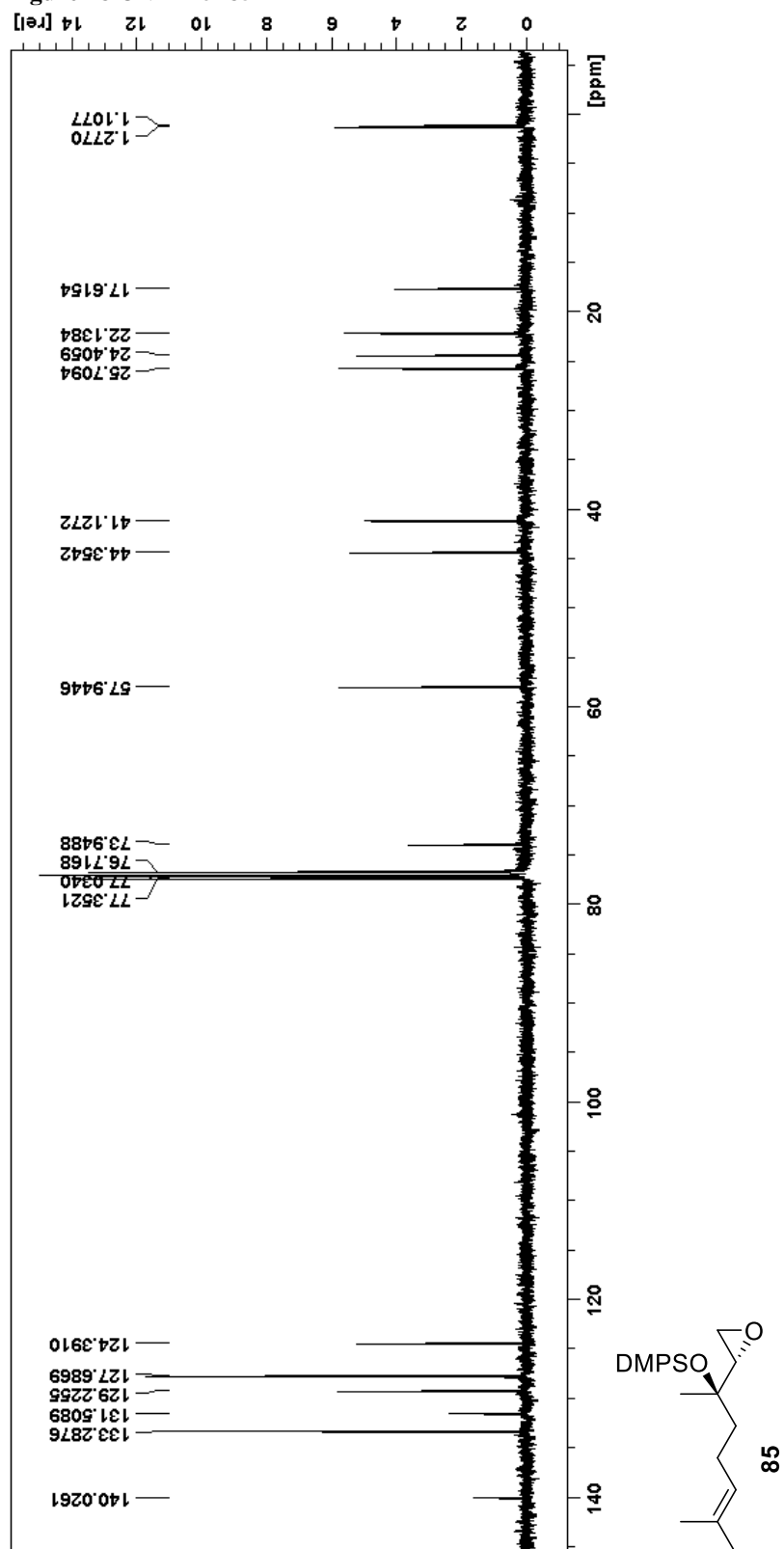


Figure 78 CNMR of 85



**26**

Chemical structure of **26**: CC(C)=CC(C)(O)C(C(=O)C=Cc1ccccc1)c2ccccc2

<sup>1</sup>H NMR spectrum (CDCl<sub>3</sub>) of compound **26**. The x-axis represents the chemical shift in ppm, ranging from 0 to 8. The y-axis represents the intensity in arbitrary units. The spectrum shows several peaks, with the following chemical shifts (ppm) labeled:

- 1.9349
- 0.9968
- 1.9586
- 5.3376
- 2.4332
- 1.9420
- 1.8686
- 1.0000
- 1.9906
- 1.1273
- 1.1942
- 2.9399
- 1.9420
- 1.8686
- 0.9634
- 0.8246
- 1.6840
- 5.5653
- 2.5023
- 7.8485
- 7.8956
- 7.8956
- 1.4825
- 7.5096
- 3.9225



Figure 80 HNMR of 101

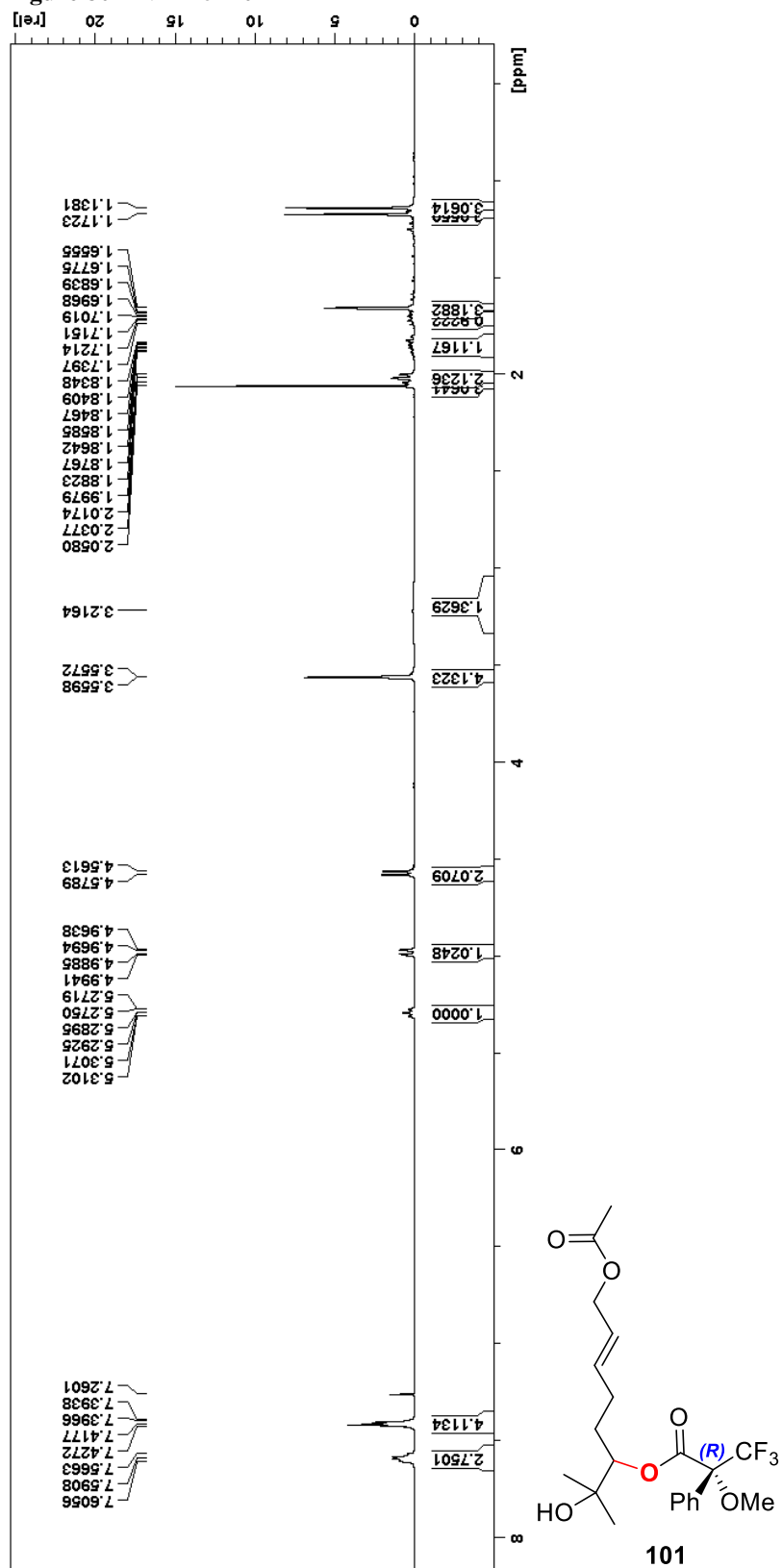
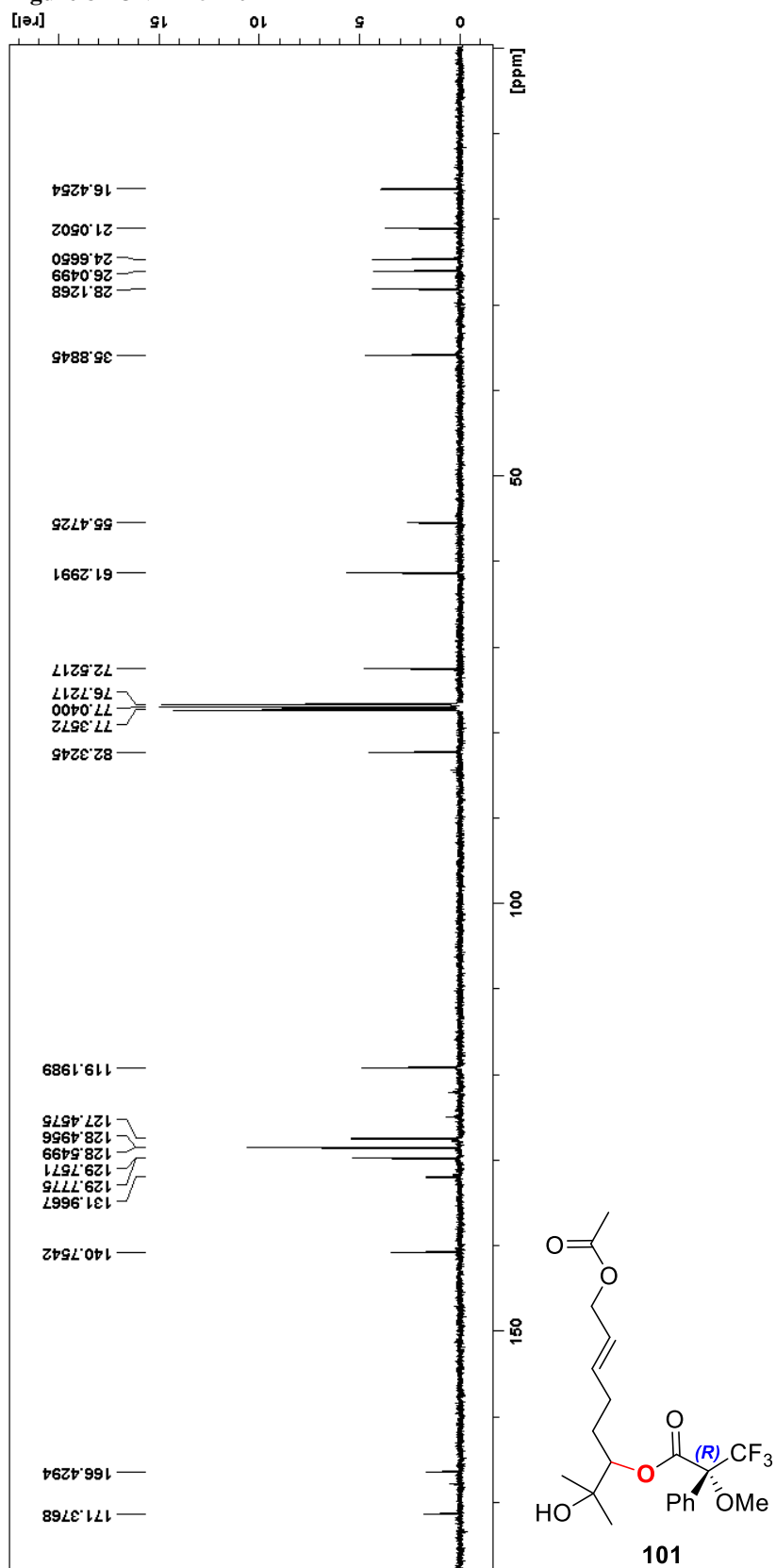


Figure 81 CNMR of 101



<sup>1</sup>H NMR spectrum of poly(2-vinylpyridine) in CDCl<sub>3</sub>. The x-axis represents the chemical shift in ppm (δ) from 0 to 8. The y-axis represents the intensity in arbitrary units. The spectrum shows several peaks corresponding to the protons in the polymer chain. The integration values are provided below the peaks.

| Chemical Shift (ppm)   | Integration |
|--|-------------|
| 7.6308, 7.6229, 7.6161, 7.6080, 7.4135, 7.4054, 7.3971, 7.2594   | 2.0097      |
| 3.0820   | 3.0820      |
| 2.0366   | 2.0366      |
| 1.0000, 1.0348   | 1.0000      |
| 3.5613, 3.5643   | 3.5613      |
| 3.0367, 1.9908, 1.2349, 3.7939, 1.6131   | 3.0367      |
| 3.1717, 3.1125   | 3.1717      |
| 2.0464, 1.9356, 1.9169, 1.8959, 1.7840, 1.7785, 1.7635, 1.7578, 1.7488, 1.7431, 1.7294, 1.7262, 1.7207, 1.7071, 1.7014, 1.6826, 1.6476, 1.6394, 1.6378, 1.6223, 1.6100, 1.5847, 1.5691, 1.5640, 1.2145, 1.1541 | 2.0464      |

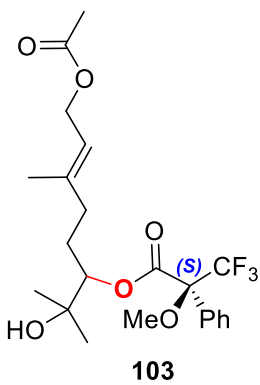
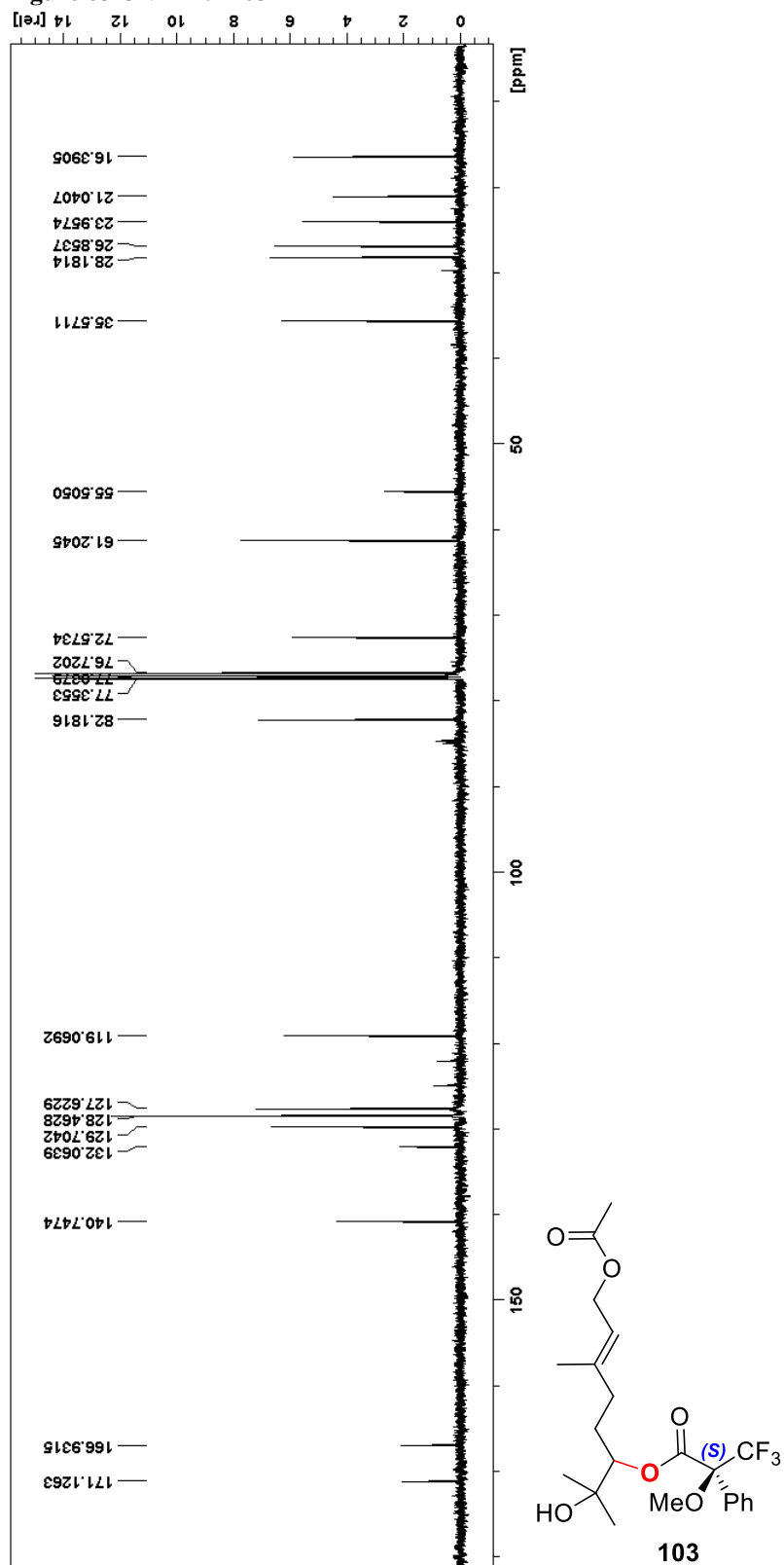


Figure 83 CNMR of 103



## REFERENCES

1. Snyder, S. A.; Treitler, D. S., Et<sub>2</sub>SBr·SbCl<sub>5</sub>Br: An Effective Reagent for Direct Bromonium-Induced Polyene Cyclizations. *Angewandte Chemie International Edition* **2009**, 48 (42), 7899-7903.
2. González, M. A.; Molina-Navarro, S., Attempted Synthesis of Spongidines by a Radical Cascade Terminating onto a Pyridine Ring. *The Journal of Organic Chemistry* **2007**, 72 (19), 7462-7465.
3. (a) CDC Malaria Facts. <http://www.cdc.gov/malaria/about/facts.html> (accessed October 8, 2013); (b) WHO Malaria Fact Sheet. <http://www.who.int/mediacentre/factsheets/fs094/en/> (accessed March 18, 2015); (c) Strowig, T.; Ploss, A., Plasmodium Falciparum Parasite Development in Humanized Mice: Liver And Blood Stages. In *Humanized Mice for HIV Research*, Poluektova, L. Y.; Garcia, J. V.; Koyanagi, Y.; Manz, M. G.; Tager, A. M., Eds. Springer New York: 2014; pp 519-528; (d) WHO, *World malaria report 2014*. World Health Organization: Geneva, Switzerland, 2014.
4. Anthony, M.; Burrows, J.; Duparc, S.; Jmoehrle, J.; Wells, T., The global pipeline of new medicines for the control and elimination of malaria. *Malar J* **2012**, 11 (1), 1-25.
5. Malaria Life-Cycle. <http://malariamedicalbreakthrough.weebly.com/life-cycle.html> (accessed October 27, 2014).
6. CDC Malaria Disease. <http://www.cdc.gov/malaria/about/disease.html> (accessed March 19, 2015).
7. Nasci, R. S. Z.-G., E.; Wirtz, R. A.; Brogdon, W. G., *CDC Health Information for International Travel* Oxford University Press.
8. (a) Pribluda, V.; Evans, L., III; Barillas, E.; Marmion, J.; Lukulay, P.; Chang, J., Were medicine quality and pharmaceutical management contributing factors in diminishing artemisinin efficacy in Guyana and Suriname? *Malar J* **2014**, 13 (1), 1-5; (b) Gbotosho, G.; Happi, C.; Ganiyu, A.; Ogundahunsi, O.; Sowunmi, A.; Oduola, A., Potential contribution of prescription practices to the emergence and spread of chloroquine resistance in south-west Nigeria: caution in the use of artemisinin combination therapy. *Malar J* **2009**, 8 (1), 1-8; (c) Mohammed, A.; Ndaro, A.; Kalinga, A.; Manjurano, A.; Mosha, J.; Mosha, D.; van Zwetselaar, M.; Koenderink, J.; Mosha, F.; Alifrangis, M.; Reyburn, H.; Roper, C.; Kavishe, R., Trends in chloroquine resistance marker, Pfcrt-K76T mutation ten years after chloroquine withdrawal in Tanzania. *Malar J* **2013**, 12 (1), 1-7.
9. Laurent, D.; Pietra, F., Antiplasmodial Marine Natural Products in the Perspective of Current Chemotherapy and Prevention of Malaria. A Review. *Mar Biotechnol* **2006**, 8 (5), 433-447.
10. (a) Kubanek, J.; Prusak, A. C.; Snell, T. W.; Giese, R. A.; Hardcastle, K. I.; Fairchild, C. R.; Aalbersberg, W.; Raventos-Suarez, C.; Hay, M. E., Antineoplastic Diterpene-Benzoate Macrolides from the Fijian Red Alga *Callophycus serratus*. *Organic Letters* **2005**, 7 (23), 5261-5264; (b) Nyadong, L.; Hohenstein, E.; Galhena, A.; Lane, A.; Kubanek, J.; Sherrill, C. D.; Fernández, F., Reactive desorption electrospray ionization mass spectrometry (DESI-MS) of natural products of a marine alga. *Anal Bioanal Chem* **2009**, 394 (1), 245-254.

11. Kubanek, J.; Prusak, A. C.; Snell, T. W.; Giese, R. A.; Fairchild, C. R.; Aalbersberg, W.; Hay, M. E., Bromophycolides C–I from the Fijian Red Alga *Callophycus serratus*. *Journal of Natural Products* **2006**, 69 (5), 731-735.
12. (a) Lane, A. L.; Nyadong, L.; Galhena, A. S.; Shearer, T. L.; Stout, E. P.; Parry, R. M.; Kwasnik, M.; Wang, M. D.; Hay, M. E.; Fernandez, F. M.; Kubanek, J., Desorption electrospray ionization mass spectrometry reveals surface-mediated antifungal chemical defense of a tropical seaweed. *Proceedings of the National Academy of Sciences* **2009**, 106 (18), 7314-7319; (b) Lane, A. L.; Stout, E. P.; Hay, M. E.; Prusak, A. C.; Hardcastle, K.; Fairchild, C. R.; Franzblau, S. G.; Le Roch, K.; Prudhomme, J.; Aalbersberg, W.; Kubanek, J., Callophycic Acids and Callophycols from the Fijian Red Alga *Callophycus serratus*. *The Journal of Organic Chemistry* **2007**, 72 (19), 7343-7351.
13. (a) Lane, A. L.; Stout, E. P.; Lin, A.-S.; Prudhomme, J.; Le Roch, K.; Fairchild, C. R.; Franzblau, S. G.; Hay, M. E.; Aalbersberg, W.; Kubanek, J., Antimalarial Bromophycolides J–Q from the Fijian Red Alga *Callophycus serratus*. *The Journal of Organic Chemistry* **2009**, 74 (7), 2736-2742; (b) Kubanek, J. M.; Hay, M. E.; Le Roch, K. G.; Stout, E. P.; Lane, A. L.; Lin, A.-S. Compounds and compositions useful in the treatment of malaria. US20110190338A1, 2011.
14. Esquenazi, E.; Dorrestein, P. C.; Gerwick, W. H., Probing marine natural product defenses with DESI-imaging mass spectrometry. *Proceedings of the National Academy of Sciences* **2009**, 106 (18), 7269-7270.
15. (a) Lin, A.-S.; Stout, E. P.; Prudhomme, J.; Roch, K. L.; Fairchild, C. R.; Franzblau, S. G.; Aalbersberg, W.; Hay, M. E.; Kubanek, J., Bioactive Bromophycolides R–U from the Fijian Red Alga *Callophycus serratus*. *Journal of Natural Products* **2010**, 73 (2), 275-278; (b) Stout, E. P.; Cervantes, S.; Prudhomme, J.; France, S.; La Clair, J. J.; Le Roch, K.; Kubanek, J., Bromophycolide A Targets Heme Crystallization in the Human Malaria Parasite *Plasmodium falciparum*. *ChemMedChem* **2011**, 6 (9), 1572-1577.
16. Teasdale, M. E.; Prudhomme, J.; Torres, M.; Braley, M.; Cervantes, S.; Bhatia, S. C.; La Clair, J. J.; Le Roch, K.; Kubanek, J., Pharmacokinetics, Metabolism, and in Vivo Efficacy of the Antimalarial Natural Product Bromophycolide A. *ACS Medicinal Chemistry Letters* **2013**, 4 (10), 989-993.
17. Chai, A.; Chevli, R.; Fitch, C., Ferriprotoporphyrin IX Fulfills the Criteria for Identification as the Chloroquine Receptor of Malaria Parasites. *Biochemistry* **1980**, 19 (8), 1543-1549.
18. Goldberg, D. E.; Slater, A. F.; Cerami, A.; Henderson, G. B., Hemoglobin degradation in the malaria parasite *Plasmodium falciparum*: an ordered process in a unique organelle. *Proceedings of the National Academy of Sciences* **1990**, 87 (8), 2931-2935.
19. Fidock, D. A.; Nomura, T.; Talley, A. K.; Cooper, R. A.; Dzekunov, S. M.; Ferdig, M. T.; Ursos, L. M. B.; bir Singh Sidhu, A.; Naudé, B.; Deitsch, K. W.; Su, X.-z.; Wootton, J. C.; Roepe, P. D.; Wellems, T. E., Mutations in the *P. falciparum* Digestive Vacuole Transmembrane Protein PfCRT and Evidence for Their Role in Chloroquine Resistance. *Molecular Cell* **2000**, 6 (4), 861-871.
20. Lin, H.; Pochapsky, S. S.; Krauss, I. J., A Short Asymmetric Route to the Bromophycolide A and D Skeleton. *Organic Letters* **2011**, 13 (5), 1222-1225.
21. (a) Bhattacharyya, S.; Solakyildirim, K.; Zhang, Z.; Linhardt, R.; Tobacman, J., Chloroquine reduces arylsulphatase B activity and increases chondroitin-4-sulphate: implications for mechanisms of action and resistance. *Malar J* **2009**, 8 (1), 1-14; (b) WHO

- Malaria: Q&A on artemisinin resistance.  
[http://www.who.int/malaria/media/artemisinin\\_resistance\\_qa/en/index.html](http://www.who.int/malaria/media/artemisinin_resistance_qa/en/index.html) (accessed 7 October).
22. Chappe, B.; Musikas, H.; eacute; egrave; ne; Marie, D.; Ourisson, G., Synthesis of Three Acyclic All-*trans*-Tetraterpene Diols, Putative Precursors of Bacterial Lipids. *Bulletin of the Chemical Society of Japan* **1988**, 61 (1), 141-148.
  23. Yu, X.-J.; Zhang, H.; Xiong, F.-J.; Chen, X.-X.; Chen, F.-E., An Improved Convergent Strategy for the Synthesis of Oligoprenols. *Helvetica Chimica Acta* **2008**, 91 (10), 1967-1974.
  24. (a) Stockton, K. P.; Greatrex, B. W.; Taylor, D. K., Synthesis of allo- and epi-Inositol via the NHC-Catalyzed Carbocyclization of Carbohydrate-Derived Dialdehydes. *The Journal of Organic Chemistry* **2014**, 79 (11), 5088-5096; (b) Vlad, P. F.; Ungur, N. D.; Aricu, A. N.; Andreeva, I. Y., Regioselective dehydration of axial and equatorial tertiary alcohols with  $\alpha$ -methyl group in the cyclohexane ring by Swern's reagent. *Russ Chem Bull* **1997**, 46 (4), 767-770; (c) Frija, L. M. T.; Afonso, C. A. M., Amberlyst®-15: a reusable heterogeneous catalyst for the dehydration of tertiary alcohols. *Tetrahedron* **2012**, 68 (36), 7414-7421.
  25. (a) Vidari, G.; Di Rosa, A.; Castronovo, F.; Zanoni, G., Enantioselective synthesis of each stereoisomer of the pyranoid linalool oxides: the geraniol route. *Tetrahedron: Asymmetry* **2000**, 11 (4), 981-989; (b) Khan, A. T.; Ghosh, S.; Choudhury, L. H., A Highly Efficient Synthetic Protocol for Tetrahydropyranylation/Depyranylation of Alcohols and Phenols. *European Journal of Organic Chemistry* **2005**, 2005 (22), 4891-4896.
  26. (a) Becker, H.; Soler, M. A.; Barry Sharpless, K., Selective asymmetric dihydroxylation of polyenes. *Tetrahedron* **1995**, 51 (5), 1345-1376; (b) Xu, D.; Park, C. Y.; Sharpless, K. B., Study of the regio- and enantioselectivity of the reactions of osmium tetroxide with allylic alcohols and allylic sulfonamides. *Tetrahedron Letters* **1994**, 35 (16), 2495-2498.
  27. Kurti, L. C., B., *Strategic Applications of Named Reactions in Organic Synthesis*. Elsevier Academic Press: San Diego, California, 2005.
  28. Katsuki, T.; Sharpless, K. B., The first practical method for asymmetric epoxidation. *Journal of the American Chemical Society* **1980**, 102 (18), 5974-5976.
  29. van der Klei, A., de Jong, Robertus L. P., Lugtenburg, J. and Tielens, Aloysius G. M., Synthesis and Spectroscopic Characterization of [1'-<sup>14</sup>C]Ubiquinone-2, [1'-<sup>14</sup>C]-5-Demethoxy-5-hydroxyubiquinone-2, and [1'-<sup>14</sup>C]-5-Demethoxyubiquinone-2. *European Journal of Organic Chemistry* **2002**, 17, 3015-3023.
  30. Zhang, P., Roundtree, I. A., Morken, J. P., Ni- and Pd-Catalyzed Synthesis of Substituted and Functionalized Allylic Boronates *Organic Letters* **2012**, 14 (6), 1416-1419
  31. Inoue, A., Kitagawa, K., Shinokubo, H., Oshima, K., Selective Halogen-Magnesium Exchange Reaction via Organomagnesium Ate Complex *The Journal of Organic Chemistry* **2001**, 66 (12), 4333-4339
  32. Smith, A. B., Risatti, C. A., Atasoylu, O., Bennett, C. S., Liu, J., Chengm H., TenDyke, K., Xu, Q., Design, Synthesis, and Biological Evaluation of Diminutive Forms

of (+)-Spongistatin 1: Lessons Learned *Journal of the American Chemical Society* **2011** 133 (35), 14042-14053

33. Hashimoto, M., Harigaya, H., Yanagiya, M., Shirahama, H., Total synthesis of the meso-triterpene polyether teurilene *The Journal of Organic Chemistry* **1991** 56 (7), 2299-2311
34. Mander, L. N., McLachlan, M. M., The Total Synthesis of the Galbulimima Alkaloid GB 13 *Journal of the American Chemical Society* **2003** 125 (9), 2400-2401
35. Bunge, A., Hamann, H. J., Dietz, D., Liebscher, J., Enantioselective epoxidation of tertiary allylic alcohols by chiral dihydroperoxides *Tetrahedron* **2013** 125 (11) 2446-2450
36. Trost, B., Merlic, C. A., Diastereoselectivity control elements. Acyclic diastereocontrol in formation and reactions of .gamma.-hydroxy sulfones *Journal of the American Chemical Society* **1988** 110 (15), 5216-5218
37. Vidari, G., Rosa, A. D., Castronovo, F., Zanoni, G., Enantioselective synthesis of each stereoisomer of the pyranoid linalool oxides: the geraniol route *Tetrahedron: Asymmetry* **2000** (2000) 11 981-989
38. Hoyer, T. R., Jeffrey, C. S., Shao, F., Mosher ester analysis for the determination of absolute configuration of stereogenic (chiral) carbinol carbons *Nature Protocols* **2007** 10 (2) 2451-2458
39. Brimble, M., Rowan, D., Spicer, J., Enantioselective Synthesis of the Apple Aroma Constituent 1,3,3-trimethyl-2,7-dioxabicyclo[2.2.1]heptane via Asymmetric Dihydroxylation *Synthesis* **1995** 10 1263-1266
40. Miyaoka, H., Kajiura, Y., Hara, Y., Yamada, Y., Total Synthesis of Dysidiolide *Journal of Organic Chemistry* **2001** 66 (4) 1429-1435
41. Hutchins, R. O., Learn, K., Regio- and stereoselective reductive replacement of allylic oxygen, sulfur, and selenium functional groups by hydride via catalytic activation by palladium(0) complexes *The Journal of Organic Chemistry* **1982** 47 (22), 4380-4382